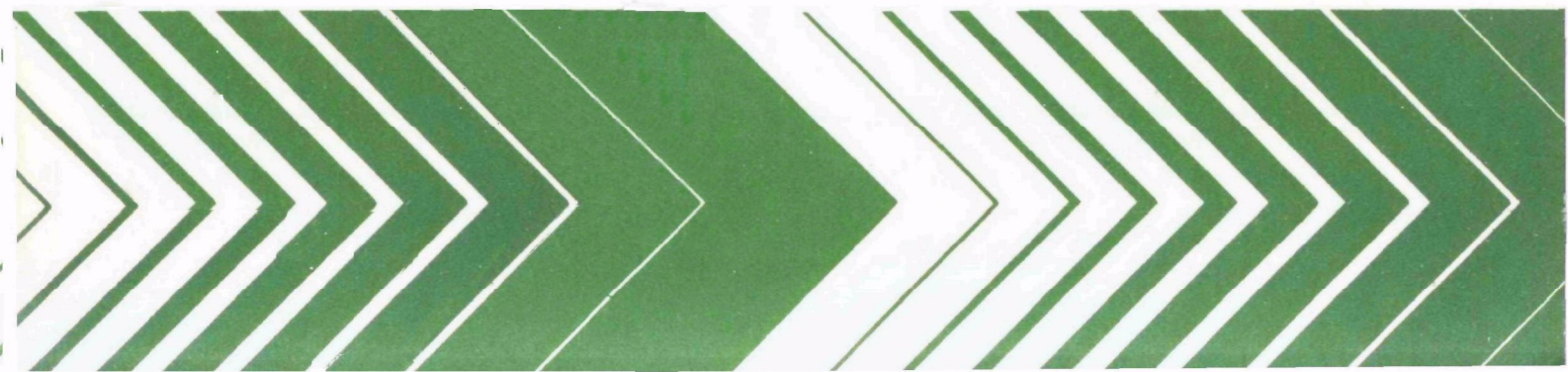


Research and Development



# Oxidant-Precursor Relationships Under Pollutant Transport Conditions

Outdoor Smog  
Chamber Study  
Volume 1.



## **RESEARCH REPORTING SERIES**

Research reports of the Office of Research and Development, U.S. Environmental Protection Agency, have been grouped into nine series. These nine broad categories were established to facilitate further development and application of environmental technology. Elimination of traditional grouping was consciously planned to foster technology transfer and a maximum interface in related fields. The nine series are:

1. Environmental Health Effects Research
2. Environmental Protection Technology
3. Ecological Research
4. Environmental Monitoring
5. Socioeconomic Environmental Studies
6. Scientific and Technical Assessment Reports (STAR)
7. Interagency Energy-Environment Research and Development
8. "Special" Reports
9. Miscellaneous Reports

This report has been assigned to the ECOLOGICAL RESEARCH series. This series describes research on the effects of pollution on humans, plant and animal species, and materials. Problems are assessed for their long- and short-term influences. Investigations include formation, transport, and pathway studies to determine the fate of pollutants and their effects. This work provides the technical basis for setting standards to minimize undesirable changes in living organisms in the aquatic, terrestrial, and atmospheric environments.

This document is available to the public through the National Technical Information Service, Springfield, Virginia 22161.

EPA-600/3-79-078a  
August 1979

OXIDANT-PRECURSOR RELATIONSHIPS UNDER POLLUTANT TRANSPORT CONDITIONS

Outdoor Smog Chamber Study

Volume 1

by

J. E. Sickles, II

L.A. Ripperton

W. C. Eaton

R. S. Wright

Research Triangle Institute

Research Triangle Park, North Carolina 27709

Contract No. 68-02-2207

Project Officers:

J. J. Bufalini

B. W. Gay, Jr.

Atmospheric Chemistry and Physics Division

Environmental Sciences Research Laboratory

Research Triangle Park, North Carolina 27711

ENVIRONMENTAL SCIENCES RESEARCH LABORATORY

OFFICE OF RESEARCH AND DEVELOPMENT

U.S. ENVIRONMENTAL PROTECTION AGENCY

RESEARCH TRIANGLE PARK, NORTH CAROLINA 27711

## DISCLAIMER

This report has been reviewed by the Environmental Sciences Research Laboratory, U.S. Environmental Protection Agency, and approved for publication. Approval does not signify that the contents necessarily reflect the views and policies of the U.S. Environmental Protection Agency, nor does mention of trade names or commercial products constitute endorsement or recommendation for use.

## ABSTRACT

A total of 146 multiple-day experiments was conducted in the four outdoor smog chambers that comprise the RTI smog chamber facility. These experiments were conducted to investigate the influence of simulated transport on ozone generation by various combinations of a surrogate urban hydrocarbon mixture and nitrogen oxides. The simulation of transport was accomplished by progressively diluting the contents of the chambers with purified air.

Maximum first-day ozone concentrations were reduced under dilution conditions. First-day ozone maxima were found to be sensitive both to the dilution rate and the time in the experiment that dilution was initiated. Second and third-day ozone maxima were reduced by increasing dilution rates but the reduction was less than proportional to the extent of dilution. Second and third-day ozone maxima were reduced by dilution but the ozone-generative potential, as measured by net ozone concentrations, was not. The ozone-generative potential of an aged photochemical system contained in the RTI smog chambers generally exceeded 0.08 ppm.

Additional experiments were conducted to examine the ozone-generative potential of low reactivity hydrocarbons, to provide data for testing and validation of a computer-based photochemical simulation model, and to compare the behavior of two types of outdoor smog chambers.

Volume 1 contains all textual material. Volume 2 (Appendixes) contains individual hydrocarbon analyses from each experiment as well as concentration ( $O_3$ , oxidant, nitrogen oxides, THC,  $CH_4$ , NMHC, HCHO, CN, and Freon-12) and environmental (solar radiation and temperature) data from each experiment.

This report was submitted in fulfillment of Contract No. 68-02-2207 by the Research Triangle Institute under the sponsorship of the U. S. Environmental Protection Agency. This report covers the period June 6, 1975 to June 23, 1978.



## CONTENTS

Abstract . . . . .	iii
Figures . . . . .	vii
Tables . . . . .	x
Acknowledgments . . . . .	xii
1. Introduction . . . . .	1
2. Conclusions . . . . .	3
3. Recommendations . . . . .	5
4. Experimental . . . . .	15
Overview . . . . .	15
RTI Smog Chamber Facility . . . . .	18
Air purification unit . . . . .	22
Reactant injection system . . . . .	22
Sampling system . . . . .	25
Smog chamber operating characteristics . . . . .	25
Mixing . . . . .	27
Performance of air purification system . . . . .	27
Chamber tightness . . . . .	27
Dilution . . . . .	31
Sample line losses . . . . .	32
Characterization experiments . . . . .	33
Reagents . . . . .	41
Measurement methods . . . . .	44
Ozone . . . . .	46
Oxidant . . . . .	46
Nitrogen oxides (NO, NO <sub>2</sub> , and NO <sub>x</sub> ) . . . . .	47
Nitrogen dioxide . . . . .	48
Total hydrocarbons, methane, nonmethane hydrocarbons, and carbon monoxide . . . . .	48
Individual hydrocarbons . . . . .	49
Formaldehyde . . . . .	51
Condensation nuclei . . . . .	52
Freon-12 . . . . .	52
Solar radiation . . . . .	53
Environmental variables . . . . .	53
Data reduction and handling . . . . .	53
Procedure . . . . .	55

## CONTENTS

5. Results and Discussion . . . . .	57
Overview . . . . .	57
Basic research program . . . . .	57
Analysis of overall data set . . . . .	58
Analysis of individual experiments . . . . .	65
Experiments conducted to provide data for model testing . . . . .	78
Ozone-generative potential of low reactivity hydro- carbons . . . . .	80
Comparison between two outdoor smog chamber facilities: matched experiments . . . . .	85
Cross calibration comparisons . . . . .	87
Background conditions . . . . .	90
The matched experiment of 20-21 September 1976 . .	90
The matched experiment of 5 November 1976 . . . . .	100
Discussion . . . . .	107
References . . . . .	109



## FIGURES

<u>Number</u>		<u>Page</u>
1	Shape of growth function of mixed layer for St. Louis based on 1976 RAPS data . . . . .	7
2	Fractional distribution of $\text{NO}_x$ as $\text{NO}_2$ along a south-to-north cross-section of St. Louis from 0500 to 0700 CST and from 1100 to 1500 CST on June 8, 1976 . . . . .	9
3	Fractional distribution of $\text{NO}_x$ as $\text{NO}_2$ along a west-to-east cross-section of St. Louis from 0500 to 0700 CST and from 1100 to 1500 CST on June 8, 1976 . . . . .	10
4	Ozone distribution along a south-to-north cross-section of St. Louis from 0500 to 0700 CST, from 1100 to 1500 CST and for the maximum hourly concentration on June 8, 1976 . . .	11
5	Ozone distribution along a west-to-east cross-section of St. Louis from 0500 to 0700 CST, from 1100 to 1500 CST and for the maximum hourly concentration on June 8, 1976 . . .	12
6	Ozone concentrations aloft and on the ground during the flight of Da Vinci II on June 8-9, 1976 . . . . .	13
7	General design of RTI outdoor smog chambers . . . . .	20
8.	Overall system design of RTI Smog Chamber Facility . . . .	21
9.	Air purification unit for RTI Smog Chamber Facility . . . .	23
10.	Reactant injection system for RTI Smog Chamber Facility . .	24
11.	Sampling system for RTI Smog Chamber Facility . . . . .	26
12	First-day maximum ozone concentrations versus initial hydrocarbon concentrations for all experiments and for static experiments . . . . .	59
13	First-day maximum ozone concentrations versus initial $\text{NO}_x$ concentrations for all experiments and for static experiments . . . . .	60

## FIGURES

<u>Number</u>		<u>Page</u>
14	First-day maximum ozone concentrations versus initial hydrocarbon-to-NO <sub>x</sub> ratios for all experiments and for static experiments . . . . .	61
15	Third-day net ozone concentrations versus sunrise hydrocarbon concentrations for all experiments and for static experiments . . . . .	63
16	Third-day net ozone concentrations versus sunrise NO <sub>x</sub> concentrations for all experiments and for static experiments . . . . .	64
17	Maximum and net ozone concentrations for static experiments and for dilution experiments initiated at sunrise . . . . .	66
18	Maximum and net ozone concentrations for static experiments and for dilution experiments initiated at crossover . . . . .	67
19	Maximum and net ozone concentrations for static experiments and for dilution experiments initiated at 1700 . . . . .	68
20	Maximum ozone concentrations plotted by case number and day for dilution beginning at sunrise, 1700 and crossover . . . . .	71
21	Net ozone concentrations plotted by case number and day for dilution beginning at sunrise, 1700 and crossover . . . . .	72
22	Maximum ozone concentrations under dilution conditions relative to the maximum ozone concentration obtained under static conditions . . . . .	77
23	Comparison of the designs and sizes of the RTI and UNC outdoor smog chambers . . . . .	88
24	Total solar radiation profiles for UNC and RTI on September 20, 1976 . . . . .	95
25	Nitric oxide, nitrogen dioxide and ozone concentration profiles for RTI Chamber 1 and RTI Chamber 2 on September 20, 1976 . . . . .	96
26	Nitric oxide, nitrogen dioxide and ozone concentration profiles for RTI Chamber 3 and RTI Chamber 4 on September 20, 1976 . . . . .	97
27	Nitric oxide, nitrogen dioxide and ozone concentration profiles for UNC Red Chamber and UNC Blue Chamber on September 20, 1976 . . . . .	98
28	Ozone concentration profiles for the two UNC chambers and the four RTI chambers on September 20, 1976 . . . . .	99

# FIGURES

<u>Number</u>		<u>Page</u>
29	Total solar radiation profiles for UNC and RTI on November 5, 1976 . . . . .	103
30	Nitric oxide, nitrogen dioxide and ozone concentration profiles for UNC Blue Chamber and RTI Chamber 2 on November 5, 1976 . . . . .	104
31	Nitric oxide, nitrogen dioxide and ozone concentration profiles for UNC Red Chamber and RTI Chamber 2 on November 5, 1976 . . . . .	105

## TABLES

<u>Table</u>		<u>Page</u>
1	Summertime Mixing Heights and Apparent Dilution Factors in Selected Urban Areas . . . . .	7
2	Summary of Experimental Conditions for Urban Mix Runs . . . . .	16
3	Summary of Experimental Conditions for Runs not Involving Urban Mix as Reactant . . . . .	17
4	Basic Research Program . . . . .	19
5	Hydrocarbon Concentrations in the RTI Smog Chambers Following Air Cleanup Operations . . . . .	28
6	Dilution in RTI Smog Chambers . . . . .	30
7	Maximum Ozone Concentration Achieved in RTI Smog Chambers During Purified Air Irradiation Experiments . . . . .	35
8	Ozone Half-Lives in RTI Smog Chambers . . . . .	36
9	NO Oxidation in RTI Smog Chambers . . . . .	37
10	Summary of Ozone Half-Lives for Various Smog Chambers . . . . .	39
11	Reagents . . . . .	42
12	Analyses of Hydrocarbon Mixtures Used in Urban Mix Experiments .	43
13	Measurement Methods . . . . .	45
14	Summary of Results from Experiments Conducted to Provide Data For Model Testing . . . . .	79
15	Comparison of RTI Outdoor Smog Chamber Results with Results From SAPRC Indoor Chamber. . . . .	81
16	Summary of Results for Low Reactivity Experiments. . . . .	84
17	Maximum Ozone Concentrations Generated in Various Smog Chambers Using Low Reactivity Hydrocarbons . . . . .	86

# TABLES

<u>Table</u>		<u>Page</u>
18	Comparison of Physical and Chemical Characteristics of Research Triangle Institute and University of North Carolina Outdoor Smog Chambers . . . . .	89
19	Measurement of Preinjection Chamber Contents and Background Ambient Air . . . . .	91
20	Summary of Results for Matched Experiments on 20 and 21 September 1976. . . . .	92
21	Summary of Results for Matched Experiment on 5 November 1976 . . . . .	101

## ACKNOWLEDGMENTS

This project was conducted by the Research Triangle Institute under Contract Number 68-02-2207 for the U.S. Environmental Protection Agency. The support of this agency is gratefully acknowledged as is the advice and guidance of the EPA personnel who contributed to the project: Dr. Basil Dimitriadis, who initiated the project, and Dr. J. J. Bufalini, and Mr. B. W. Gay, Jr. who served as Project Officers.

Several persons in the Environmental Measurements Department of the Research Triangle Institute contributed substantially to this project. Mr. C. E. Decker was Laboratory Supervisor for the project. Mr. D. L. Ewald and Mr. D. P. Dayton conducted day-to-day chamber operations, data reduction, and data verification. Messrs. R. B. Denyszyn, L. T. Hackworth, and P. M. Grohse developed the gas chromatographic procedures used and, along with Mr. D. L. Hardison, conducted all the GC analyses. Mrs. A. L. Turner conducted the wet chemical determinations. Mrs. S. K. Burt transferred the data into a computer-capatible format. Dr. L. M. Worsham served as a consultant to RTI during analysis of selected data.

The matched smog chamber experiments described in this report were conducted and analyzed jointly by the authors and Mr. R. M. Kamens and Dr. H. E. Jeffries of the University of North Carolina at Chapel Hill.

We gratefully acknowledge these individuals for their efforts in bringing this project to a successful conclusion.

## SECTION 1

### INTRODUCTION

Anthropogenic activity accounts for the high concentrations of ozone precursors that accumulate in urban areas during the early morning hours. Frequently by mid-morning the high concentrations of hydrocarbons and nitrogen oxides that were trapped within the lowest 200 to 400 meters over an urban center become diluted by atmospheric convective mixing processes that are promoted by solar heating. Thus, these emissions experience significant dilution on the day of their release. They also experience approximately 12 hours of irradiation. As an urban plume is transported downwind of a city, it may experience several diurnal cycles of irradiation and continued dilution with nonurban air.

Until recently most smog chamber simulations of photochemical smog employed initial reactant concentrations that are typical of those in urban areas, usually Los Angeles, during the early morning hours. Most experiments were conducted with indoor chambers that used artificial irradiation. In addition, the duration of these irradiations was usually short, e.g. 2 to 6 hours.

The current study was designed to investigate various aspects of photochemical ozone production under conditions that simulate the ambient atmosphere more closely than had been accomplished in previous smog chamber investigations. Multiple-day experiments were conducted in outdoor smog chambers that are designed to permit the simulation of atmospheric dilution conditions. The purpose was to investigate the influence of dilution on ozone generation by various combinations of a surrogate urban hydrocarbon mixture and nitrogen oxides. The relationship between ozone and ozone precursors (hydrocarbons and nitrogen oxides) were examined under various dilution conditions and repeated diurnal cycles of temperature and solar radiation.





## SECTION 2

### CONCLUSIONS

Smog chamber experiments were employed to investigate the influence of simulated transport on ozone generation by various combinations of a surrogate urban hydrocarbon mixture and nitrogen oxides. The basic research plan called for three-day smog chamber experiments to be conducted in the four outdoor smog chambers that comprise the RTI Smog Chamber Facility. Chamber contents were diluted to simulate the dispersion of an air parcel during transport. Experiments were conducted at four target initial reactant concentrations and at four dilution rates with initiation of dilution occurring at three different times on the first day of an experiment.

Findings from this study are summarized as follows:

1. For those experiments where dilution was initiated before the first-day maximum ozone concentrations occurred, the maxima were reduced in comparison to the maxima obtained under static conditions. In no case examined in the current study did dilution cause first-day ozone levels to exceed those of corresponding static experiments.
2. First-day ozone maxima were found to be sensitive both to the dilution rate and to the time at which dilution was initiated. Maximum ozone concentrations were reduced approximately in proportion to the extent of dilution when it was initiated at sunrise. When dilution was begun at NO-NO<sub>2</sub> crossover, however, maximum ozone concentrations were reduced, but the reduction was less than proportional to the extent of dilution.
3. The time required to achieve the first-day [O<sub>3</sub>]<sub>max</sub> concentration was reduced under dilution conditions relative to the times observed under static conditions.

4. Under both static and dilution conditions, first-day ozone maxima were greater than second-day maxima, which in turn, were greater than third-day maxima.
5. Minimum ozone concentrations on both the second and third days of an experiment were reduced with increasing dilution rates.
6. Second and third-day ozone maxima were reduced by dilution, but the ozone-generative potential as measured by net ozone concentrations was not.
7. Second and third-day ozone maxima were reduced with increasing dilution rates; however, the decrease was less than proportional to the extent of dilution.
8. Second-day net ozone concentrations at 39 or 77 percent dilution were greater than the corresponding levels under static conditions.
9. Second and third-day net ozone concentrations generally ranged from 0.08 to 0.30 ppm. Thus, in smog chambers, aged photochemical systems have relatively high ozone-generative potential.

Ancillary experiments were conducted to address additional points.

Major findings from these studies are listed below:

1. Maximum first-day ozone concentrations generated by low reactivity hydrocarbons, such as propane, in the presence of  $\text{NO}_x$  are highly temperature sensitive and decrease sharply with decreasing temperature.
2. If the classification of organics as low reactivity species is based on whether or not these species can produce 0.08 ppm of ozone during smog chamber investigations, then the results of the current study indicate that ethane, acetylene and propane must be considered to be reactive hydrocarbons.
3. Comparison of results from two same-day matched experiments conducted in the RTI and UNC outdoor smog chambers revealed good agreement both for propane/ $\text{NO}_x$  and for propene/ $\text{NO}_x$  experiments. This should increase confidence in the reliability of data obtained in outdoor smog chambers.

### SECTION 3

#### RECOMMENDATIONS

Based on findings in the current study, first-day-ozone generative potential is sensitive not only to the dilution rate experienced by a reacting photochemical system but also to the time at which this dilution is initiated. It is recommended that efforts in the next phase of this research program be directed at improving the understanding of these effects. The following questions should be addressed:

1. Is the effect of dilution one of simply reducing HC and  $\text{NO}_x$  at a constant HC/ $\text{NO}_x$  ratio to lower absolute concentrations?
2. Is the sensitivity of the photochemical smog system to dilution a manifestation of nonlinear effects resulting from the photochemical mechanism?
3. At what point in the sequence of events leading to the photochemical generation of ozone is the sensitivity to dilution the greatest, and does it occur during the time period leading to NO- $\text{NO}_2$  crossover?
4. How is the point of maximum sensitivity related to dilution rate?

Experiments designed to elucidate these issues can be conducted in smog chambers.

A topic currently of interest to those individuals who are responsible for planning and implementing oxidant control strategies is the impact of transported ozone on urban air quality. This issue can also be addressed by smog chamber studies. Chamber operation, however, must be carefully controlled to simulate both urban chemistry and meteorology.

To define the operating conditions required to simulate the meteorology, the extent of dilution that an urban air parcel experiences must first be defined.

Nocturnal surface-based inversions exist in most urban areas during evening and early morning hours. Urban emissions accumulate within this layer until shortly after sunrise when the convective activity resulting from solar heating causes this layer to erode and mixing to occur to the daily maximum mixing height. Mean summertime early morning and afternoon mixing heights are tabulated for selected cities in Table 1<sup>1</sup>. If it is assumed that the increase in mixing height during a day roughly reflects the extent of dilution experienced by a typical early morning urban air parcel, then the average extent of dilution for these urban areas is 78 percent.

The next point that must be addressed is the manner in which dilution occurs--the shape function for growth of the mixed layer. This function has been defined empirically from data collected in the RAPS Study<sup>2</sup> and is shown in Figure 1. During the first hour after sunrise the inversion begins to erode, and 2 percent of the total volumetric exchange occurs. During the next hour, 10 percent occurs. From 0830 to 0930 CST the inversion is dissipated, so that by 1000 CST, 58 percent of the total volumetric exchange has occurred. Most of the exchange, 85 percent, has occurred by noon, and the maximum mixing height is established by 1500 CST. This suggests that to a first approximation a uniform dilution rate of  $30\% \text{ hr}^{-1}$  should be employed in smog chamber simulation of these events. The duration of dilution should be 5 to 6 hours; it should begin at two hours past sunrise and terminate at noon.

With the major meteorological parameters defined, the chemical parameters should be defined as well. There is evidence to suggest that the maximum ozone concentration is determined by the total mass of ozone precursors injected into a smog chamber divided by the total mixing volume at the time of the maximum<sup>3</sup>. Thus, the procedure commonly employed in smog chamber studies of introducing the HC and  $\text{NO}_x$  reactants as a batch injection just prior to sunrise is a reasonable approach.

It is recommended that a surrogate urban mix be designed and employed. Such a mix could be as simple as the two-component EKMA mix recently employed in EPA's computer modeling efforts<sup>4-6</sup> or as complex as to contain not only alkane, alkene, and aromatic hydrocarbons, but aldehydes as well.

Table 1. Summertime Mixing Heights and Apparent Dilution Factors in Selected Urban Areas<sup>1</sup>

Urban Area	<u>Mixing Heights, m</u>		Dilution Factor <sup>†</sup>
	Morning	Afternoon	
Dayton, OH	349	1661	0.21
Nashville, TN	417	1845	0.23
New York, NY	662	1512	0.44
Peoria, IL	272	1498	0.18
Pittsburgh, PA	333	1794	0.19
Washington, DC	378	1884	0.20

<sup>†</sup> Dilution factor is the ratio of the morning to afternoon mixing heights; extent of dilution  $\approx 1 - \text{dilution factor}$ .

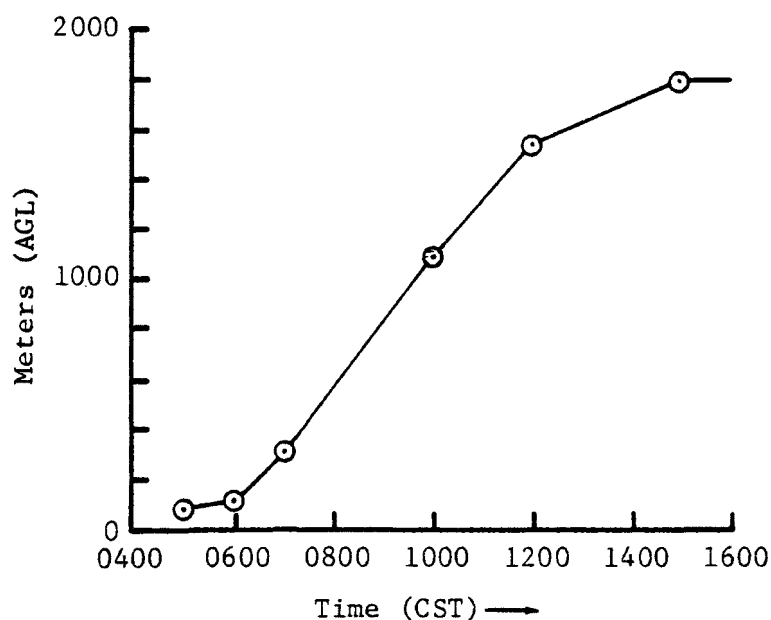


Figure 1. Shape of growth function of mixed layer for St. Louis based on 1976 RAPS data.<sup>2</sup>

In previous smog chamber studies the initial fraction of  $\text{NO}_x$  as  $\text{NO}_2$  has been 10 to 25 percent. Examination of data collected in St. Louis during the flight of the DaVinci II has shown this fraction to be much greater<sup>7</sup>. The fractional distribution of  $\text{NO}_x$  as  $\text{NO}_2$  is presented along South to North and West to East axes in Figures 2 and 3. The corresponding ozone distribution is shown in Figures 4 and 5. On 8 June 1976, for the 0500 to 0700 CST hours, approximately 65 percent of  $\text{NO}_x$  was as  $\text{NO}_2$ . For the 1100-1500 CST hours this value had increased to 80 percent. Although the mean early morning  $\text{NO}_2/\text{NO}_x$  percentage on this day was 65 percent, within the urban area where the ozone concentrations were insufficient to oxidize all of the NO to  $\text{NO}_2$ , approximately half of the total  $\text{NO}_x$  existed as  $\text{NO}_2$ . This finding has also been noted by others<sup>8</sup>. Thus, it is recommended that the fraction of  $\text{NO}_x$  as  $\text{NO}_2$  to be employed in future smog chamber experiments be increased to 50 percent.

If experiments conducted to simulate the urban atmosphere require dilution, then the chemical composition of the diluent air must be defined as well. To a first approximation this air is normally very low in ozone precursors<sup>5,6</sup>. It may contain considerable amounts of ozone, however, as is indicated by data collected in the DaVinci II experiment<sup>7</sup>.

Hourly ozone concentration data collected on and beneath the DaVinci II are presented in Figure 6. These data suggest that between 1000 and 1700 CST, on this day, the atmosphere was reasonably well mixed from ground level to the altitude of DaVinci II. Near sunset, surface cooling resulted in the establishment and growth of a surface-based radiation inversion. This permitted the accumulation of ozone-destructive agents near the surface. Ozone within this layer was depleted rapidly by surface deposition and by reaction with emitted destructive agents. The ozone above the nocturnal radiation inversion was insulated from the ground and the destructive agents released at the ground. On the evening of 8 June and the morning of 9 June the ozone aloft decayed at a very slow rate with a half-life of 116 hours. Thus, during a single nighttime period, ozone was transported aloft essentially undiminished over a distance of 300 km from St. Louis, MO to Evansville, IN.

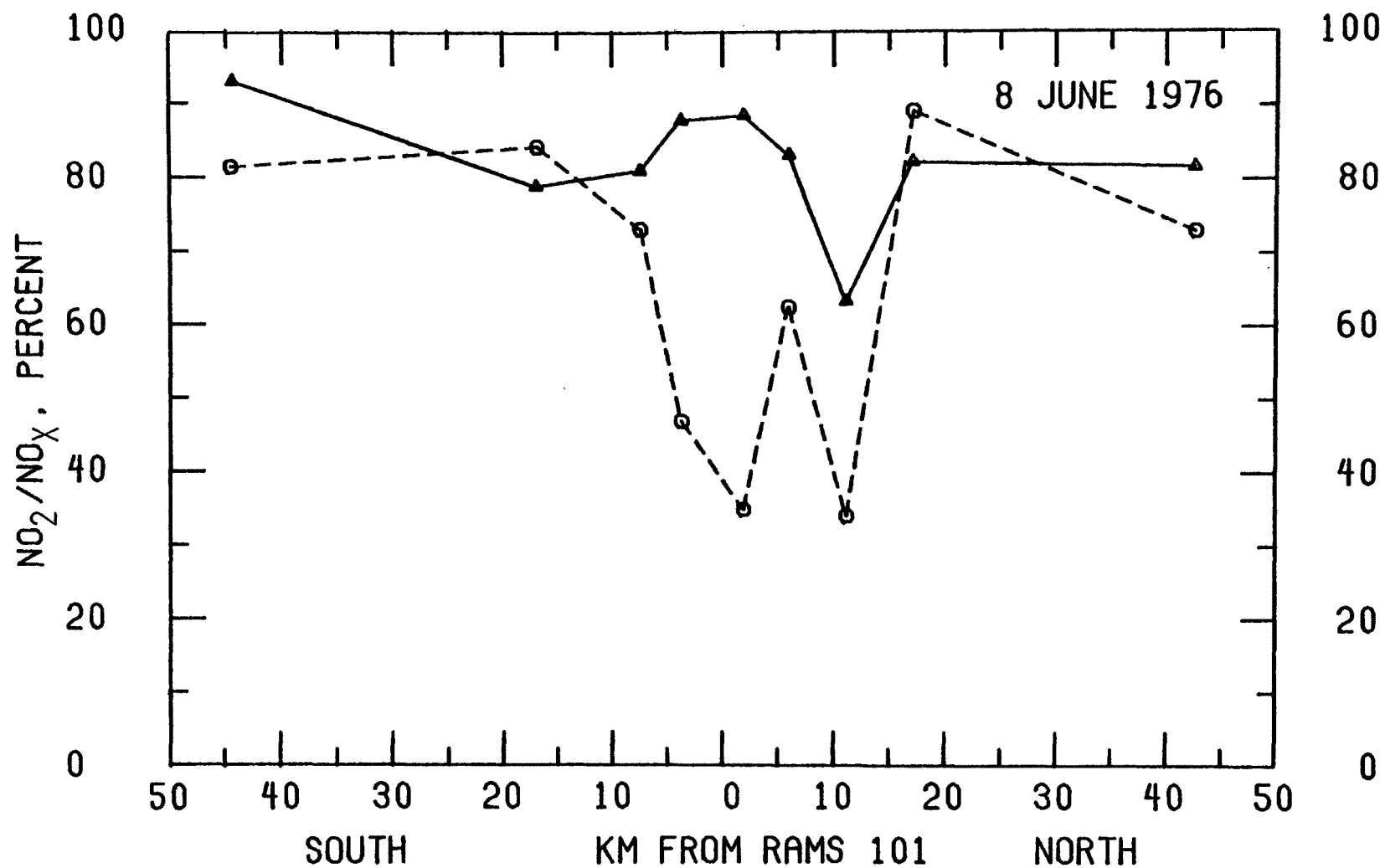


Figure 2. Fractional Distribution of NO<sub>x</sub> as NO<sub>2</sub> Along A South-To-North Cross-Section of St. Louis from 0500 to 0700 CST (o) and from 1100 to 1500 CST (Δ) on June 8, 1976.

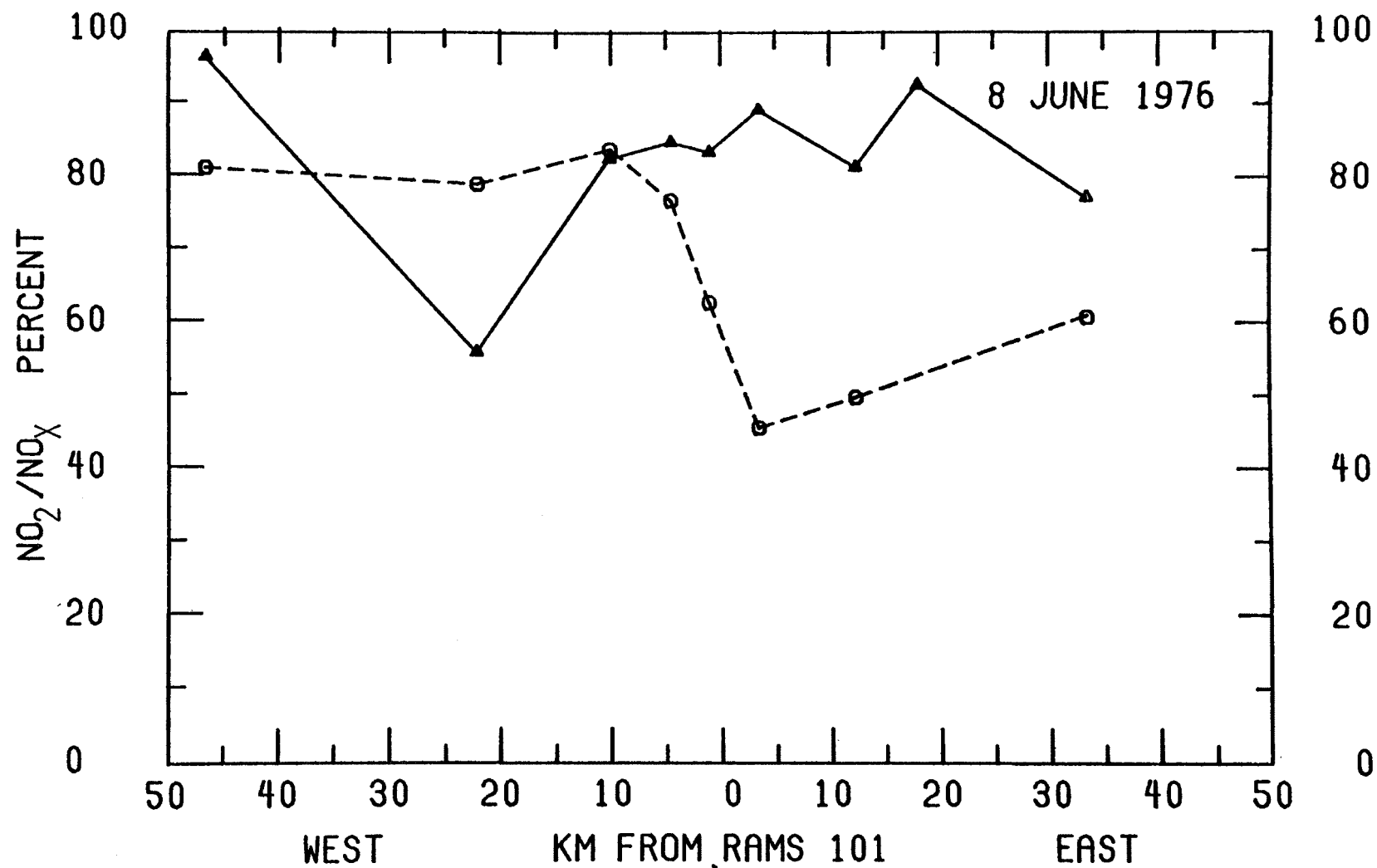


Figure 3. Fractional Distribution of NO<sub>x</sub> as NO<sub>2</sub> Along A West-To-East Cross-Section of St. Louis from 0500 To 0700 CST (0) and from 1100 to 1500 CST on June 8, 1976.



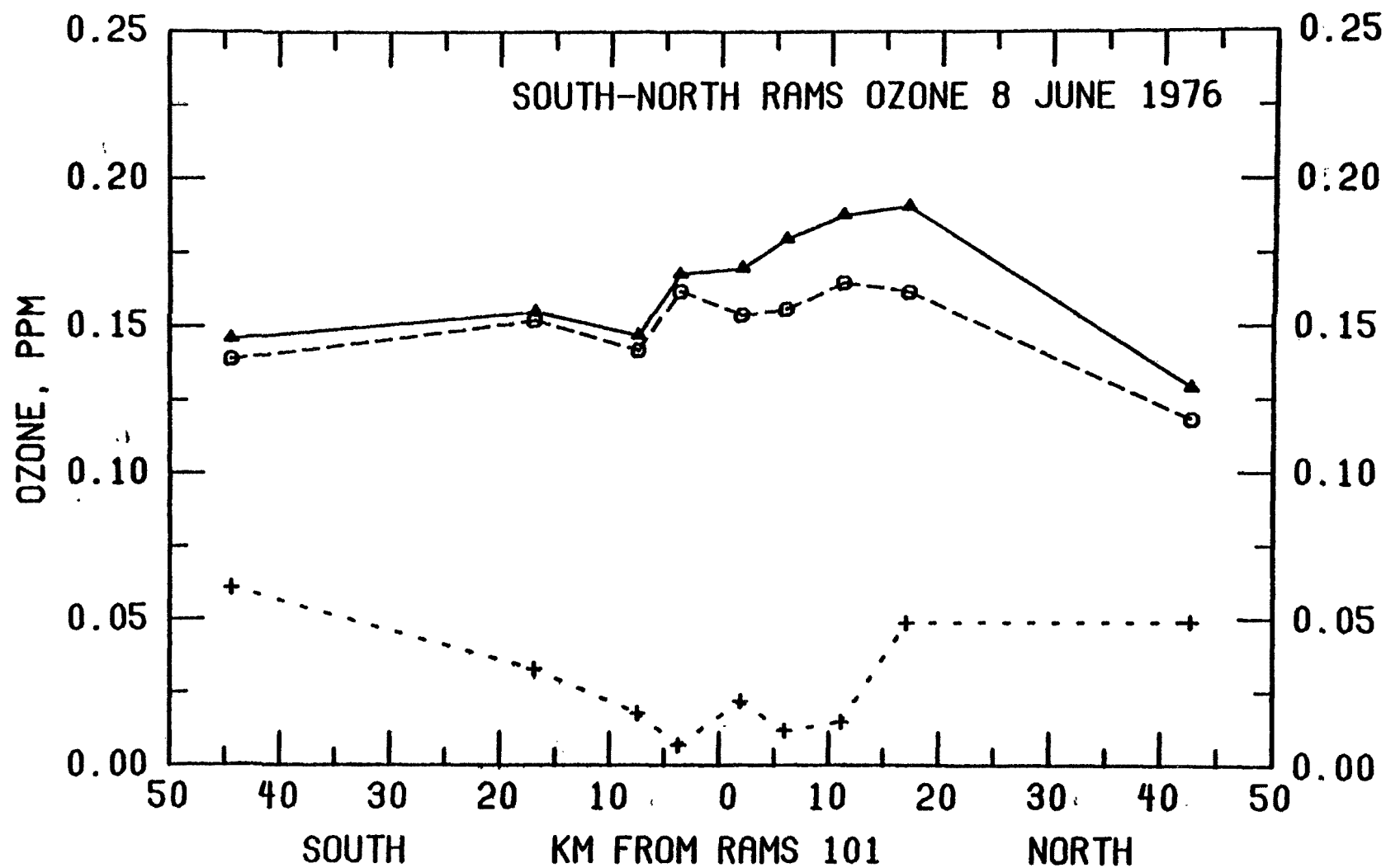


Figure 4. Ozone Distribution Along A South-To-North Cross-Section of St. Louis From 0500 to 0700 CST (+), from 1100 to 1500 CST (o) and for the Maximum Hourly Concentration (Δ) on June 8, 1976.

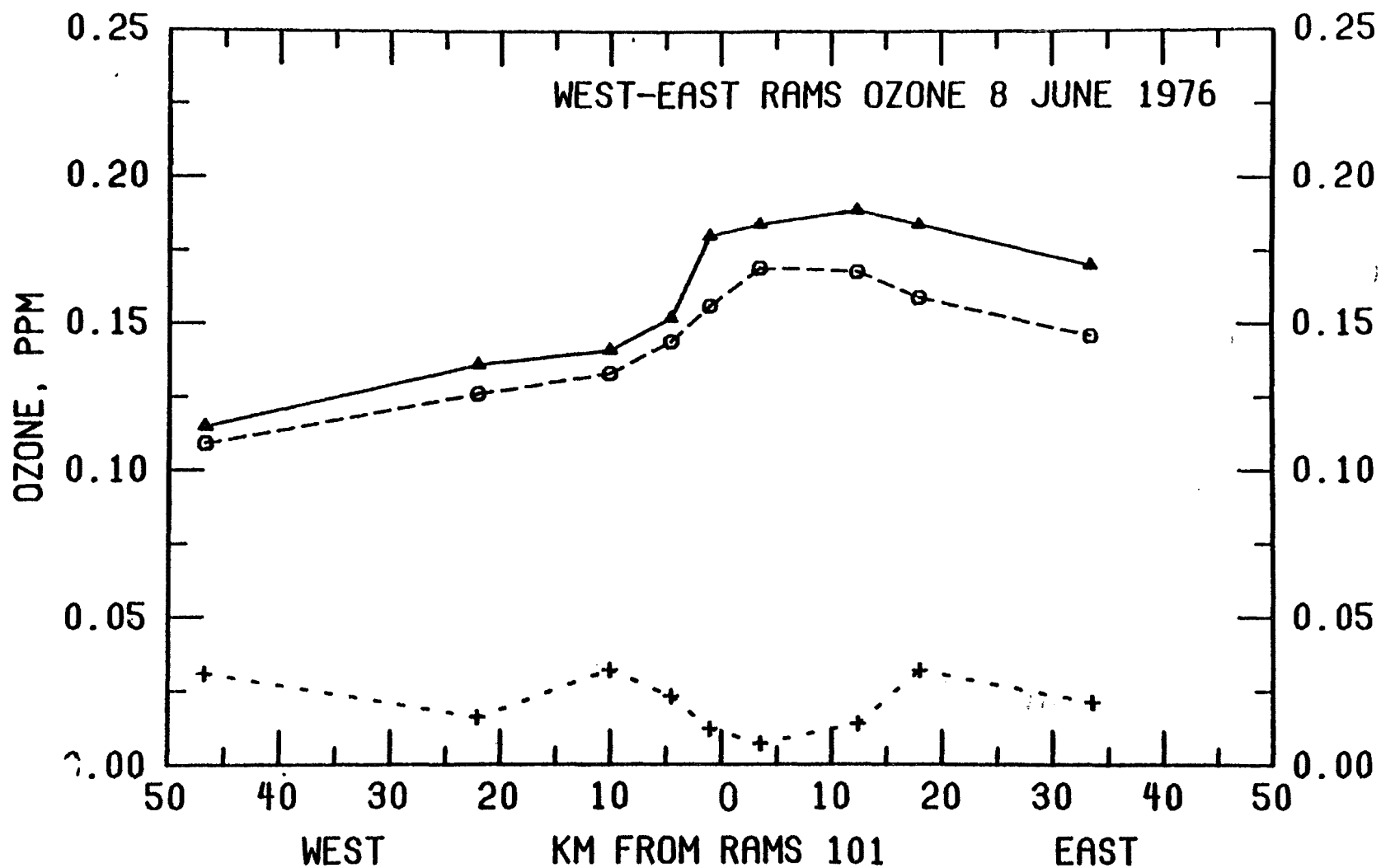


Figure 5. Ozone Distribution Along A West-To-East Cross-Section of St. Louis from 0500 to 0700 CST (+), from 1100 to 1500 CST (o) and for the Maximum Hourly Concentration (Δ) on June 8, 1976.

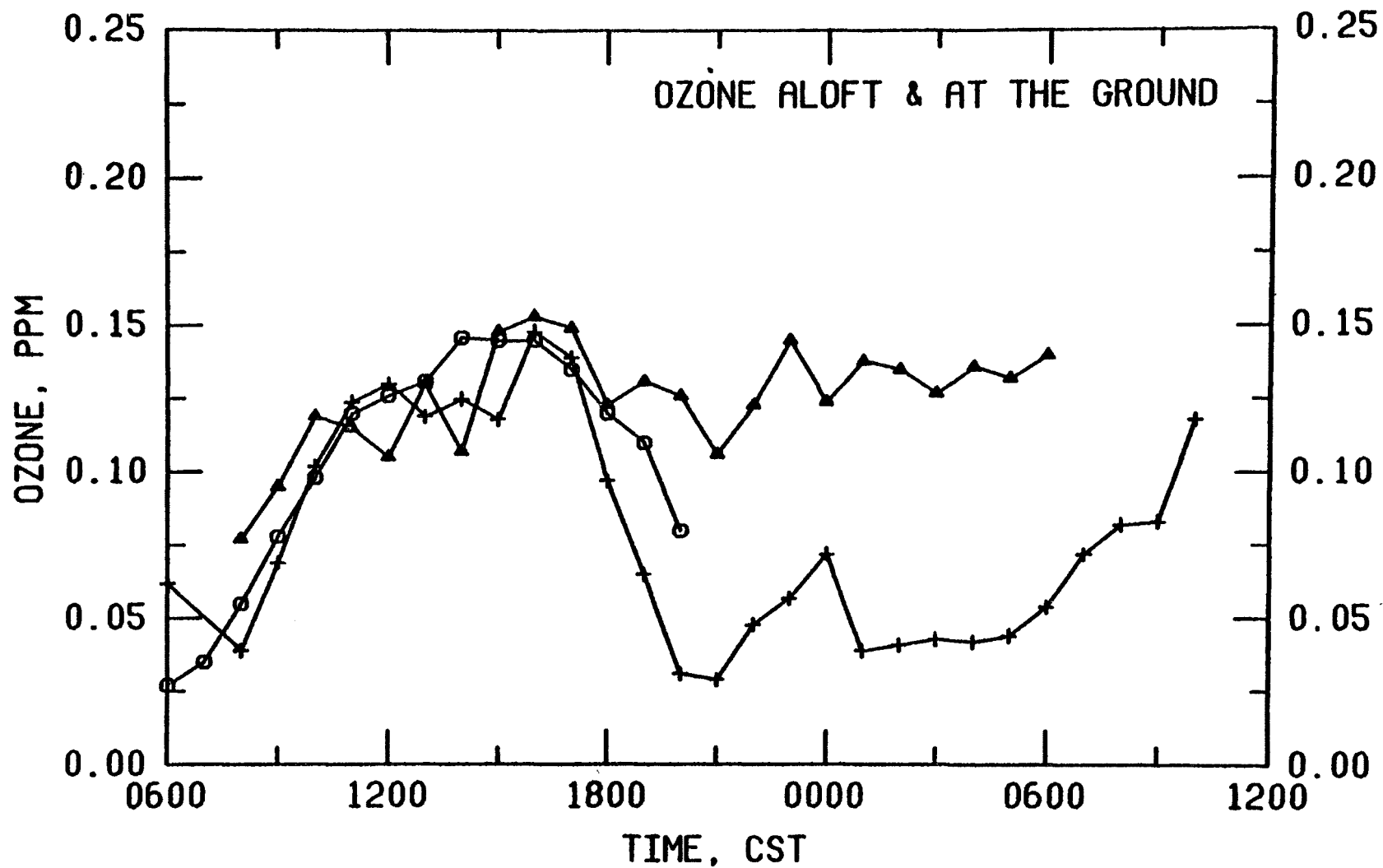


Figure 6. Ozone Concentrations Aloft and on the Ground During the Flight of DaVinci II on June 8-9, 1976. ( $\Delta$  = DaVinci II, + = Mobile Van Underneath DaVinci II and o = Nearest RAMS Station).

On the morning of 9 June, the breakup of the radiation inversion resulted in the downward mixing of transported ozone to the surface. The solar radiation that causes the breakup of the inversion is also instrumental in photochemical processes that generate ozone. Since precursors are emitted at the ground, it is likely that the ozone-generative potential was greater near the ground than aloft. The relative contributions of transport and synthesis to increasing ozone concentrations observed at the ground on the morning of 9 June cannot be separated in this case.

Transported ozone plays several roles in defining air quality within a region. It may be mixed to the ground, enhancing local concentrations; it may hasten additional ozone synthesis by early conversion of NO to NO<sub>2</sub>; or it may modify the ozone-producing potential of a reacting photochemical system in some as yet undefined way.

Modeling results have suggested that when ozone is added to an alkane-NO<sub>2</sub> photochemical system it can act as a net radical source or radical sink depending on the initial HC/NO<sub>2</sub> ratio<sup>9</sup>. These roles are reflected by differences in net ozone production. The impact of "so called" transported ozone on the ozone-generative potential of a photochemically reacting urban mix is an issue that should be addressed. The following questions are particularly relevant and amenable to experimental investigation:

1. What are the effects of adding ozone directly to a nondiluted reacting photochemical HC/NO<sub>x</sub> systems?
2. Is the time of introduction of this ozone important (e.g. at sunrise, at time of NO-NO<sub>2</sub> crossover, at time of [NO<sub>x</sub>]<sub>max</sub>)?
3. Are the effects of added ozone sensitive to initial HC and NO<sub>x</sub> concentrations and their ratios?
4. Under dilution conditions, how does adding ozone to the diluent air influence the maximum ozone concentrations achieved in experiments designed to simulate urban conditions?

It is recommended that the next phase of this research program be directed toward extending the current understanding of the effects of dilution on ozone production and toward defining the effects of transported ozone on ozone production.

## SECTION 4

### EXPERIMENTAL

#### OVERVIEW

This subsection describes the experimental design and provides a general overview of the experiments that were conducted in this study. Detailed descriptions of the smog chamber facility, reagents, measurement methods, data reduction and handling, and procedures are provided in subsequent subsections.

A total of 170 experiments was conducted in the four outdoor smog chambers that comprise the RTI smog chamber facility. Two types of experiments were conducted: those that involved the irradiation of a surrogate urban hydrocarbon mix in the presence of  $\text{NO}_x$  and those that dealt with other chemical systems. The urban mix experiments are identified in Table 2. The current investigation is a continuation of an earlier contract, EPA 68-02-1296<sup>10</sup>. To provide a complete summary of the research program, the 73 urban mix experiments conducted under the current study, EPA 68-02-2207, as well as the 24 urban mix experiments conducted in the earlier study, are identified in Table 2. The data collected during these experiments are tabulated in Appendixes A and B (printed under a separate cover as Volume 2 of this report).

The 73 experiments that did not involve the urban mix are identified in Table 3. These smog chamber runs were comprised of chamber characterization experiments, experiments with low reactivity hydrocarbons, runs designed for comparison with predictions of EPA's photochemical kinetics simulation model, and experiments designed to permit comparison of the behavior of the RTI and UNC outdoor smog chambers. The data collected during these experiments, except for the chamber characterization runs which are summarized in the text, are also listed in Appendixes A and B (Volume 2).

The basic research plan involved the urban mix and called for 3-day smog chamber runs with four different target initial reactant concentrations, four different dilution rates, and three different times at which

TABLE 2. SUMMARY OF EXPERIMENTAL CONDITIONS FOR URBAN MIX RUNS<sup>a</sup>

Starting Date	Time of Initiation of Dilution	Percent <sup>b</sup> Dilution in 24 Hrs	Measured Initial Conditions <sup>c</sup> HC (ppmC)/NO <sub>x</sub> (ppm)				Comments
			Chamber No.				
			1	2	3	4	
7/17/75	Sunrise	95	6.6/0.44 <sup>f</sup>	3.6/.13	3.4/.38	1.2/.06	d
7/22/75	1700	95	11.5/1.0	4.5/.25	4.1/.73	1.8/.11	d
7/28/75	NO-NO <sub>2</sub> Crossover	95	7.0/1.0	4.2/.25	4.0/.77	1.2/.11	d
8/4/75	NO-NO <sub>2</sub> Crossover	77	7.4/1.0	4.4/.24	4.4/.71	1.0/.11	d
8/8/75	NO-NO <sub>2</sub> Crossover	77	5.9/.78	3.5/.37	3.1/.51	0.93/.15	d
8/12/75	Static	0	7.7/1.0	4.3/.24	3.8/.71	1.6/.11	d
8/17/75	1700	77	7.8/.96	4.8/.23	4.8/.69	0.99/.10	e
8/21/75	Sunrise	39	8.7/.91	4.3/.22	4.5/.66	0.98/.10	e
8/27/75	NO-NO <sub>2</sub> Crossover	39	9.2/1.0	4.9/.26	4.1/.73	1.1/.15	e
9/25/75	Sunrise	95	6.4/1.1	3.9/.28	3.7/.80	1.3/.13	
9/29/75	Sunrise	95	10.0/1.0	3.7/.24	5.1/.73	1.2/.10	
10/8/75	Sunrise	39	10.9/.98	3.6/.22	5.3/.70	0.58/.09	
10/14/75	NO-NO <sub>2</sub> Crossover	95	9.7/1.1	3.7/.26	5.4/.80	0.73/.12	Plus NO <sub>x</sub> and HC on Second Day
10/28/75	NO-NO <sub>2</sub> Crossover	95	8.9/.94	3.7/.23	5.3/.69	0.99/.10	Plus NO <sub>x</sub> on Second Day
11/4/75	1700	39	8.9/1.0	3.8/.25	5.4/.74	1.1/.11	
11/18/75	Static	0	5.5/.25				
11/18/75	NO-NO <sub>2</sub> Crossover	77		5.2/.24			
11/18/75	NO-NO <sub>2</sub> Crossover	39			5.3/.24		
11/18/75	NO-NO <sub>2</sub> Crossover	95				4.0/.26	
1/9/76	Static	0			5.6/.34		Winter Run
4/14/76	Sunrise	95	5.7/.84	5.4/.72	4.7/.63	3.5/.63	Plus NO <sub>x</sub> and HC on Second Day in <sup>x</sup> Chambers 1 and 3
4/28/76	Static	0	1.0/.10	0.88/.14	0.92/.10	0.57/.11	Plus NO <sub>x</sub> on Second Day
5/6/76	Static	0	1.1/.40	1.5/.47	1.6/.16	1.8/.05	Plus NO <sub>x</sub> on Second Day
8/4/76	Static	0	3.5/1.1	3.7/1.1	3.3/1.1	4.0/1.1	Preceded by NO Oxidation Run <sup>e</sup>
8/24/76	Static	0	24/1.0	6.2/.74	5.6/.25	2.5/.11	e
9/13/76	Static	0	4.0/1.1	3.1/.72	3.9/.25	--/.11	e
9/23/76	Static	0	7.2/1.1	4.6/.77	3.7/.26	0.71/.11	e
11/11/76	Static	0	12/1.1	6.5/.81	6.4/.27	0.99/.12	Winter Run <sup>e</sup>

<sup>a</sup> Conducted under EPA Contract 68-02-2207, unless noted otherwise; see Volume 2 (Appendixes A and B) for data.

<sup>b</sup> Defined as target percent of initial chamber contents replaced by clean air in the 24-hour dilution period.

<sup>c</sup> Entries denoted by blanks (--) indicate that analyses are not available; unless noted otherwise, HC was determined as NMHC by Beckman 6800.

<sup>d</sup> Conducted under EPA 68-02-1296.

<sup>e</sup> NMHC not available, reported HC is the summation of the individual HC species.

<sup>f</sup> NO<sub>x</sub> concentration is estimated.

TABLE 3. SUMMARY OF EXPERIMENTAL CONDITIONS FOR RUNS NOT INVOLVING URBAN MIX AS REACTANT<sup>a</sup>

Starting Date	Time of Initiation of Dilution	Percent <sup>b</sup> Dilution in 24 Hrs	Measured Initial Conditions <sup>c</sup> HC (ppmC)/NO <sub>x</sub> (ppm)				Comments
			Chamber No.				
			1	2	3	4	
7/10/75	Static	0	0.10/.001	0.04/.001	0.16/0.0	0.24/0.0	Purified Air Irradiation <sup>d,e,f</sup>
7/11/75	Static	0	0.06/.63	0.0/.67	0.02/.62	0.02/.68	NO Oxidation <sup>d,e,f</sup>
8/1/75	Static	0	--/0.0	--/0.0	--/.001	--/.001	O <sub>3</sub> Decay <sup>d,f</sup>
1/9/76	Static	0	.35/.010				Purified Air Irradiation <sup>e,f</sup>
1/9/76	Static	0		.96/.53			Propene Run <sup>e</sup>
1/9/76	Static	0				.34/.69	NO Oxidation <sup>e,f</sup>
4/6/76	Static	0		0.0/.006	.01/.006		Purified Air Irradiation <sup>e,f</sup>
4/23/76	Static	0	.056/.001	--/.001	.065/.001	.007/.001	Purified Air Irradiation <sup>f</sup>
4/25/76	Static	0	--/--	--/--	--/--	--/--	O <sub>3</sub> Decay <sup>f</sup>
6/24/76	Static	0	.16/--				Purified Air Irradiation <sup>f</sup>
6/24/76	Sunrise	95		.039/--	.073/--	.063/--	Purified Air Irradiation <sup>f</sup>
6/25/76	Static	0	--/--				Purified Air Irradiation <sup>f</sup>
6/25/76	Sunrise	95		--/--	--/--	--/--	Purified Air Irradiation <sup>f</sup>
8/3/76	Static	0	.02/1.0	.03/1.0	.01/1.0	.02/1.1	NO Oxidation <sup>f</sup>
8/28/76	Static	0	--/.02	--/.02	--/.02	--/.02	Purified Air Irradiation <sup>f</sup>
9/8/76	Static	0	6.9/.17				Ethane
9/8/76	Static	0		12/.18			Propane
9/8/76	Static	0			5.6/.16		Acetylene
9/8/76	Static	0				.07/.17	Control (NO <sub>x</sub> added)
9/17/76	Static	0	--/.82	--/.82	--/.77	--/.80	NO Oxidation <sup>x,f</sup>
9/20/76	Static	0	10.2/.21	11.1/.22	11.3/.21	10.3/.20	RTI/UNC Comparison, Propane
10/1/76	Static	0	--/--	--/--	--/--	--/--	O <sub>3</sub> Decay <sup>f</sup>
10/6/76	Static	0	1.3/.14	.64/.52	1.2/.53		Runs for EPA Model, Propene
10/6/76	Static	0				.023/.10	Runs for EPA Model, Control
10/11/76	Static	0	.68/1.6	2.4/1.7	1.3/.55	1.2/.50	Runs for EPA Model, Propene
10/27/76	Static	0	5.5/.10	10/.22	3.1/.056		Propene
10/27/76	Static	0				.01/.056	Control (NO <sub>x</sub> added)
11/5/76	Static	0	1.7/.55	3.3/.56			RTI/UNC Comparison, Propene
11/5/76	Static	0			2.6/.05	2.8/.047	Propene

<sup>a</sup> Conducted under EPA Contract 68-02-2207, unless specified otherwise; see Volume 2 (Appendixes A and B) for data.

<sup>b</sup> Defined as percent of initial chamber volume replaced by clean air in the 24-hour dilution period.

<sup>c</sup> Entries denoted by blanks (--) indicate that analyses are not available; unless noted otherwise, HC was determined as individual HC species or sum of these species.

<sup>d</sup> Conducted under EPA 68-02-1296.

<sup>e</sup> Determined as NMHC by Beckman 6800.

<sup>f</sup> Chamber characterization experiment; results of these experiments are summarized in text and are NOT listed in Appendixes.

dilution was to have been initiated. Dilution of chamber contents with purified air was employed to simulate atmospheric transport conditions. Static operation (no dilution) was used to simulate stagnation conditions. Following reactant injection, each experiment was begun in the static mode and, if the experimental design called for simulated transport, dilution was initiated on the first day at one of three times: sunrise, NO-NO<sub>2</sub> cross-over, or 1700 EST. One of four target dilution rates was employed such that 95, 77, 39, or 0 percent of a tracer present at the start of dilution would have been removed by the end of the 24-hour dilution period. Dilution was terminated 24 hours after it had been initiated. The chamber was then operated in the static mode until the experiment was terminated at 1700 EST on the third day. Target initial conditions called for initial HC/NO<sub>x</sub> ratios between 7 and 20 with the initial [NMHC] of 1 to 10 ppmC and the initial [NO<sub>x</sub>] (20 percent NO<sub>2</sub>) of 0.1 to 1.0 ppm. The target experimental conditions and the dates on which the corresponding experiments were conducted are identified in Table 4.

#### RTI SMOG CHAMBER FACILITY

The Research Triangle Institute Smog Chamber Facility consists of four cylindrically shaped smog chambers. Each chamber has a surface area of 51 m<sup>2</sup>, a volume of 27 m<sup>3</sup>, and a surface-to-volume ratio of 1.9 m<sup>-1</sup>. Figure 7 illustrates the general design. The chambers are located outdoors, and irradiation is provided by natural sunlight. The walls are fabricated from 0.13-mm thick (5 mil) fluorinated ethylene propylene (FEP) Type A Teflon<sup>®</sup> film. The Teflon walls are supported by an interior aluminum framework. The floors are 0.25 mm (10 mil) thick FEP Teflon film laid over a reflective layer of aluminum foil, which serves to raise the light intensity within the chambers and thus compensate for transmission losses through the walls. Mixing in each chamber is provided by a 0.45-m diameter aluminum fan blade on a shaft that is driven at 345 RPM by a 185-W (1/4 hp) motor using a belt-pulley system.

In addition to the chambers proper, provisions were made for air purification, reactant injection, and sample collection with subsequent instrumental and wet chemical analyses. The overall system is illustrated in Figure 8.



TABLE 4. BASIC RESEARCH PROGRAM

Time of Initiation of Dilution	Target Dilution (%)	Target Initial Reactant Concentrations HC/NO <sub>x</sub> (ppmC/ppm)				Starting Date of Experiment
		Chamber 1	Chamber 2	Chamber 3	Chamber 4	
Static	0	10/1.0	5.0/0.24	5.0/0.71	1.0/0.10	8-12-75 <sup>a</sup>
	0	5.0/0.24				11-18-75 <sup>b</sup>
	0	10/1.0	5.0/0.24	5.0/0.71	1.0/0.10	8-4-76
	0	10/1.0	5.0/0.24	5.0/0.71	1.0/0.10	8-24-76
	0	10/1.0	5.0/0.24	5.0/0.71	1.0/0.10	9-13-76
	0	10/1.0	5.0/0.24	5.0/0.71	1.0/0.10	9-23-76
Sunrise	39	10/1.0	5.0/0.24	5.0/0.71	1.0/0.10	8-21-75 <sup>a</sup>
	39	10/1.0	5.0/0.24	5.0/0.71	1.0/0.10	10-8-75
	95	10/1.0	5.0/0.24	5.0/0.71	1.0/0.10	7-17-75
	95	10/1.0	5.0/0.24	5.0/0.71	1.0/0.10	9-25-75
	95	10/1.0	5.0/0.24	5.0/0.71	1.0/0.10	9-29-75 <sup>a</sup>
Crossover	39	10/1.0	5.0/0.24	5.0/0.71	1.0/0.10	8-27-75 <sup>a</sup>
	39			5.0/0.24		11-18-75 <sup>b</sup>
	77	10/1.0	5.0/0.24	5.0/0.71	1.0/0.10	8-4-75 <sup>a</sup>
	77	10/1.0	5.0/0.24	5.0/0.71	1.0/0.10	8-8-75
	77		5.0/0.24			11-18-75 <sup>b</sup>
	95	10/1.0	5.0/0.24	5.0/0.71	1.0/0.10	7-28-75 <sup>a</sup>
	95				5.0/0.24	11-18-75 <sup>b</sup>
1700	39	10/1.0	5.0/0.24	5.0/0.71	1.0/0.10	11-4-75 <sup>a</sup>
	77	10/1.0	5.0/0.24	5.0/0.71	1.0/0.10	8-17-75 <sup>a</sup>
	95	10/1.0	5.0/0.24	5.0/0.71	1.0/0.10	7-22-75 <sup>a</sup>

<sup>a</sup>Experiments considered in the analysis of individual experiments.<sup>b</sup>Multiple dilution experiment.

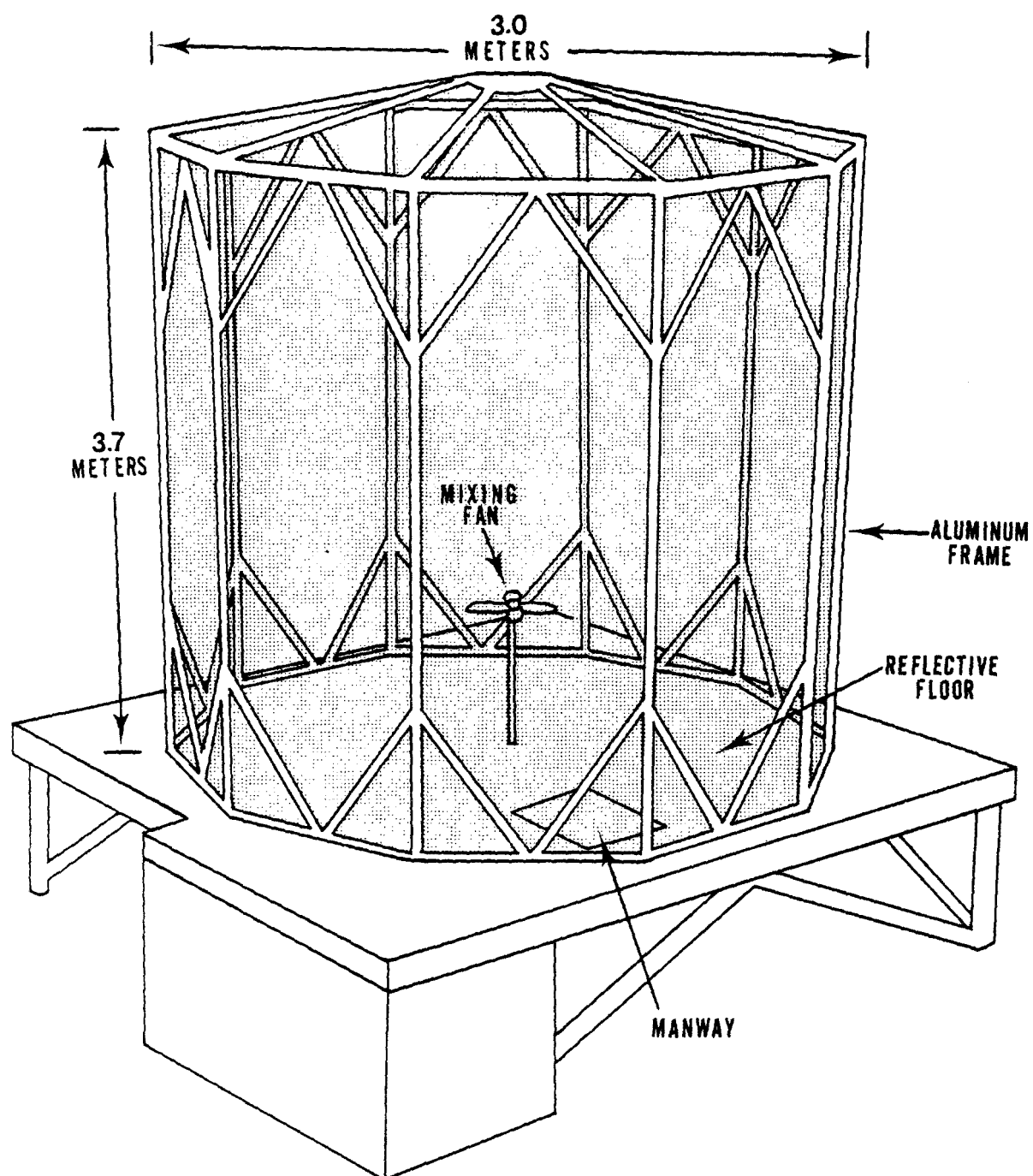


Figure 7. General Design of RTI Outdoor Smog Chambers.

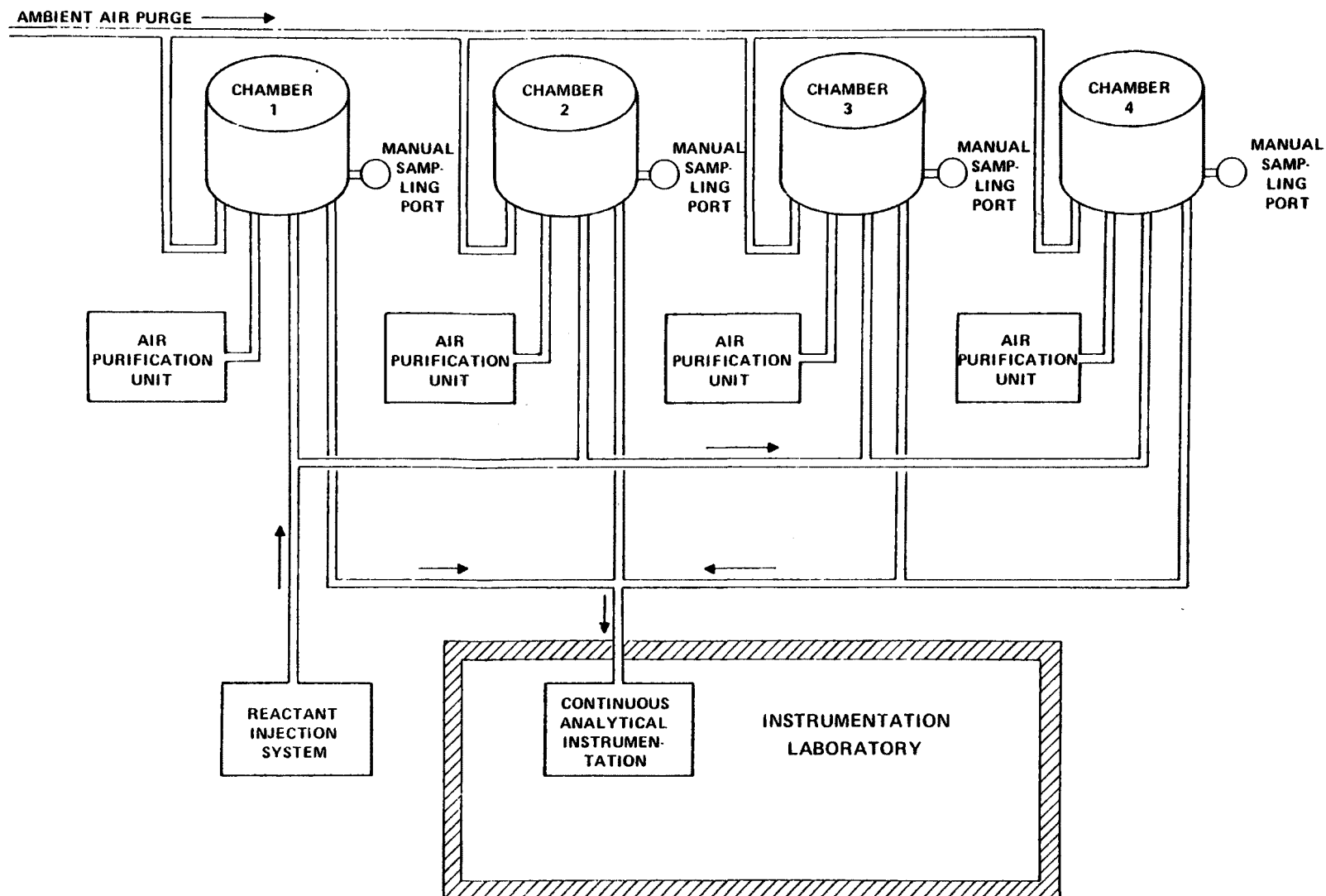


Figure 8. Overall System Design of RTI Smog Chamber Facility.

## Air Purification Unit

Details of the air purification unit are shown in Figure 9. This unit has three modes of operation: purge, cleanup, and dilution.

During the purge mode, air is supplied by a blower from a 10-m tower. By opening a manway in the floor and allowing the tower blower to force air through each chamber, purge flow rates of up to  $2.3 \text{ m}^3 \text{ min}^{-1}$  are attained.

After purging with ambient air, the chambers are sealed, and air is recirculated through the purification unit in the cleanup mode. The purification unit contains the following equipment:

1. Desiccant column (6.5 kg of 4A molecular sieves);
2. Two HEPA particle filters;
3. Heated catalyst column (5 kg of 0.5 percent Pd on alumina catalyst; operating temperature:  $200\text{-}475^\circ \text{C}$ );
4. Air cooler;
5. Purafil<sup>®</sup> column (6.5 kg of Purafil for  $\text{NO}_x$  and  $\text{O}_3$  removal); and
6. Humidifier.

Solenoid-driven valving allows the inclusion or exclusion of this equipment as may be appropriate in achieving desired experimental conditions. In this study, items 2, 3, 4, and 5 were included for the cleanup and dilution operations. The purification or "cleanup" operation requires 8 to 12 hours at a flow rate of approximately  $0.28 \text{ m}^3 \text{ min}^{-1}$ . Pollutant removal efficiency of the purification unit is discussed in a subsequent subsection.

To effect dilution, the chamber contents are recirculated through the purification unit at flow rates corresponding to the desired dilution rate. Flow rates for this operation mode between  $0.0085$  and  $0.058 \text{ m}^3 \text{ min}^{-1}$  are employed for 24 hours to simulate between 39 and 95 percent dilution. Of course, the purification unit was not employed (zero flow rate) to simulate static conditions.

## Reactant Injection System

A schematic of the reactant injection system is seen in Figure 10. There are three injection manifolds from cylinders of compressed gases. The flow rates are controlled by calibrated fine metering valves, and the quantity of each injection is controlled by timed, manual operation of the appropriate solenoid valves. The hydrocarbon mix, toluene, and carbon

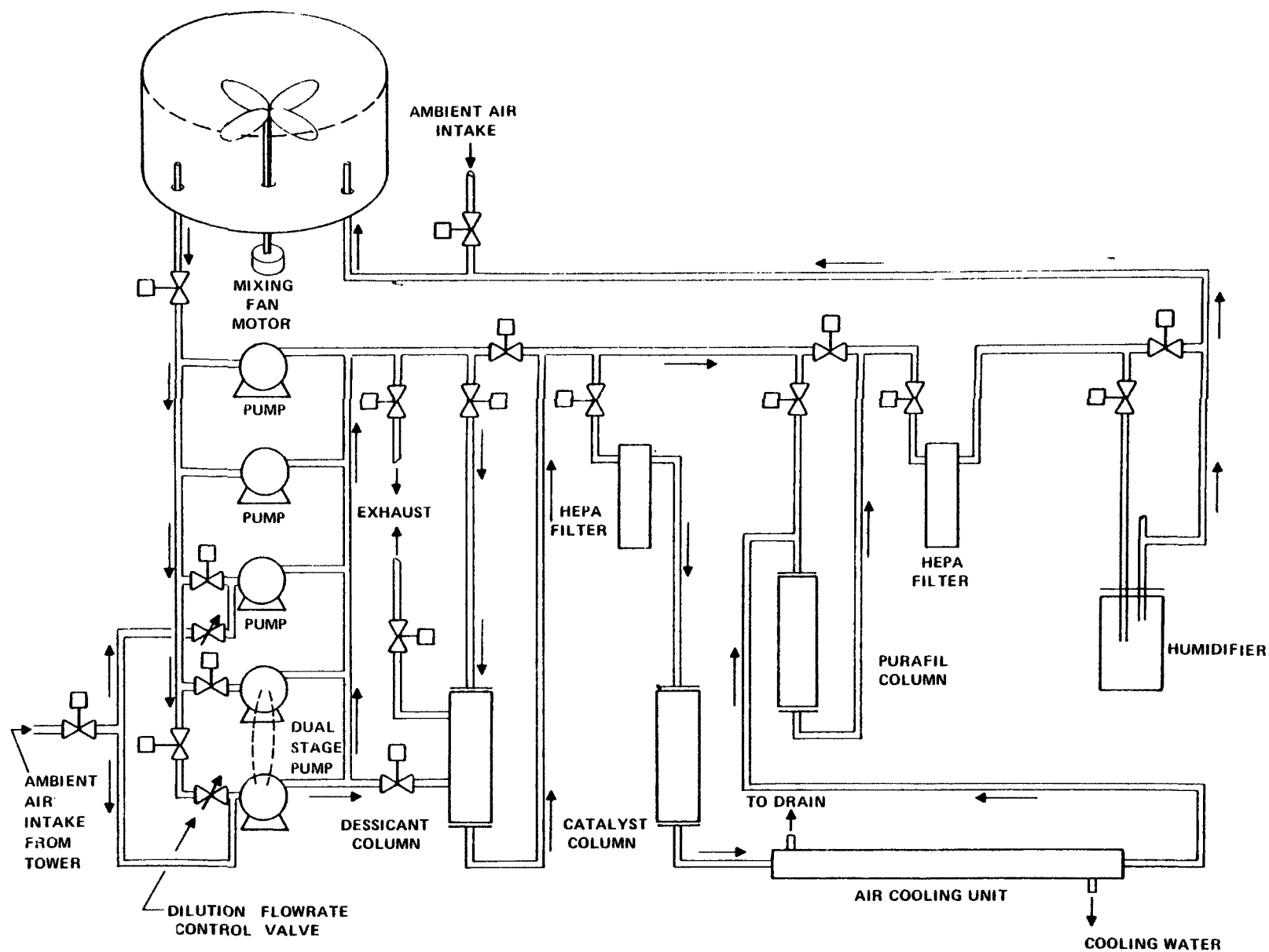


Figure 9. Air Purification Unit for RTI Smog Chamber Facility.

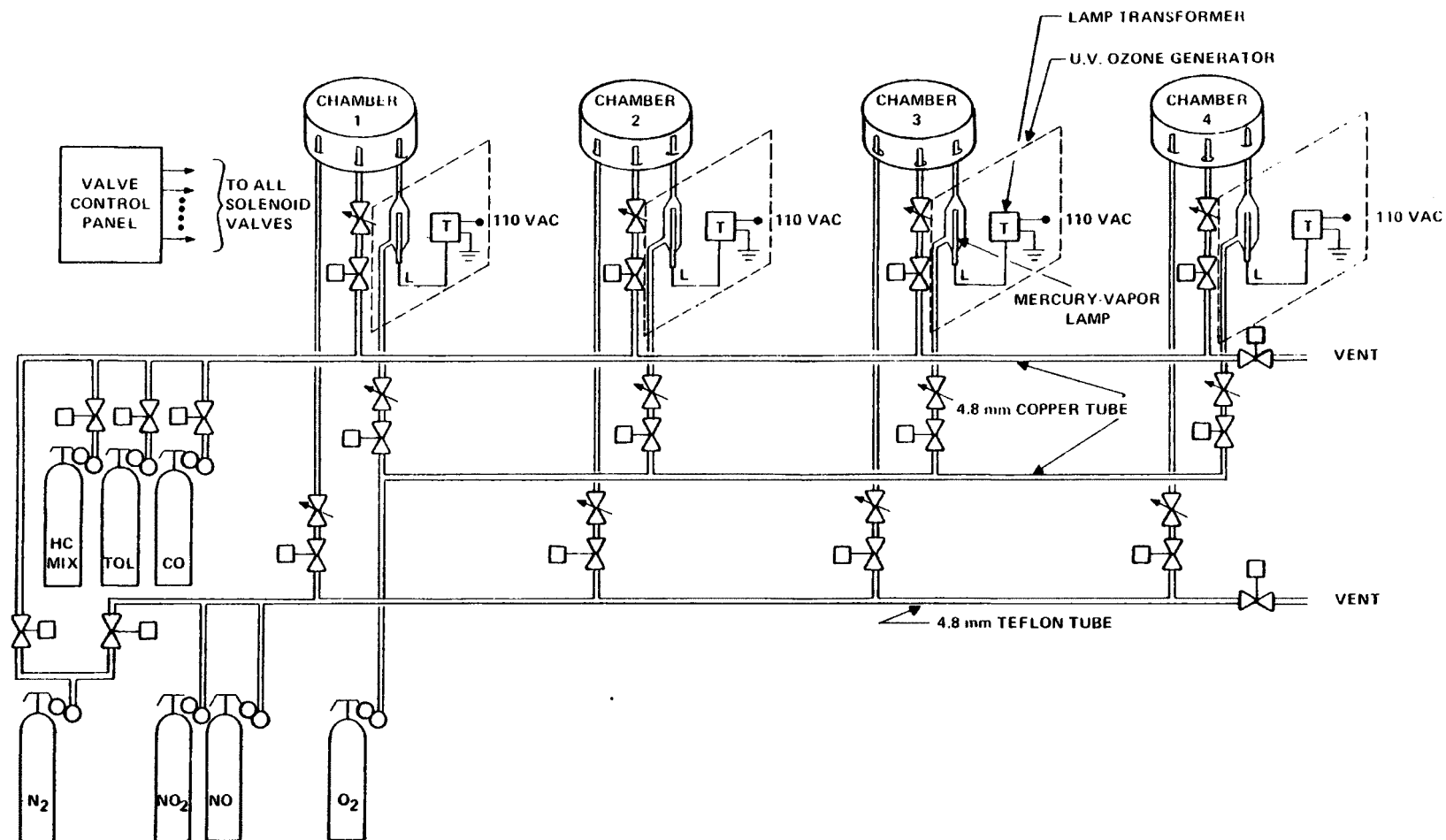


Figure 10. Reactant Injection System for RTI Smog Chamber Facility.

monoxide (CO) are injected sequentially from a copper manifold. Nitric oxide and NO<sub>2</sub> are injected sequentially from a Teflon manifold. Ozone may be added by injecting O<sub>2</sub> from a copper manifold through an O<sub>3</sub> generator, located at each chamber; this feature was employed in O<sub>3</sub> decay experiments. After the reactants have been injected, each of the manifolds is flushed with nitrogen.

### Sampling System

The sampling system is illustrated in Figure 11. An automatic timer activates the appropriate sampling solenoid valves and provides for a 10-minute sample from each chamber once per hour. During the remaining 20 minutes of each hour, the instruments sample ambient air from the 10-m tower, they are used to analyze bag samples, or they are calibrated.

The sampled air must pass from a chamber to the laboratory through lengths of 4.8-mm ID TFE Teflon tubing that range from 26 to 48 m, depending on the chamber. The sample is drawn at a flow rate of 0.005 m<sup>3</sup> min<sup>-1</sup> (5 lpm) by a Metal-Bellows pump located in the laboratory. A Metal-Bellows MB-21 was used until 11 September 1975, and an MB-41 was used thereafter. The sample is delivered to a glass manifold from which the instruments draw their samples. The residence time in the sampling line is less than 10 seconds. The instruments include an O<sub>3</sub> analyzer, a NO-NO<sub>2</sub>-NO<sub>x</sub> analyzer, and an environmental chromatograph and have a total volumetric flow requirement of 0.003 m<sup>3</sup> min<sup>-1</sup> (3 lpm).

In addition to the automated sampling system described above, a 1-m long, 4.8-mm ID FEP Teflon tube is located under each chamber for periodic manual grab sampling. Wet bubbler samples for oxidant, NO<sub>2</sub>, and formaldehyde (HCHO) determinations are collected at this location. Samples for individual hydrocarbon analyses are also collected at this point in 10-liter Tedlar<sup>®</sup> bags. These samples are drawn through the 1-m long sampling tube with a Metal-Bellows MB-41 pump and exhausted into the Tedlar bags. Typically, grab samples were collected manually twice a day from each chamber (see Appendixes A and B for exact times).

### Smog Chamber Operating Characteristics

Operating characteristics of the chambers comprising the RTI Smog Chamber Facility are documented in the following paragraphs. This informa-

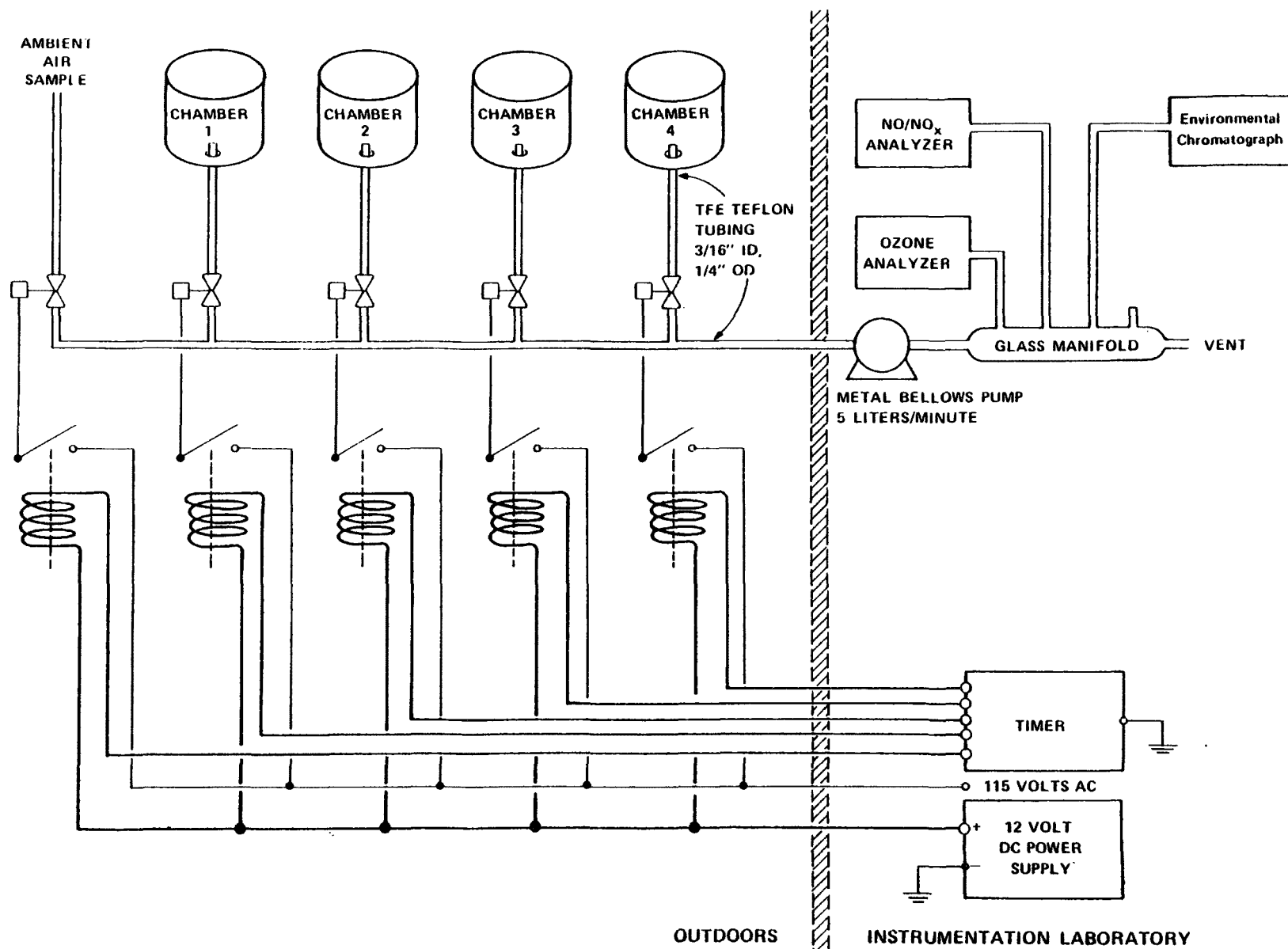


Figure 11. Sampling System for RTI Smog Chamber Facility



tion is reported to provide a basis for assessing the performance of the RTI chambers and to permit comparison with other chambers.

#### Mixing--

As noted earlier, mixing in each chamber is provided by a fan designed for that purpose. Unless specified otherwise, the fan operated continually during each experiment.

Air velocity measurements have been conducted within each chamber. The minimum air velocity was measured to be greater than  $0.05 \text{ m sec}^{-1}$  within 0.02 m of the floor. Air velocities increased with distance from the walls to a maximum that was greater than  $4.0 \text{ m sec}^{-1}$  near the moving fan blade.

If a smog chamber can be considered to be an agitator-stirred tank, then a published relationship can be used to estimate the time required for complete mixing.<sup>11</sup> This procedure indicates that the mixing of an injected gas should be 90 percent complete within 24 seconds and 99 percent complete within 43 seconds after injection.

#### Performance of Air Purification System--

The air purification system routinely reduces the  $\text{NO}_x$  content of the purified air to a measured zero (minimum detectable concentration [MDC]: 0.005 ppm). The catalytic hydrocarbon oxidation system typically reduces  $\text{C}_2$  to  $\text{C}_{10}$  hydrocarbons measured by gas chromatography to less than 20 ppbC (MDC: 0.1 ppb [v/v]). Typical "postcleanup" hydrocarbon levels minus the ethane + ethene and the toluene components are shown in Table 5 for each chamber. The correction was made because of possible sampling line and bag contamination. This point is discussed in detail in a subsequent subsection (see "Individual Hydrocarbons").

#### Chamber Tightness--

Exchange of chamber contents with the ambient atmosphere is expected. Chamber leaks may be attributed to replacement of the volume required by sampling and to chamber "breathing" caused by diurnal temperature variations and buffeting by winds. The sampling flow rate of  $0.005 \text{ m}^3 \text{ min}^{-1}$  for 10 minutes per hour corresponds to a loss coefficient of  $0.002 \text{ hr}^{-1}$  or dilution of 5 percent in 24 hours.

TABLE 5. HYDROCARBON CONCENTRATIONS IN THE RTI SMOG CHAMBERS  
FOLLOWING AIR CLEANUP OPERATIONS

Date	[HC] <sup>a</sup> , ppmC			
	Chamber No. 1	Chamber No. 2	Chamber No. 3	Chamber No. 4
8-17-75	0.012	0.002	0.008	0.014
8-27-75	0.009 <sub>b</sub>	0.008	0.013	0.050
9-4-75	_____	0.005	0.006	_____
9-29-75	0.007	0.009	0.016	_____
11-18-75	0.038	0.057	0.008	0.074
4-23-76	0.023	_____	0.015	0.002
6-24-76	0.039	0.011	0.018	0.016
8-3-76	0.008	0.011	0.004	0.009
8-24-76	0.009	0.009	0.010	0.008
9-23-76	0.002	0.017	0.004	0.020
10-6-76	0.010	0.018	0.003	0.001
10-11-76	0.006	0.017	0.011	0.023
10-14-76	0.013	0.035	0.006	0.010
10-27-76	0.043	0.009	0.004	0.008
11-1-76	0.010	0.034	0.023	0.019
11-5-76	0.003	0.018	0.015	0.011
11-11-76	0.008	0.030	0.031	0.030

<sup>a</sup>[HC] is summation of concentrations of individual C<sub>2</sub> to C<sub>10</sub> hydrocarbon species less ethane + ethene and toluene.

<sup>b</sup>Blanks indicate that no analysis is available.

To quantify chamber leakage, first order leak rate coefficients were estimated by least squares regressions of  $\ln$  [tracer] versus time data. During the course of the current experimental program CO, NO<sub>x</sub>, and Freon-12<sup>®</sup> were used as tracers to assess chamber leakage. Results from these experiments are summarized in the portion of Table 6 that corresponds to a target 24-hour dilution of zero.

Most of the experiments in the basic research program shown in Table 4 had been completed between June 1975 and the end of April of 1976. The mean leak rate coefficient across all four chambers during this period is  $0.008 \pm 0.004 \text{ hr}^{-1}$ .

Based on the results in Table 6, chamber 2 had the lowest leak rate, chambers 4 and 1 had slightly higher leak rates, and chamber 3 had the highest value. The leak rate coefficient in each chamber generally increased between June 1975 and January 1977. They ranged from approximately  $0.005 \text{ hr}^{-1}$  to greater than  $0.015 \text{ hr}^{-1}$  which correspond to dilutions of 11 to 30 percent in 24 hours. The increased leakage over the intervening 19-month period is due to weathering caused by continuous exposure of the chambers to "the elements."

As noted earlier, sample replacement corresponds to a leak rate coefficient of  $0.002 \text{ hr}^{-1}$ . If  $0.010 \text{ hr}^{-1}$  is taken to be typical for the current program, then environmental factors account for most of the leakage. Many of the leak coefficients listed in Table 6 for the 0 dilution condition were determined from data collected over one or more 24-hour periods. Although the data reflecting this behavior are not presented in this report, leak rate coefficients exhibit diurnal cycles that correspond qualitatively with wind speed. Daytime leak rate coefficients exceeded nighttime values by from 50 to as much as 200 percent.

Initially, the leak rates for the RTI chambers were approximately  $0.005 \text{ hr}^{-1}$ . The Teflon chamber walls were replaced in May of 1977, and leak rate coefficients were redetermined with Freon-12 as the tracer. Values of 0.004, 0.005, 0.004 and  $0.004 \text{ hr}^{-1}$  were again found. These leak rate coefficients as well as those listed in Table 6 agree well with the  $0.01 \text{ hr}^{-1}$  value reported for the newly constructed UNC outdoor chambers.<sup>12</sup> Concentration data in the present study were not adjusted for dilution.

TABLE 6. DILUTION IN RTI SMOG CHAMBERS

Date	Target Dilution	Dilution Coefficients <sup>a</sup>			
		Chamber 1	Chamber 2	Chamber 3	Chamber 4
7/17/75	95 <sup>b</sup>	0.1437	0.1687	0.1635	0.1747
7/22/75	95	0.1428	0.1655	0.1530	0.1724
7/28/75	95	0.1467	0.1797	0.1695	0.1839
9/25/75	95	0.1334	0.1462	0.1542	0.1583
9/29/75	95	0.1333	0.1460	0.1527	0.1543
10/14/75	95	0.1285	0.1500	0.1511	0.1922
10/28/75	95	0.1040	0.1156	0.1190	0.1190
11/18/75	95	--	--	--	0.1527
4/14/76	95	0.1251	0.1205	0.1344	0.1354
6/24/76	95	--	0.1327	0.1518	0.1612
8/4/75	77 <sup>c</sup>	0.0868	0.0969	0.103	0.0933
8/8/75	77	0.0829	0.0965	0.0960	0.0899
8/17/75	77	0.0793	0.0859	0.0848	0.0775
11/18/75	77	--	0.0957	--	--
8/21/75	39 <sup>d</sup>	0.0539	0.0547	0.0506	0.0347
8/27/75	39	0.0214	0.0446	0.0235	0.0413
10/8/75	39	0.0439	0.0360	0.0748	0.0320
11/4/75	39	0.0221	0.0334	0.0300	0.0296
11/18/75	39	--	--	0.0309	--
7/11/75	0 <sup>e</sup>	--	--	0.0082	0.0089
8/13,14/75	0	0.0022	0.0025	0.0072	0.0072
8/17/75	0	--	--	--	0.0079
11/4/75	0	0.0113	--	0.0153	0.0137
11/18,19,20/75	0	0.0037	--	--	--
1/9,10,11/76	0	0.0056	0.0031	0.0058	0.0065
1/9,10,11/76	0 <sup>e</sup>	--	--	--	0.0109
4/28,29,30/76	0	0.0080	0.0063	0.0134	0.0089
5/6,7,8/76	0	0.0114	0.0085	0.0228	0.0104
6/24/76	0	0.0170	--	--	--
8/3/76	0 <sup>e</sup>	0.0164	0.0076	0.0213	0.0123
9/17,18/76	0 <sup>e</sup>	0.0143	0.0134	0.0201	0.0129
12/16,17,18,19/76	0 <sup>f</sup>	0.0131	0.0072	0.0191	0.0082
12/20,21,22/76	0 <sup>f</sup>	0.0205	0.0160	0.0270	0.0141
1/13/77	0 <sup>f</sup>	0.0227	0.0089	0.0183	0.0110

<sup>a</sup>First order loss coefficient as determined from the slope of least squares regression of  $\ln_{-1}[\text{tracer}]$  versus time data; unless noted otherwise the tracer is CO; units:  $\text{hr}^{-1}$ .

<sup>b</sup>The target dilution coefficient required to achieve 95 percent dilution in 24 hours is  $0.125 \text{ hr}^{-1}$ .

<sup>c</sup>The target dilution coefficient required to achieve 77 percent dilution in 24 hours is  $0.061 \text{ hr}^{-1}$ .

<sup>d</sup>The target dilution coefficient required to achieve 39 percent dilution in 24 hours is  $0.021 \text{ hr}^{-1}$ .

<sup>e</sup> $\text{NO}_x$  is the tracer.

<sup>f</sup>Freon-12 is the tracer.

## Dilution--

Target recirculation flow rates through the purification unit that were employed in this study are 0.058, 0.029, 0.010, and 0.0 m<sup>3</sup> min<sup>-1</sup>. These rates correspond to target 24-hour dilution rates of 95, 77, 39, and 0 percent and may be interpreted to mean that, after 24 hours of operation, 95, 77, 39, or 0 percent of a tracer present at the start of dilution would have been removed. A manual control valve is used to set the recirculation flow rate through the purification unit. The valve setting is established manually prior to each run in which dilution is to be employed.

To quantify the dilution for each experiment, first order dilution coefficients were estimated, using CO as a tracer, by least squares regressions of ln [CO] versus time data. These estimates are summarized in Table 6, and should be considered by those who desire to model individual experiments by computer simulation.

The actual dilution rates are subject to losses due to sample replacement, to chamber leakage, and to leakage by the air purification system during dilution operations. Since the target recirculation flow rates were set without regard for these factors, the actual dilution rates are generally greater than the target values.

Freon-12 tracer experiments conducted at the highest dilution rate (95 percent) in December 1976 and January 1977 suggest that a significant portion, perhaps half of the dilution air volume, was ambient air rather than air that had been completely recirculated through the air purification system. This is considered to be a worst case estimate, and the ambient air fraction is expected to be much lower at the lower dilution rates.

A target 24-hour dilution of 95 percent corresponds to a dilution coefficient of 0.125 hr<sup>-1</sup>. The mean of the measured dilution coefficients across all four chambers is 0.148 ± 0.002 hr<sup>-1</sup> and corresponds to a 24-hour dilution of 97 percent.

At a target 24-hour dilution of 77 percent the dilution coefficient is 0.061 hr<sup>-1</sup>, while the mean of the measured values is 0.090 ± 0.008 hr<sup>-1</sup>. This corresponds to an actual 24-hour dilution of 88 percent.

The target 24-hour dilution of 39 percent corresponds to a dilution coefficient of 0.021 hr<sup>-1</sup>. The mean of the measured dilution coefficients is 0.039 ± 0.014 hr<sup>-1</sup> and corresponds to a 24-hour dilution of 61 percent.

As discussed in the previous subsection, chamber leakage and sample replacement account for dilution of the chamber contents under zero dilution conditions. A dilution coefficient under these conditions of  $0.010 \text{ hr}^{-1}$  is considered typical for the current program and corresponds to an actual 24-hour dilution of 21 percent.

The target dilution rates were arbitrarily chosen to permit the investigation of the photochemical ozone production by HC-NO<sub>x</sub> systems under a variety of simulated transport conditions. The average measured 24-hour dilution rates of 97, 88, 61, and 21 percent offer a reasonable spread of experimental conditions for examining the effects of simulated transport. The discrepancies between the target and measured dilution rates are therefore of little consequence in achieving this objective.

#### Sample Line Losses--

The most distant chamber is 48 m from the instruments in the laboratory. When NO, NO<sub>2</sub>, and O<sub>3</sub> are present in a chamber during periods of irradiation, a small reduction of NO and O<sub>3</sub> and a slight increase in NO<sub>2</sub> may occur in the dark sample line due to the dark-phase reaction of NO and O<sub>3</sub>.<sup>13</sup> In view of the short residence time (10 seconds), this contribution should be small in most cases, and the data were not corrected for these effects.

The sampled air volume must pass through a considerable length of sampling line (26 to 48 m) and a pump before it is delivered to the instruments for analysis. Sample modification is therefore expected. A 20 percent loss of ozone between the chambers and laboratory was reported on contract EPA 68-02-1296.<sup>10</sup> A thorough investigation of sampling line loss rates was conducted on the current contract and has shown the initially reported loss rate to be in error. In this study, single-component mixtures of air and O<sub>3</sub>, NO, and NO<sub>2</sub> were prepared in Teflon bags at 3 to 5 concentrations ranging between 0.08 and 1.0 ppm. Concentrations were determined by sampling each bag directly at the instrument in the laboratory. Next, concentrations were determined by connecting the bag to the sampling line located within each chamber and by sampling in the usual manner. Sampling line losses for O<sub>3</sub>, NO, and NO<sub>2</sub> were found to be less than 1 percent and to be independent of concentration. The O<sub>3</sub>, NO, and NO<sub>2</sub> data reported in Appendix B for EPA 68-02-1296 and EPA 68-02-2207 were therefore not corrected for sampling line losses.

Grab samples for individual hydrocarbon analyses were collected at each chamber, were drawn through a 1-m long, 4.8-mm ID FEP Teflon tube and a  $\text{MnO}_2$  scrubber with a Metal-Bellows MB-41 pump, and were exhausted into 10-liter Tedlar bags. A recent evaluation of sample collection containers for hydrocarbon sampling has demonstrated that  $\text{C}_2$  to  $\text{C}_5$  hydrocarbons are stable for up to 18 days when stored in Tedlar bags.<sup>7</sup> However, high background levels of FID-responsive species in the  $\text{C}_6$  to  $\text{C}_{10}$  range were also found in Tedlar bags. In the current study, the high background may prevent the accurate determination of compounds such as toluene that fall within the  $\text{C}_6$  to  $\text{C}_{10}$  range.

A  $\text{MnO}_2$  scrubber located in-line at the intake of the HC sampling pump was employed to remove  $\text{O}_3$  from the sampled air. A recent evaluation of this technique has shown the  $\text{MnO}_2$  to pass  $\text{C}_2$  to  $\text{C}_5$  hydrocarbons quantitatively.<sup>7</sup> The scrubber, however, was shown to be much less than 100 percent efficient at removing ozone. It is therefore anticipated that the ozone passed by the  $\text{MnO}_2$  scrubber would have reacted with  $\text{O}_3$ -reactive hydrocarbons, primarily the olefins. This could have occurred in most of the HC samples except those collected on the morning of the first day of a run and would be reflected as a low bias for the reported olefin concentrations. Recently, FEP Teflon tubing has been found to release considerable quantities of ethene to a passing gas stream.<sup>7</sup> The use of FEP Teflon tubing in the collection or transfer of samples may have prevented the accurate determination of ethane plus ethene.

#### Characterization Experiments--

The role of surface-mediated reactions in smog chamber investigations is unclear. Contamination or "dirty chamber" effects have been observed in glass, aluminum, and Teflon chambers.<sup>14,15</sup> The levels of background FID-responsive contaminants that are released by Teflon film vary from batch to batch.<sup>7,16</sup> Teflon film is the currently accepted material of choice for the fabrication of smog chamber walls. However, the experimental conditions for which the influence of chamber-associated contaminants may be safely neglected are yet to be defined.

Three types of chamber characterization experiments were conducted to document the behavior of the RTI smog chambers with respect to contaminant-

associated effects: purified air irradiations,  $O_3$  decays, and NO oxidations. The results of these experiments are presented in Tables 7, 8, and 9.

The purpose of the purified air irradiations was to document the concentrations of ozone,  $[O_3]_{\max}$ , that accumulated in the RTI smog chambers when purified air was irradiated. The ozone results from photochemical processes involving trace levels of nitrogen oxides and organics. These contaminants either remain in the air after purification or desorb from the chamber walls. Results from these experiments are summarized in Table 7. Ozone levels generated in the RTI chambers on the first day of purified air irradiations ranged from 0.03 to 0.17 ppm. A seasonal effect is apparent: the largest  $[O_3]_{\max}$  occurred on July 10, 1975, whereas the smallest  $[O_3]_{\max}$  occurred on January 9, 1976. The results of multiple-day experiments indicate that, on the first day, ozone levels near 0.08 ppm could be achieved. Also, second- and third-day maximum ozone concentrations could exceed the first-day levels. The  $[O_3]_{\max}$  values presented in Table 7 compare favorably with the value of 0.14 ppm reported for the outdoor UNC facility<sup>12</sup> and with the values of 0.04<sup>15</sup>, 0.05<sup>17</sup>, 0.10<sup>18</sup>, and 0.22<sup>15</sup> ppm reported for indoor chambers.

It is unclear how the results from purified air irradiations may be related to results from HC/NO<sub>x</sub> experiments. While purified air irradiations may indicate the level of chamber-associated contaminants relative to other purified air irradiations they may not be accurate indicators of the effects of these contaminants in HC/NO<sub>x</sub> experiments. These effects may be overshadowed completely in photochemically reactive HC/NO<sub>x</sub> systems. It is expected that as the absolute reactant concentrations and their ratio change, the impact of chamber effects on the overall behavior of the system will also change. Chamber influences are anticipated to be nonlinear with changing reactant concentration, and the experimental conditions at which chamber-related influences begin to dominate the behavior of chemical systems remain to be defined.

It should be noted that the  $[O_3]_{\max}$  that accumulates during a single irradiation period is the net result of both ozone-formation and destruction reactions that occur within a smog chamber. It is possible for a given chamber to have a low light-phase ozone-destructive component, low absolute concentrations of background contaminants (ozone precursors) and yet achieve



TABLE 7. MAXIMUM OZONE CONCENTRATION ACHIEVED IN RTI SMOG  
CHAMBERS DURING PURIFIED AIR IRRADIATION EXPERIMENTS

Date	%SS <sup>a</sup>	T <sub>max</sub> , °C	[O <sub>3</sub> ] <sub>max</sub> , ppm				Comments <sup>b</sup>
			Chamber 1	Chamber 2	Chamber 3	Chamber 4	
7/10/75	76	30.0	.155	.149 <sup>c</sup>	.154	.170 <sup>c</sup>	Run followed a propene/NO <sub>x</sub> experiment
1/9/76	100	0.0	.032	-- <sup>d</sup>	--	--	
4/6/76	89	22.2	--	.070	.080	--	Three-day experiment
4/7/76	93	22.8	--	.101	.123	--	
4/8/76	77	22.2	--	.086	.117	--	
4/23/76	97	31.1	.108	.043	.078	.078	Two-day experiment
4/24/76	92	32.2	.149	.079	.121	.124	
6/24/76	85	28.8	.155	.081 <sup>e,f</sup>	.063 <sup>e,g</sup>	.048 <sup>e,h</sup>	12-hour dilution from dawn until dusk
6/25/76	86	32.2	.142	.117	.099	.102	Four-day experiment with 24-
6/26/76	41	30.0	.134	.061 <sup>e</sup>	.050 <sup>e</sup>	.049 <sup>e</sup>	hour dilution from dawn of
6/27/76	38	30.6	.095	.050	.053	.064	6/26/76 until dawn of 6/27/76
6/28/76	91	31.7	.152 <sup>c</sup>	.102 <sup>c</sup>	.124 <sup>c</sup>	.137 <sup>c</sup>	
8/28/76	52	31.1	.089	.111	.099	.147	Three-day experiment
8/29/76	66	33.9	.062	.049	.099	.188	
8/30/76	72	26.1	.093 <sup>c</sup>	.062 <sup>c</sup>	.152 <sup>c</sup>	.235	

<sup>a</sup>Duration of solar radiation reported as percent of possible minutes of direct sunshine (see text).

<sup>b</sup>Unless noted otherwise, each experiment was preceded by a cleanup and was conducted in the static mode (no dilution).

<sup>c</sup>Last measurement of experiment.

<sup>d</sup>Blanks denote that no experiment was conducted.

<sup>e</sup>Experiment was conducted under dilution conditions.

<sup>f</sup>Dilution rate based on CO loss was 13.3 percent hr<sup>-1</sup>.

<sup>g</sup>Dilution rate based on CO loss was 15.2 percent hr<sup>-1</sup>.

<sup>h</sup>Dilution rate based on CO loss was 16.1 percent hr<sup>-1</sup>.

TABLE 8. OZONE HALF-LIVES IN RTI SMOG CHAMBERS

Date	%SS <sup>a</sup>	Chamber 1		Chamber 2		Chamber 3		Chamber 4	
		[O <sub>3</sub> ]i <sup>b</sup>	t <sub>1/2</sub> <sup>c</sup>	[O <sub>3</sub> ]i	t <sub>1/2</sub>	[O <sub>3</sub> ]i	t <sub>1/2</sub>	[O <sub>3</sub> ]i	t <sub>1/2</sub>
8/1/75 <sup>d</sup>	Dark	0.915	21.0	0.905	27.4	0.907	23.0	0.910	31.2
4/25,26/76 <sup>e</sup>	Dark	0.830	26.2	0.803	38.9	0.663	18.9	0.603	24.8
10/1,2/76 <sup>f</sup>	Dark	0.442	16.8	0.944	31.6	0.937	23.7	0.507	40.0
10/2,3/76 <sup>e</sup>	Dark	0.363	18.7	0.468	30.1	0.382	23.1	0.368	27.0
8/1/75 <sup>g</sup>	65	0.755	10.1	0.776	10.7	0.760	11.1	0.798	10.4
4/26/76 <sup>h</sup>	78	0.635	14.0	0.668	18.0	0.459	12.8	0.453	11.2
10/1/76 <sup>i</sup>	0	0.690	17.6	0.688	17.4	0.682	16.6	0.687	25.5
10/2/76 <sup>i</sup>	0	0.266	11.4	0.759	16.3	0.700	13.5	0.411	19.8
10/3/76 <sup>j</sup>	8	0.245	15.1	0.351	16.5	0.260	17.4	0.276	19.6

<sup>a</sup>Duration of solar radiation reported as percent of possible minutes of direct sunshine (see text).

<sup>b</sup>Initial ozone concentration in ppm.

<sup>c</sup>Half-life in hours; calculated from the slope of least squares regression of  $\ln [O_3]$  versus time data.

<sup>d</sup>Experiment was conducted from 0000 until 0400 EST.

<sup>e</sup>Experiment was conducted from 1900 EST until 0500 EST.

<sup>f</sup>Experiment was conducted from 1800 EST until 0500 EST.

<sup>g</sup>Experiment was conducted from 0600 EST until 1500 EST.

<sup>h</sup>Experiment was conducted from 0600 EST until 1100 EST.

<sup>i</sup>Experiment was conducted from 0600 EST until 1700 EST.

<sup>j</sup>Experiment was conducted from 0600 EST until 1000 EST.

TABLE 9. NO OXIDATION IN RTI SMOG CHAMBERS

Date	%SS <sup>a</sup>	Chamber 1		Chamber 2		Chamber 3		Chamber 4	
		[NO]i <sup>b</sup>	R <sup>c</sup>	[NO]i	R	[NO]i	R	[NO]i	R
1/9/76	Dark	--	--	--	--	--	--	0.48	3.0(1.6)
1/10/76	Dark	--	--	--	--	--	--	0.32	2.6(1.5)
8/3/76	Dark	0.63	1.6(1.2)	0.72	1.3(1.1)	0.56	2.2(1.3)	0.67	1.6(1.0)
9/17/76	Dark	0.81	1.2 <sup>d</sup>	0.80	1.1 <sup>d</sup>	0.79	1.6(0.8)	0.82	1.4(0.9)
9/18/76	Dark	0.53	1.8(0.9)	0.48	1.7(0.7)	0.45	2.4(1.0)	0.51	1.5(0.7)
7/11/75	10	0.58	2.9	0.61	0.9	0.58	2.6	0.62	2.0
1/9/76	100	--	--	--	--	--	--	0.61	2.2
1/10/76	88	--	--	--	--	--	--	0.36	2.5
1/11/76	18	--	--	--	--	--	--	0.27	4.7
8/3/76	22	0.80	1.2	0.82	0.5	0.80	2.1	0.86	1.4
9/17/76	65	0.74	3.2	0.73	4.0	0.71	4.6	0.73	3.4

<sup>a</sup>Duration of solar radiation reported as percent of possible minutes of direct sunshine (see text).

<sup>b</sup>Initial NO concentration in ppm.

<sup>c</sup>Ratio of experimentally determined second order rate constant for oxidation of NO to the established (literature) value  $k_{\text{expt}}/k_{\text{lit}}$ ; ratios in parentheses have been corrected for chamber leakage; ratios not in parentheses have not been corrected for chamber leakage.

<sup>d</sup>Variability of NO<sub>x</sub> data did not permit the determination of a leak rate coefficient.

a higher  $[O_3]_{\max}$  than another more contaminated chamber with a higher light-phase ozone-destructive component. Thus, the ozone-destructive component under irradiation should be considered when comparing  $[O_3]_{\max}$  values achieved in clean air irradiation experiments conducted in various chambers.

Ozone can disappear inside a chamber by interacting heterogeneously with the walls or by reacting homogeneously with contaminants present inside the chamber. Ozone decay rates reported as half-lives under both dark conditions and irradiation have been used as measures of smog chamber reactivity. For fixed-volume smog chambers, the apparent  $O_3$  half-life is influenced by chamber leakage. Leak rates were not determined for the  $O_3$  decay experiments in the current study. The  $O_3$  half-lives for the RTI chambers listed in Table 8 have not been corrected for leakage. These tabulated results indicate consistent behavior from chamber to chamber. Apparent dark-phase half-lives range from 16.8 to 40.0 hours with an overall mean of  $26.4 \pm 6.7$  hours. The corresponding values under exposure to natural irradiation range from 10.1 to 25.5 hours. Based on these results, 10 hours may be considered to be a reasonable estimate of the ozone half-life in the RTI chambers on a sunny summer day. The reduced half-life for irradiated conditions has been attributed mainly to secondary reactions following ozone photolysis (such as  $O(^1D) + H_2O$ ,  $O_3 + OH$ , and  $O_3 + HO_2$ ).<sup>9</sup>

Ozone half-lives reported for various smog chambers are summarized in Table 10. Comparison of the ozone half-lives for the RTI chambers with those reported for other chambers indicates that the RTI chamber surfaces are relatively unreactive with  $O_3$ . In addition, the dark-phase  $O_3$  half-lives listed in Table 8 are in accord with a recently reported value of 116 hours that was estimated for an elevated air parcel that was traveling downwind of the St. Louis area.<sup>7</sup>

The oxidation of NO should proceed in the dark by the third-order thermal reaction,  $NO + NO + O_2 \rightarrow 2 NO_2$ . In the dark, in the absence of reactive organic species, the above thermal reaction should be the major pathway for NO disappearance. Apparent second order rate constants for NO disappearance were determined from the slope of least squares regressions of  $[NO]^{-1}$  versus time data. For fixed-volume smog chambers, the apparent second order rate constant must be corrected for chamber leakage. Leak rate coefficients based on the dark-phase loss of  $NO_x$  were estimated for each

TABLE 10. SUMMARY OF OZONE HALF-LIVES FOR VARIOUS SMOG CHAMBERS

Chamber		Volume, l	Half-lives, hr <sup>a</sup>		Illumi- nation <sup>b</sup>	Reference
Identity	Construction Material		Dark	Light		
Bureau of Mines	Al, Teflon film	1.8 x 10 <sup>3</sup>	12	1 (54° C) 3.6 (34° C)	A	18
Bureau of Mines	Al, glass	2.8 x 10 <sup>3</sup>	14	6	A	18
Battelle	Al, Teflon film	1.7 x 10 <sup>4</sup>	8	1.5 (27° C)	A	19
Shell	Stainless steel	4.0 x 10 <sup>2</sup>	1.7-6 (24° C)	1.3-2.5 (30° C)	A	20
Exxon	Al, Teflon film	4.3 x 10 <sup>3</sup>	13.9	2.7	A	21
SRI	Teflon-coated Al	7.7 x 10 <sup>3</sup>	20	7.8	A	22
CSARB	Glass	3.1 x 10 <sup>4</sup>	==	5.8	A	23
SAPRC	Teflon-coated Al	5.8 x 10 <sup>3</sup>	6.8	4.2 (29° C)	A	17
--	Teflon bag	1 x 10 <sup>2</sup>	9.5	--	A	24
Lockheed	Glass	1.9 x 10 <sup>3</sup>	7.2 (35° C)	3.0 (35° C)	A	25
General Motors	Stainless steel	8.4 x 10 <sup>3</sup>	10.0	2.0	A	26
--	Tedlar Bag	4.4 x 10 <sup>2</sup>	11.9	--	A	27
UNC	Al, Teflon film	1.6 x 10 <sup>5</sup>	49-75 <sup>c</sup>	16-23 <sup>c</sup> (Nov. & Dec. 1973)	N	12
UNC	Al, Teflon film	2.0 x 10 <sup>5</sup>	21.2	9.4 (June 1974)	N	28
--	Teflon bags	1.0 x 10 <sup>2</sup>	45-150 <sup>d</sup> (25° C)	9-16 <sup>d</sup> (June 1975)	N	9
RTI	Al, Teflon film	2.7 x 10 <sup>4</sup>	17-40 <sup>e</sup>	10-26 <sup>e</sup>	N	Current Study

<sup>a</sup> Measured at approximately 1.0 ppm ozone.

<sup>b</sup> Artificial: A; natural sunlight: N, taken under sunny conditions unless stated otherwise.

<sup>c</sup> Range presented for simultaneous experiments in two chambers.

<sup>d</sup> Half-lives varied over this range with water vapor concentration.

<sup>e</sup> Range of half-lives reported in Table 8.

experiment from the slope of least squares regressions of  $\ln [\text{NO}_x]$  versus time data. The apparent second order rate constants for NO disappearance were corrected for chamber leakage.<sup>17</sup> Ratios of both the apparent and leak-corrected rate constants to the established value of  $1.77 \times 10^{-2} \text{ ppm}^{-1} \text{ hr}^{-1}$ <sup>29</sup> are presented in Table 9. The dark-phase loss rate coefficients for  $\text{NO}_x$  range from 0.003 to 0.011  $\text{hr}^{-1}$  with a mean of  $0.0072 \pm 0.0025 \text{ hr}^{-1}$ . The uncorrected ratios of rate constants range from 1.1 to 3.0 and the corrected ratios range from 0.7 to 1.6. These ratios suggest good agreement between the established value of the dark phase NO oxidation rate constant and the value as determined in the RTI chambers.

Loss rates of NO under irradiation in excess of the thermal rate may be attributed to participation of organic contaminants in the normal photochemical NO-oxidation reactions. Dimitriadis has suggested that the rate of NO loss under irradiated conditions provides a measure of chamber contamination levels.<sup>18</sup> Apparent second order rate constants for NO disappearance were determined by the technique noted above using data collected under irradiation. For these conditions  $\text{NO}_x$  loss was much greater than under dark conditions--the  $\text{NO}_x$  loss rate coefficients range from 0.008 to 0.032  $\text{hr}^{-1}$  with a mean of  $0.019 \pm 0.007 \text{ hr}^{-1}$ . Although increased daytime wind speeds may increase the daytime leak rate, the contribution of leakage to the current  $\text{NO}_x$  loss rates is unclear. Gas-phase or surface-mediated reactions that lead to the formation of  $\text{N}_2\text{O}_5$  and  $\text{HNO}_3$  with the subsequent loss of  $\text{NO}_x$  may also contribute to the loss of  $\text{NO}_x$ . The data therefore do not permit correction of the apparent light-phase rate constants for leakage.

The uncorrected ratios of rate constants determined for irradiated conditions compare favorably with those determined under dark conditions and range from 0.5 to 4.7. These results for the RTI chambers also compare favorably with the value of 4.0 for the Bureau of Mines chamber<sup>18</sup> and to values of 4.8 and 3.0 for the outdoor UNC facility.<sup>12</sup>

In addition to the above characterization experiments, matched experiments conducted during the experimental program show consistent behavior from chamber to chamber. For example, a matched urban mix experiment was conducted on 4 August 1976. Target initial conditions were 5 ppmC hydrocarbon and 1 ppm  $\text{NO}_x$  (20 percent  $\text{NO}_2$ ). The NO- $\text{NO}_2$  crossovers for the four chambers occurred within 6 minutes of each other at approximately 0655 EST,

and the maximum  $\text{NO}_2$  concentrations ranged from 0.79 to 0.86 ppm. The  $\text{O}_3$  maxima on the first day of the experiment occurred during the 1500 hour and were in good agreement: 1.05, 1.07, 1.04, and 1.06 ppm.

A second matched experiment was conducted on 20 September 1976 with target initial conditions of 12.0 ppmC propane and 0.2 ppm  $\text{NO}_x$  (20%  $\text{NO}_2$ ). The  $\text{NO}$ - $\text{NO}_2$  crossovers occurred within 26 minutes of each other, and the maximum  $\text{NO}_2$  concentrations ranged from 0.150 to 0.158 ppm. The first day  $[\text{O}_3]_{\text{max}}$  values were also in reasonable agreement: 0.20, 0.26, 0.18, and 0.21 ppm. These results are discussed in detail in a subsequent section of this report. The good agreement demonstrated in these and other matched experiments increases confidence in the reliability of data obtained in the RTI smog chambers.

#### REAGENTS

Air used in the smog chamber experiments was supplied from the air purification systems that are located under each chamber. The gaseous reagents that were employed are identified in Table 11. These gases were used as received from the suppliers without further purification.

The  $\text{O}_2$  that was used for  $\text{O}_3$  injections was zero (Z-2) grade. The  $\text{N}_2$  that was used to purge the injection lines was Matheson "Oxygen Free" grade. Nitrogen oxides were introduced from separate tanks that contained  $\text{NO}$  in  $\text{N}_2$  and  $\text{NO}_2$  in  $\text{N}_2$ .

Several different hydrocarbons were used in runs that did not involve the urban mix (see Table 3). Ethane, acetylene, and propane were injected as pure gases. The propene-air mixture that was used in several experiments was blended at RTI from 99 percent propene (Phillips Petroleum Company) and hydrocarbon-free air (Airco).

The hydrocarbon mixtures that were used in the urban mix runs (see Table 2) were supplied by Matheson Gas Products. Two different mix tanks were employed: one was used until it was depleted in late November of 1975; the second was used for all the urban mix runs that were conducted in 1976. The individual hydrocarbon analyses for each tank were supplied by Matheson and are listed in Table 12. It should be noted that the first mix did not contain acetylene or toluene--normal constituents of polluted urban air. In the 1975 urban mix experiments, acetylene was introduced by syringe injection.

TABLE 11. REAGENTS

Reagents	b.p. <sup>a</sup>	Purity	Supplier
Air	---	b	Airco
Oxygen	-183.0	99.95% <sup>b</sup>	Scientific Gas Products
Nitrogen (Oxygen Free)	-195.8	99.998% <sup>b</sup>	Matheson Gas Products
Nitric Oxide	-151.7	220 ppm in N <sub>2</sub>	Matheson Gas Products
Nitrogen Dioxide	21.1	115 ppm in N <sub>2</sub>	Matheson Gas Products
Ethane	- 88.2	>99%	Phillips Petroleum Company
Acetylene	- 75.0	99.6%	Matheson Gas Products
Propane	- 42.1	99.5%	Linde
Propene	- 47.7	99%	Phillips Petroleum Company
Propene	- 47.7	244 ppm (v/v) in air	RTI Blend
Carbon Monoxide	-191.5	20,300 ppm in N <sub>2</sub>	Matheson Gas Products
Toluene	110.6	28 ppm (v/v) in N <sub>2</sub>	Matheson Gas Products
Hydrocarbon Mix I <sup>b</sup>	---	212 ppm (v/v) in N <sub>2</sub>	Matheson Gas Products
Hydrocarbon Mix II <sup>c</sup>	---	563 ppm (v/v) in N <sub>2</sub>	Matheson Gas Products

<sup>a</sup>Boiling Point, °C.<sup>30</sup>

<sup>b</sup>Contains less than 0.5 ppmC total hydrocarbons.

<sup>c</sup>Mix used in 1975 urban mix runs, see Table 12 for analysis.

<sup>d</sup>Mix used in 1976 urban mix runs, see Table 12 for analysis.



TABLE 12. ANALYSES OF HYDROCARBON MIXTURES USED IN URBAN MIX EXPERIMENTS<sup>a</sup>

Compound	<u>Hydrocarbon Mix I<sup>b</sup></u>		<u>Hydrocarbon Mix II<sup>c</sup></u>	
	ppm (v/v)	ppmC	ppm (v/v)	ppmC
Acetylene	-	-	99	198
Propane	26	78	50	150
N-Butane	66	264	154	616
Isopentane	33	165	77	385
Cyclopentane	1	5	4.4	22
Ethene	51	102	105	210
Propene	11	33	27.9	83.7
1-Butene	10	40	17.6	70.4
Trans-2-Butene	8	32	18.8	75.2
2-Methyl-2-Butene	6	24	9.4	37.6

<sup>a</sup>These analyses were provided by gas supplier, Matheson Gas Products.

<sup>b</sup>Mix used in 1975 urban mix runs, see Table 2.

<sup>c</sup>Mix used in 1976 urban mix runs, see Table 2.

tion as a pure gas; whereas toluene was injected from a separate tank that contained toluene in  $N_2$ . Acetylene was included in the second hydrocarbon mixture; therefore, only toluene injections were required in the 1976 urban mix experiments.

The hydrocarbon mixture was blended so as to permit the injection, in combination with separate injections of acetylene and toluene, of a reasonable surrogate of urban air. The composition of the surrogate urban mix was specified by EPA such that on a carbon basis, the target relative fractions of alkanes, alkenes, aromatics, and acetylene were 0.49, 0.22, 0.20, and 0.09. Propane, n-butane, isopentane, and cyclopentane comprised the alkane fraction with propane representing itself; n-butane the straight chain alkanes; isopentane the branched chain alkanes; and cyclopentane the cyclic alkanes. Ethene, propene, 1-butene, trans-2-butene, and 2-methyl-2-butene comprised the alkene fraction with ethene and propene representing themselves; 1-butene the terminally double-bonded olefins, trans-2-butene the internally double-bonded olefins, and 2-methyl-2-butene the branched chain olefins. Toluene represented aromatic compounds, and acetylene represented itself. The relative amounts of each model species within its class were chosen based on data reported for Los Angeles air.<sup>31</sup>

In addition to the hydrocarbon mix, acetylene, and toluene injections, CO was injected from a separate tank that contained CO in  $N_2$ . Although CO is a normal constituent of polluted urban air, CO was injected as a tracer in the urban mix experiments at a constant initial target concentration of 10 ppm.

## MEASUREMENT METHODS

The measurement methods employed in the chamber studies are described below. A summary of these methods is presented in Table 13.

Both instrumental and manual analytical techniques were employed. Ozone, NO,  $NO_2$ , total hydrocarbons (THC), methane ( $CH_4$ ), and CO concentration data from automated instruments were recorded from each chamber once per hour during the corresponding 10-minute sampling period. The reported  $O_3$ , NO, and  $NO_2$  concentrations were reduced from strip chart records at the eighth minute of each 10-minute sampling period. The THC,  $CH_4$ , and CO concentrations were reduced from the strip chart records of the second

TABLE 13. MEASUREMENT METHODS

Measured Quantity	Method	Manufacturer	Range	MDC <sup>a</sup>
O <sub>3</sub>	Chemiluminescent	Bendix Model 8002	0-1 ppm	0.001 ppm
Oxidant	NBKI (Wet Bubbler)	---	0-1 ppm	0.001 ppm
NO, NO <sub>2</sub> , NO <sub>x</sub>	Chemiluminescent	Thermo-Electron Model 14B	0-1 ppm	0.001 ppm
NO <sub>2</sub>	Saltzman (Wet Bubbler)	---	0-5 ppm	0.005 ppm
THC, CH <sub>4</sub> , NMHC, CO	Gas Chromatography/ Flame Ionization	Beckman Model 6800	0-10 ppmC	0.01 ppmC
Individual HC	Gas Chromatography Flame Ionization	Perkin Elmer Model 900	>0.1 ppb(v/v) <sup>b</sup> >50 ppb(v/v) <sup>c</sup>	0.1 ppb(v/v) <sup>b</sup> 50 ppb(v/v) <sup>c</sup>
HCHO	Chromotropic Acid (Wet Bubbler)	---	0-1 ppm	0.015 ppm
Condensation Nuclei (CN)	Photoelectric Nucleus Counter	Gardner Associates, Type CN	0-10 <sup>7</sup> CN/cm <sup>3</sup>	100 CN/cm <sup>3</sup>
Freon-12	Long Path Infrared Spectroscopy	Wilks Scientific Miran I	0-700 ppm (0-1 AU)	0.08 ppm
Solar Radiation <sup>d</sup>	Pyranometer	Eppley Model 2	0-2 Langleys	---
% Possible Minutes Sunshine <sup>e</sup>	Photoelectric Cells	Foster Sunshine Switch	---	---
Ambient Temperature <sup>e</sup>	---	---	---	---

<sup>a</sup>Minimum detectable concentration as reported by the manufacturer.

<sup>b</sup>This value is for cryogenic sample concentration.

<sup>c</sup>This value is for direct injection of a 1 ml volume of sample.

<sup>d</sup>Data collected by the U.S. EPA, Division of Meteorology, Research Triangle Park, North Carolina.

<sup>e</sup>Data collected by NWS Forecast Office at RDU<sup>32</sup>.

5-minute cycle of each 10-minute sampling period. The sampling frequency of the data reported in Volume 2 (Appendix B) is once per hour for each chamber.

Oxidant,  $\text{NO}_2$ , and  $\text{HCHO}$  were determined by wet chemical techniques. Samples were collected twice daily from each chamber at midmorning and midafternoon (see Volume 2 [Appendix B]) for exact times). Individual hydrocarbon concentrations were determined by gas chromatographic analyses of grab samples collected in Tedlar bags twice daily at sunrise and late afternoon. Hydrocarbon analyses from the chamber runs, as well as the exact times of sample collection, are reported in Volume 2 (Appendix A).

### Ozone

Ozone was monitored with a Bendix Model 8002 Ozone Analyzer. The principle of operation employs the chemiluminescent gas-phase reaction between ozone and ethene. The instrument operates in the continuous mode with a range of 0 to 1 ppm and an MDC of 0.001 ppm. Calibration was performed prior to each experiment using a stable ultraviolet light ozone generator. The output of the  $\text{O}_3$  generator was determined by gas-phase titration of  $\text{O}_3$  with known  $\text{NO}$  concentrations that were blended from air and certified standard mixtures of  $\text{NO}$  in nitrogen.<sup>33</sup> A recent intercomparison of the  $\text{NO}$  calibration cylinder with four other certified calibration cylinders indicated that the  $[\text{NO}]$  in the original cylinder was 7.0 percent less than the label value. The reported ozone data have been corrected, and a correction factor (multiplier) of 1.070 has been applied to the raw data to arrive at the ozone concentrations reported in Volume 2 (Appendix B).

### Oxidant

For chamber studies, photochemical oxidant concentrations were measured by the NBKI technique.<sup>33,34</sup> This involved passing a known volume of chamber air through two all-glass midjet impingers in series; each contained a 1% neutral-buffered potassium iodide (NBKI) solution. These solutions were subsequently analyzed with a Bausch and Lomb Spectronic 100 spectrophotometer. Calibration curves and blanks were prepared periodically according to the referenced procedures. The sampling duration was normally 10 minutes, and the flow rates ranged from 600 to 700  $\text{ml min}^{-1}$ . Flow rate was controlled by a calibrated hypodermic needle protected from overspray by a dessicant

cartridge and glass wool trap. The reported data have not been corrected for interferences from nitrogen dioxide, peroxyacyl nitrates or other oxidizing species. In the reported data (Volume 2 [Appendix B]), the time assigned to a wet chemical measurement for a chamber is the automated instrument sampling period for that chamber which is closest to the beginning of the bubbler sampling period.

#### Nitrogen Oxides (NO, NO<sub>2</sub>, and NO<sub>x</sub>)

Nitrogen oxides were monitored with a Thermo-Electron (TECO) Model 14B NO-NO<sub>x</sub> Analyzer. The principle of operation employs the chemiluminescent gas-phase reaction between NO and O<sub>3</sub>. Two modes of operation are required to determine NO, NO<sub>2</sub>, and NO<sub>x</sub>. Nitric oxide is measured first using the reaction of NO and O<sub>3</sub>. The determination of NO<sub>2</sub> and NO<sub>x</sub>, however, requires catalytic reduction of NO<sub>2</sub> to NO prior to the reaction of NO with ozone. After reduction of NO<sub>2</sub> to NO, the signal from the total NO in the sample is taken to be the NO<sub>x</sub> concentration. Electronic subtraction of the original NO signal from the NO<sub>x</sub> signal yields the NO<sub>2</sub> concentration. The instrument operates with a 90-second cycle time: NO concentration is updated at the end of the first portion of the cycle; and NO<sub>2</sub> and NO<sub>x</sub> concentrations are updated at the end of the cycle.

The instrument was calibrated prior to each experiment. Calibration of the NO and NO<sub>x</sub> channels was performed by dilution of a known concentration of NO from a certified cylinder of NO in nitrogen. Calibration of NO<sub>2</sub> was performed by using the NO<sub>2</sub> produced from the gas-phase titration of known NO concentrations with O<sub>3</sub> from the calibrated ozone generator. As was noted in the earlier discussion of the ozone calibration procedure, recently the [NO] in the calibration cylinder was found to be 7.0 percent less than the label value. The reported NO, NO<sub>2</sub>, and NO<sub>x</sub> data have been corrected, and a correction factor (multiplier) of 1.070 has been applied to the raw data to arrive at the NO, NO<sub>2</sub>, and NO<sub>x</sub> concentrations reported in Volume 2 (Appendix B).

The NO<sub>x</sub> analyzer was usually operated on the 0 to 1 ppm full scale (FS) range, although both the 0 to 0.2 and the 0 to 0.5 ppm FS ranges were used occasionally. In contrast to the MDC of 0.001 ppm as specified by the manufacturer, the effective MDC in the current study was approximately

0.005 ppm on the 0 to 1 ppm FS range. This is determined by instrument noise and the width of the strip chart trace. In addition, the zero baseline for the NO and the NO<sub>x</sub> channels displayed a strong temperature dependence. Diurnal variations of the room temperature could produce as much as 10 percent FS shift in the zero baseline over the course of an experiment. Frequent zero checks reduced the impact of this behavior. The data in Appendix B that are suspected of having residual error due to zero drift have been identified. The NO<sub>2</sub> channel did not exhibit this behavior because NO<sub>2</sub> is the difference between the NO<sub>x</sub> and NO channels which were both shifting by equal amounts.

It has been demonstrated that nitric acid, PAN, and ethyl nitrate interfere with NO<sub>2</sub> and NO<sub>x</sub> determinations in instruments of the type employed in this study.<sup>35</sup> The interfering species were not determined in this study. Therefore, the reported NO<sub>2</sub> and NO<sub>x</sub> data have not been corrected for interferences.

#### Nitrogen Dioxide

In addition to the chemiluminescent measurements, the Saltzman method was used to determine NO<sub>2</sub> levels in the chambers.<sup>36</sup> Chamber air was drawn through a glass, fritted Mae West bubbler containing Griess-Saltzman reagent. The sampling duration was normally 15 minutes, and the flow rates ranged from 600 to 800 ml min<sup>-1</sup>. Flow rate was controlled by a calibrated hypodermic needle protected from overspray by a dessicant cartridge and glass wool trap. Samples were analyzed with a Bausch and Lomb Spectronic 100 spectrophotometer. Calibration curves and blanks were prepared periodically according to the referenced procedure. The reported data have not been corrected for interferences from ozone or peroxyacyl nitrates. In the reported data (Volume 2 [Appendix B]), the time assigned to a wet chemical measurement for a chamber is the automated instrument sampling period for that chamber which is closest to the beginning of the bubbler sampling period.

#### Total Hydrocarbons, Methane, Nonmethane Hydrocarbons, and Carbon Monoxide

Total hydrocarbon, CH<sub>4</sub>, NMHC, and CO were determined by a Beckman Model 6800 Air Quality Chromatograph that employs a flame ionization detector (FID). The instrument operates with a 5-minute cycle time and provides THC,

CH<sub>4</sub>, and CO concentrations once per cycle. Thus, once per hour during each 10-minute sampling period two sets of measurements were performed on the air sampled from each chamber. Only the second set of measurements were reduced and reported.

The NMHC concentration is a calculated quantity that is computed by subtraction of the CH<sub>4</sub> from the THC concentration. In the instrument, THC is determined by injection of a portion of the sampled air directly to the FID. A second portion of the sampled air is injected into a Porapak Q stripper column that separates CH<sub>4</sub> and CO from CO<sub>2</sub>, H<sub>2</sub>O, and the C<sub>2</sub>-and-heavier hydrocarbons. As the CH<sub>4</sub> and CO emerge from the stripper column in a single peak, they are diverted to a molecular sieve column. Here CH<sub>4</sub> and CO are separated into two peaks with CH<sub>4</sub> eluting first. They are then passed through a nickel catalyst methanator before introduction to the FID. Methane passes through the methanator unaffected and is detected as methane by the FID. Carbon monoxide is converted to methane in the methanator, and is detected as methane by the FID.

Calibration was performed daily. Certified mixtures of CH<sub>4</sub> and CO in hydrocarbon-free air that were supplied by Scott Research Laboratories were employed as calibration gases. The calibration procedure was similar to the present Federal Reference Method.<sup>37</sup> This approach should provide accurate determinations of CH<sub>4</sub> and CO. It should be noted, however, that the subsequent determination of NMHC may be subject to a substantial low bias. Most NMHC species yield a lower FID response on a per-atom-carbon basis than methane. Results from a recent study that employed a Beckman 6800 have indicated that the effective carbon numbers for typical urban NMHC species range from 0.42 to 0.60 relative to methane.<sup>38</sup> Thus, to correct NMHC data for this reduced response efficiency, a correction factor (multiplier) of 1.7 to 2.4 may be necessary. To maintain consistency with the Federal Reference Method, however, the NMHC data in Appendix B have NOT been corrected.

#### Individual Hydrocarbons

The concentrations of individual hydrocarbon species were determined by gas chromatographic separation with flame ionization detection. The results of these determinations are listed in Volume 2 (Appendix A).

Samples were collected from each chamber at sunrise and sunset on each day of an experiment. Each sample was drawn through a 1-m long 4.8-mm ID Teflon tube and a  $\text{MnO}_2$  scrubber by a Metal-Bellows MB-41 pump and was exhausted into a 10-liter Tedlar bag. A specific volume of sample from this bag was cryogenically trapped in a 3.2-mm OD stainless steel loop that had been immersed in liquid oxygen. The trap was connected to the modified Perkin-Elmer Model 900 gas chromatograph that was employed in the current study. Next, the trap was heated, and its contents passed into the column.

Low molecular weight hydrocarbons ( $\text{C}_2$ - $\text{C}_5$ ) were separated on a 1.8-m x 3.2-mm OD stainless steel column packed with n-octane on Porasil. The column temperature was 23° C, and the helium carrier flow rate was 12 ml  $\text{min}^{-1}$ .

High molecular weight hydrocarbons (including aromatics) were separated on a 1.8-m x 3.2-mm OD stainless steel column packed with GP 5% SP-1200/5% Bentone 34 on 100/120 Supelcoport. The column temperature was 75° C, and the helium flow rate was 20 ml  $\text{min}^{-1}$ .

Normally, the samples were analyzed within 8 hours after their collection. In some cases, however, longer storage periods, up to two days, were required.

A Hewlett-Packard Model HP-3352 data system acquired the output signal, integrated peak areas, and converted the areas into concentration values which were printed by a teletype. Strip chart records of output signals were maintained to supplement data system records. The MDC from the data system using the liquid oxygen trapping injection technique is less than 0.1 ppb (v/v). Occasionally HC measurements were performed by direct injection of the sample into the GC column from a 1-ml sampling loop without cryogenic concentration of the sample. This technique was generally used for experiments involving high concentrations of single hydrocarbons and is noted in Volume 2 (Appendix A). The MDC for this technique is 50 ppb (v/v).

Identification and quantification of compounds was based on comparison of retention times and peak areas with those of calibration mixtures. Cali-

---

\*If a bag initially contained 0.1 ppm  $\text{O}_3$  and 0.1 ppmV ethene, approximately 11 percent of the initially present ethene would be consumed in 8 hours by reaction with ozone. This percentage would increase for more reactive olefins. For example, under the same initial conditions 43 percent of the initially present propene would be consumed in 8 hours.



bration was performed at three-week intervals and showed a precision of  $\pm 5$  percent. The hydrocarbon calibration mixtures were supplied by Scott Research Laboratories and were certified to  $\pm 1$  percent accuracy.

Several recent findings in our laboratory<sup>7</sup> may have a significant impact on the reliability of the individual HC data reported in Appendix A.

- The concentration of  $C_2$  to  $C_5$  hydrocarbons has been shown to be stable for up to 18 days in Tedlar bags.
- High background levels of FID-responsive species in the  $C_6$  to  $C_{10}$  range have been found in Tedlar bags.
- Samples of FEP Teflon tubing have been found to release substantial quantities of ethene (or a material with a similar retention time) to a passing gas stream.
- The  $MnO_2$  scrubber that was employed to remove  $O_3$  from the HC samples has been shown to pass  $C_2$  to  $C_5$  hydrocarbons quantitatively. However, the scrubber has also been found to be less than 100 percent efficient at removing ozone.

In view of these findings, reported  $C_2$  to  $C_5$  alkane concentrations should be reliable. Ethane plus ethene concentrations may be erratic due to the use of FEP Teflon tubing during sample collection. The unstabilized or residual ozone could react with sampled olefins and provide a low bias.\* The first-day samples that were collected on the mornings of each run should not have been subject to this bias because there was no ozone present at the time of sample collection. Toluene determinations may have been obscured by the high  $C_6$  to  $C_{10}$  background of the Tedlar bags.

#### Formaldehyde

In the chamber studies, formaldehyde was determined by the chromotropic acid method.<sup>39,40</sup> A 1% sodium bisulfite solution was employed as the collection medium. Chamber air was drawn through two glass midget impingers in series. The sampling duration was normally 30 minutes, and the flow

---

\*If a bag initially contained 0.1 ppm  $O_3$  and 0.1 ppmV ethene, approximately 11 percent of the initially present ethene would be consumed in 8 hours by reaction with ozone. This percentage would increase for more reactive olefins. For example, under the same initial conditions 43 percent of the initially present propene would be consumed in 8 hours.

rates ranged from 600 to 700 ml min<sup>-1</sup>. Flow rate was controlled by a calibrated hypodermic needle which was protected from overspray by a dessicant cartridge and glass wool trap. Samples were analyzed with a Bausch and Lomb Spectronic 100 spectrophotometer after treatment with chromotropic and sulfuric acids. Calibration curves and blanks were prepared periodically according to the referenced procedures. The reported data have not been corrected for interferences from ethene, propene, or other hydrocarbons. In the reported data (Volume 2 [Appendix B]), the time that has been assigned to a wet chemical measurement for a chamber is the automated instrument sampling period for that chamber which is closest to the beginning of the bubbler sampling periods.

### Condensation Nuclei

The number of condensation nuclei per cubic centimeter of sampled air (CN) was determined with a Gardner Associates Type CN Small Particle Detector. The sampling frequency varied from experiment to experiment. Normally CN determinations were performed from one to four times per day. The samples were taken directly from each chamber through a 1-m length of 4.8-mm ID Teflon tubing. The manufacturer's calibration curve was used.

### Freon-12

Freon-12<sup>®</sup> (difluorodichloromethane) was used at initial concentrations of approximately 300 ppm as a tracer in several experiments which were designed to quantify chamber leakage under various modes of operation. It was measured by a Wilks Miran I Variable Filter Infrared Analyzer. This instrument uses a single-beam spectrophotometer in conjunction with a 20-meter variable pathlength White cell. When Freon-12 is present in the cell, the spectrum of infrared light will show a strong absorption band ( $44 \text{ atm}^{-1} \text{ cm}^{-1}$  for  $1 \text{ cm}^{-1}$  resolution) at a spectral frequency of  $930 \text{ cm}^{-1}$ . Typical instrumental resolution in this spectral region is  $20 \text{ cm}^{-1}$ . The instrument is equipped with a linear absorbance accessory which produces an output signal proportional to the Freon-12 concentration. This signal was recorded on a strip chart recorder.

The Metal Bellows pump of the sampling system was used to flush air continuously through the White cell. This was accomplished by connecting the cell's intake port to the vent of the glass sampling manifold (see Figure 11).

Bags also containing mixtures of approximately 300 ppm Freon-12 in air were prepared by injecting pure Freon-12 via a syringe into 100-liter bags which contained breathing air. Periodic span checks were made using these mixtures. The instrument's zero was established during the ambient air portion of the sampling cycle.

#### Solar Radiation

Total solar radiation data reported in this study were collected by the U.S. Environmental Protection Agency Division of Meteorology. The solar radiometer, an Eppley Precision Spectral Pyranometer was located at a point approximately 0.5 km from the RTI Smog Chamber Facility. This instrument employs a thermopile sensing element and determines light intensity at wavelengths longer than 295 nm. The hourly average values reported in Appendix B were reduced from continuous strip chart records.

#### Environmental Variables

Other environmental variables reported in this study (see Appendix B) are ambient air temperature at 3-hour intervals, the daily maximum temperature ( $T_{\max}$ ), and the percent of possible minutes of direct sunshine (% SS). The % SS is determined by a Foster Sunshine Switch, which consists of two photoelectric cells and a recorder. One cell is shaded from direct sunlight; the other is not. These cells are connected such that the recorder is actuated when the intensity of direct sunshine is sufficient to produce a shadow. The temperature and the sunshine data are collected by the National Weather Service (NWS) Forecast Office at the Raleigh-Durham Airport (RDU).<sup>32</sup> RDU is located at a distance approximately 10 km from the RTI Campus.

#### DATA REDUCTION AND HANDLING

Data have been handled in several forms in the current study. They have been transformed from continuous or discrete values into discrete computer-compatible values. Listings of these data are presented in Appendixes A and B.

Strip chart records of  $O_3$ , NO,  $NO_2$ , THC,  $CH_4$ , and CO were manually reduced into concentration units and entered onto coding forms. The  $O_3$ , NO, and  $NO_2$  concentrations were reduced at the eighth minute of each 10-minute sampling period. Strip chart traces of the THC,  $CH_4$ , and CO chromatographic

peaks were manually reduced into concentration units from the records of the second 5-minute chromatographic cycle of each 10-minute sampling period. These data were also entered at times corresponding to the eighth minute of the sampling period.

Concentrations of oxidant,  $\text{NO}_2$ , and  $\text{HCHO}$  that were determined manually by wet chemical techniques were entered onto coding forms. The time assigned to a wet chemical measurement for a chamber is that corresponding to the automated instrument sampling period for that chamber which is closest to the beginning of the bubbler sampling period. The manually determined CN data were treated similarly.

Strip chart records of continuous solar radiation data were obtained from the EPA Division of Meteorology. From these records, hourly average values of solar radiation intensity were manually calculated and entered onto coding forms.

Ambient temperature at 3-hour intervals, the maximum daily temperature, and the percent of possible minutes of direct sunshine were recorded at the NWS Forecast Office, RDU airport. Tabulated data were obtained<sup>32</sup> and transferred to coding forms.

The coded data noted above were keypunched and processed into the format shown in Volume 2 (Appendix B). The data processing program, in addition to providing a convenient format for listing the coded data, also calculated and listed time,  $\text{NO}_x$ , NMHC, and the cumulative solar radiation (CUM-SR). The following formulae were used in these computations:

$$\text{NO}_x = \text{NO} + \text{NO}_2$$

$$\text{NMHC} = \text{THC} - \text{CH}_4$$

$$\text{CUM-SR} = \sum_{i=0}^{h-1} \text{SR}(i) + \frac{m}{60} \text{SR}(h)$$

Where  $\text{SR}(i)$  is the average solar radiation for the  $i^{\text{th}}$  complete hour;

$h$  is the number of the indicated hour; and

$m$  is the number of minutes from the top of the indicated hour until the indicated time.

It should be noted that the SR data are listed in Volume 2 (Appendix B) as hourly averages in units of Langleys per minute ( $\text{cal cm}^{-2} \text{min}^{-1}$ ). The CUM-SR is a measure of the cumulative solar radiation that had occurred up to the indicated time and is expressed in Langleys ( $\text{cal cm}^{-2}$ ).

Individual hydrocarbon data were handled differently than the data noted above. Grab samples were collected manually and these samples were determined with a gas chromatograph. The analog signals from the gas chromatograph were identified and transformed by an automatic data acquisition system to species identifiers and concentration units which were printed by a teletype. These data were subsequently entered onto coding forms. The coded individual HC data were keypunched and processed into the format shown in Volume 2 (Appendix A).

Time is listed in fractional hours (EST) in Volume 2. The times of measurements were coded and keypunched as time of day in hours and minutes (EST). These data were converted by the processing programs to fractional hours (EST).

#### PROCEDURE

Two types of experiments were conducted in the present study: those that involved the irradiation of a surrogate urban hydrocarbon mix in the presence of  $\text{NO}_x$  and those that dealt with other chemical systems (see Tables 2 and 3). The basic research plan involved the urban mix and called for 3-day smog chamber runs with four different target initial reactant concentrations, four different dilution rates, and three different times at which dilution was initiated (see Table 4). The procedure employed for urban mix experiments is described in this subsection. The procedures employed in those experiments that did not involve the urban mix were similar and therefore are not addressed in this discussion.

A three-day smog chamber run requires four days of chamber activities. On the day before a run is to start, the chambers are operated in the purge mode. Starting at 0900 EST and lasting for six to eight hours each chamber is flushed with ambient air at a flow rate of up to  $2.3 \text{ m}^3 \text{ min}^{-1}$ . At approximately 1500 EST the purging operation is terminated, each chamber is sealed, and the cleanup operation is begun. Hydrocarbon and  $\text{NO}_x$  contaminants in the chamber air are removed by recirculation of the chamber contents through the air purification unit for 8 to 12 hours at a flow rate of  $0.28 \text{ m}^3 \text{ min}^{-1}$ . In the current experimental programs, the humidity of the chamber contents was not altered during the cleanup. This was accomplished by "by-passing" both the humidifier and the desiccant columns during the cleanup operation. The cleanup operation is terminated two hours before sunrise.

The next step in the procedure is reactant injection. Appropriate amounts of NO and NO<sub>2</sub> are sequentially introduced into each chamber from separate gas cylinders using the reactant injection system (see Figure 10). After the NO<sub>x</sub> injection, the hydrocarbon mix, toluene, and CO are injected from separate cylinders using the same reactant injection system. The injection procedure is completed 1 hour before sunrise. This allows time for mixing and initial reactant sampling prior to sunrise.

In the current study, target initial [NO<sub>x</sub>] (20 percent NO<sub>2</sub>) ranged between 0.1 and 1.0 ppm and target initial [NMHC] ranged from 1 to 10 ppmC, and the target initial [CO] was 10 ppm. Specific target [NMHC]: [NO<sub>x</sub>] combinations were 10 ppmC: 1.0 ppm, 5 ppmC: 0.71 ppm, 5 ppmC: 0.24 ppm and 1.0 ppmC: 0.1 ppm. In the 1975 urban mix experiments, acetylene had to be introduced into the chambers by syringe injection of the pure gas, because it had been omitted from the hydrocarbon injection mix. However, this was not the case in the 1976 urban mix experiments, since acetylene had been included in the 1976 hydrocarbon injection mix (see Table 12).

The contents of the chambers were sampled and monitored for the next three days. Ozone, NO, NO<sub>2</sub>, THC, CH<sub>4</sub>, and CO were monitored once per hour for each chamber. Typically, wet bubbler samples for oxidant, NO<sub>2</sub>, and HCHO analyses were collected from each chamber twice daily at midmorning and at mid-afternoon (see Volume 2 [Appendix B]) for exact times). Samples for hydrocarbon analyses were collected in 10-liter Tedlar bags twice daily at sunrise and late afternoon (see Volume 2 [Appendix A]) for exact times).

Dilution of chamber contents with purified air for 24 hours was employed to simulate atmospheric transport conditions. Static operation (no dilution) was used to simulate stagnation conditions. Following reactant injection, each experiment was begun in the static mode and, if the experimental design called for simulated transport, dilution was initiated on the first day at one of three times: sunrise, NO-NO<sub>2</sub> crossover, or 1700 EST. One of four dilution rates was employed such that 95, 77, 39, or 0 percent of a tracer present at the start of dilution would have been removed by the end of the 24-hour dilution period. Dilution was terminated 24 hours after it had been initiated. The chamber was then operated in the static mode until the experiment was terminated at 1700 EST on the third day. The target experimental conditions and the dates on which the corresponding experiments were conducted are identified in Table 4.

## SECTION 5

### RESULTS AND DISCUSSION

#### OVERVIEW

The results of smog chamber experiments conducted under EPA contracts 68-02-1296 and 68-02-2207 are discussed in this section. Data collected during these experiments are tabulated in Volume 2. The experimental conditions were identified previously in Tables 2 and 3. During these 60-hour experiments a surrogate urban mix in the presence of  $\text{NO}_x$  was exposed to three daylight periods of natural irradiation and two nighttime periods of darkness. Ancillary multi-day experiments involving other chemical systems were conducted as well. The basic research program was designed to permit the investigation of the influence of simulated transport on the ozone generation by various combinations of the surrogate urban hydrocarbon mix and  $\text{NO}_x$  from experiments conducted in smog chambers. The ancillary experiments did not involve the urban mix, but instead, were directed toward exploring the ozone-generative potential of low reactivity hydrocarbons, at conducting experiments for comparison (by EPA personnel) with results predicted by photochemical kinetics simulation model, and toward permitting comparison of the behavior of the RTI and UNC outdoor smog chambers.

#### BASIC RESEARCH PROGRAM

The experiments considered in this study are identified in Table 4. Eighteen four-chamber sets of experiments were considered: five sets of static experiments, twelve sets of dilution experiments, and one set of multiple dilution experiments. Dilution was initiated at sunrise in five sets, at the time of  $\text{NO}$ - $\text{NO}_2$  crossover in four sets, and at 1700 in three sets. The parameters considered in this study were selected from the following: the time at which dilution was initiated; the extent of dilution; the initial NMHC and  $\text{NO}_x$  concentrations as well as their ratio; the  $[\text{NMHC}]$ ,  $[\text{NO}_x]$ , and  $[\text{NMHC}]/[\text{NO}_x]$  at sunrise of the second and third days; the maximum  $\text{O}_3$  concentration on the first day; and the maximum, minimum, and net  $\text{O}_3$

concentrations on the second and third days.\* The parameters may be determined for each experiment from the data tabulated in Volume 2 (Appendix B).

#### Analysis of Overall Data Set

The data on each of the three days of an experiment were stratified by precursor concentration. The  $\text{NO}_x$  and NMHC concentration ranges used were chosen arbitrarily such that the concentrations did not overlap and that approximately an equal number of data would fall within each range. Since the experiments were conducted under a variety of conditions, i.e., at different temperatures, solar intensities, and times of the year, the standard deviations for the  $\text{O}_3$  concentrations within each range are large. Data were rejected when permitted by Chauvenet's criterion.<sup>41</sup>

Initially, the entire data set was considered. This data set is identified in Table 4 and is comprised of both static and dilution experiments. These data were used to determine the effects of ozone precursor concentration and their ratio on the maximum concentrations of ozone produced on the first day of an experiment. Results are presented in Figures 12, 13, and 14. Figures 12 and 13 suggest that in these experiments the maximum  $\text{O}_3$  concentration generated on the first day generally increases with increasing precursor concentration. The average  $\text{O}_3$  concentration at 0.37 ppm  $\text{NO}_x$  in

---

\*Net ozone concentration on any day is the difference between the maximum and minimum concentrations:  $\Delta\text{O}_3 = [\text{O}_3]_{\text{max}} - [\text{O}_3]_{\text{min}}$ . The accumulation of ozone in smog chambers is the net result of synthesis and destructive processes. Ozone is synthesized by photochemical processes. At night in the absence of sunlight, ozone-destructive processes prevail. During the night following the first day of an experiment, the ozone concentration declines as the ozone that was generated during the previous daylight period is destroyed by homogeneous reactions with various reactants and products and by heterogeneous interactions with the chamber walls. On the morning of the second and third days, ozone synthesis begins with the reintroduction of sunlight to the system. When the ozone synthesis rate begins to exceed the destruction rate, the concentration profile passes through a minimum and the ozone concentration increases. In the current investigation, the difference between this minimum and the maximum concentration that accumulates on any given day is known as the net ozone concentration. Since the initial (minimum) ozone concentration is always zero on the first day, the first-day maximum and net ozone concentrations are identical. This is not the case on the second and third days. The first-day net or maximum ozone concentration presumably reflects the ozone production potential of a "fresh" chemical system; whereas, the second-day net ozone represents the ozone production potential after one diurnal cycle and the third-day net ozone represents the ozone production potential after two diurnal cycles.



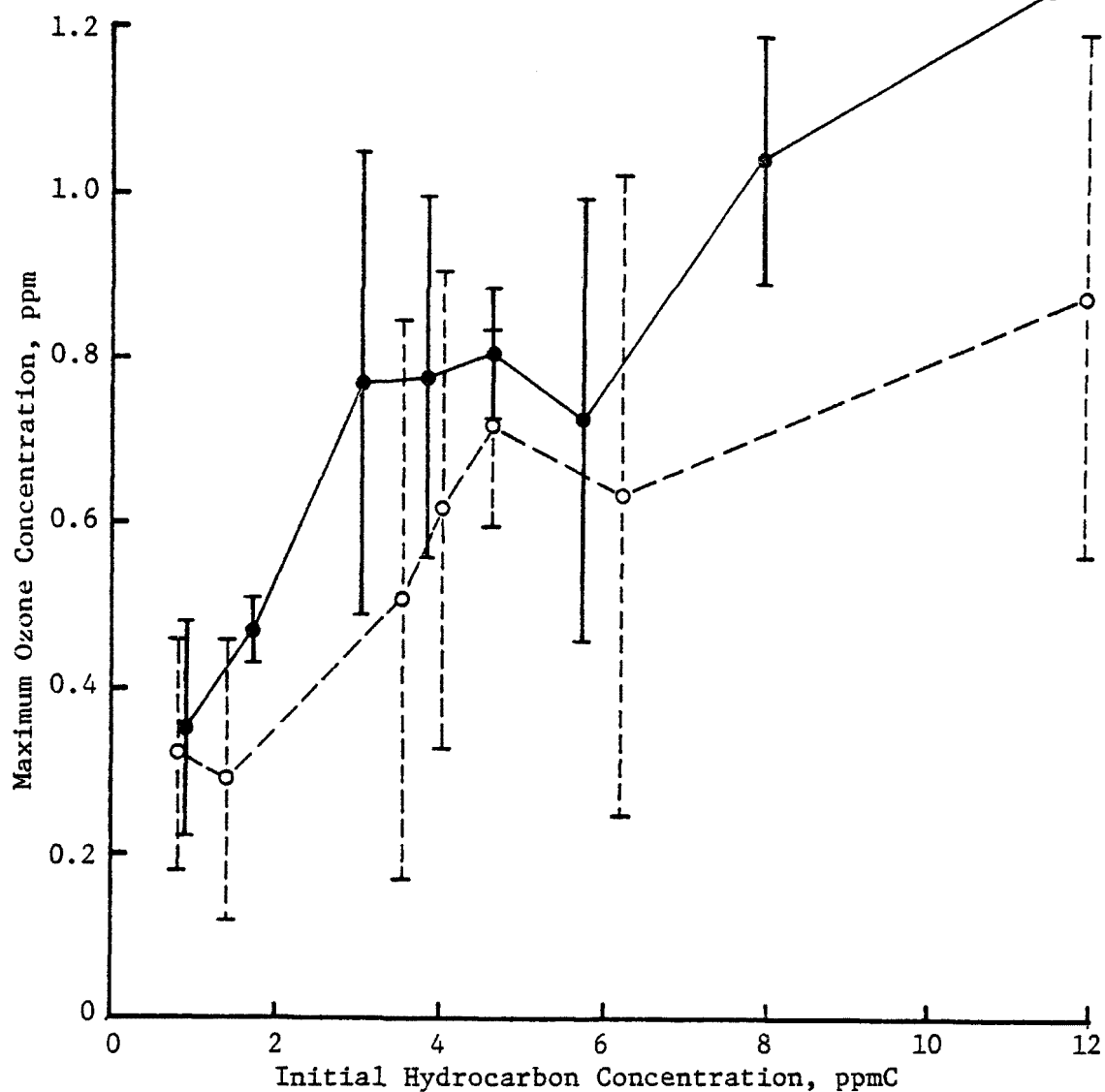


Figure 12. First-Day Maximum Ozone Concentrations Versus Initial Hydrocarbon Concentrations for All Experiments (---) and for Static Experiments (—). Points represent mean values; error bars represent  $\pm$  one standard deviation; and the absence of error bars indicates that only one data point was available.

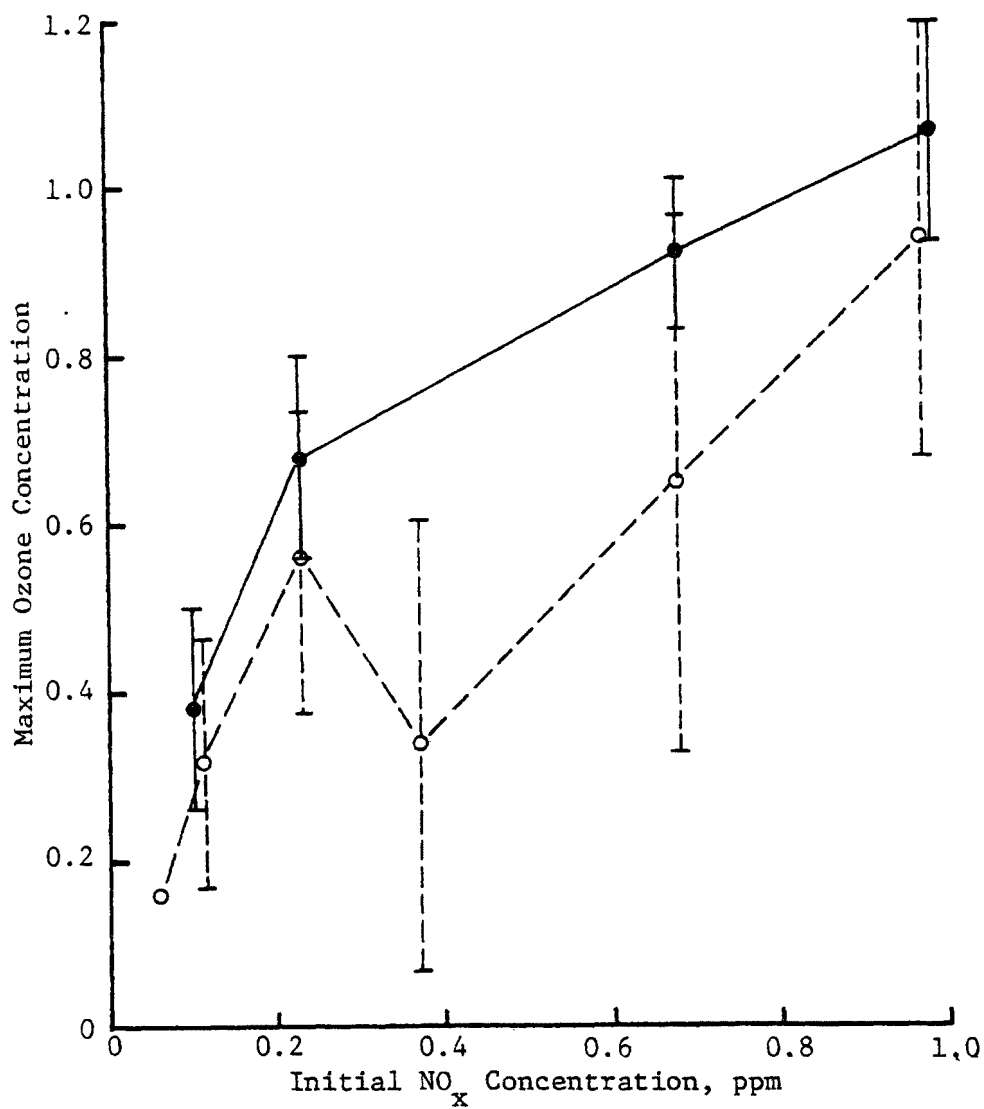


Figure 13. First-Day Maximum Ozone Concentrations Versus Initial NO<sub>x</sub> Concentrations for All Experiments (---) and for Static Experiments (—). Points represent mean values; error bars represent  $\pm$  one standard deviation; and the absence of error bars indicates that only one data point was available.

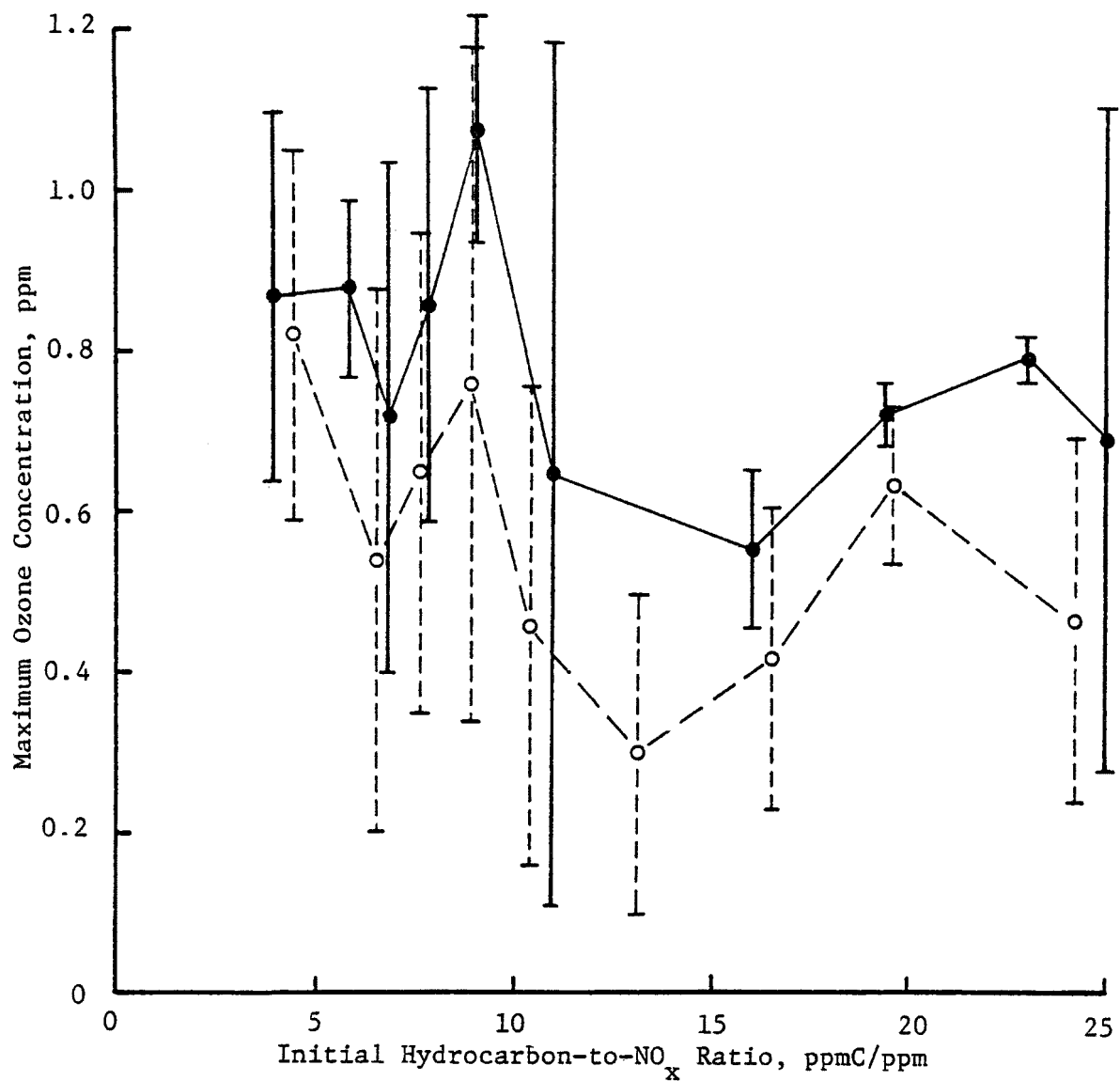


Figure 14. First-Day Maximum Ozone Concentrations Versus Initial Hydrocarbon-to-NO<sub>x</sub> Ratios for All Experiments (---) and for Static Experiments (—). Points represent mean values; error bars represent  $\pm$  one standard deviation.

Figure 13 is lower than might be anticipated. Three of the five data comprising this set are from experiments in which 95 percent dilution was initiated at sunrise and may be responsible for the indicated behavior. The results in Figure 14 are highly variable and permit few generalizations concerning the influence of initial NMHC/NO<sub>x</sub> ratio on the resulting maximum O<sub>3</sub> concentration.

Next, the data were further stratified to consider O<sub>3</sub> production under static conditions. First-day data from both static experiments and experiments in which dilution was initiated at 1700 were used, since for these dilution experiments, dilution was not commenced until after the maximum O<sub>3</sub> concentration had been achieved. The results for static conditions were treated similarly to those from the entire data set. Results are presented in Figures 12, 13, and 14 where they may be compared with those of the entire data set to permit a qualitative assessment of the effects of dilution. As shown in Figures 12 and 13, for these experiments the first-day [O<sub>3</sub>]<sub>max</sub> increases with increasing precursor concentration. Although the results in Figure 14 are highly variable, the maximum first-day O<sub>3</sub> concentration occurs at an initial NMHC/NO<sub>x</sub> ratio of approximately 9. In general, the behavior is similar for both sets of data. The effects of dilution on first-day ozone production are apparent in Figures 12, 13, and 14. In each case higher maximum O<sub>3</sub> concentrations were achieved for the static (no dilution) experiments than for the entire set of static and dilution experiments. More detailed assessments of the effects of dilution on O<sub>3</sub> production are presented in a subsequent subsection in which the results of individual experiments are analyzed.

To determine whether the net O<sub>3</sub> concentrations that were generated on subsequent days were affected by dilution, third-day results from all dilution experiments were considered. The resulting net O<sub>3</sub> concentrations are compared in Figures 15 and 16 with those from the static experiments. Similar trends are suggested by both figures--third-day net O<sub>3</sub> concentrations may increase slightly with increasing precursor concentration. In general, however, the variability of the data does not permit distinction between static and diluted conditions. Such a distinction is sought in subsequent analyses of individual experiments.

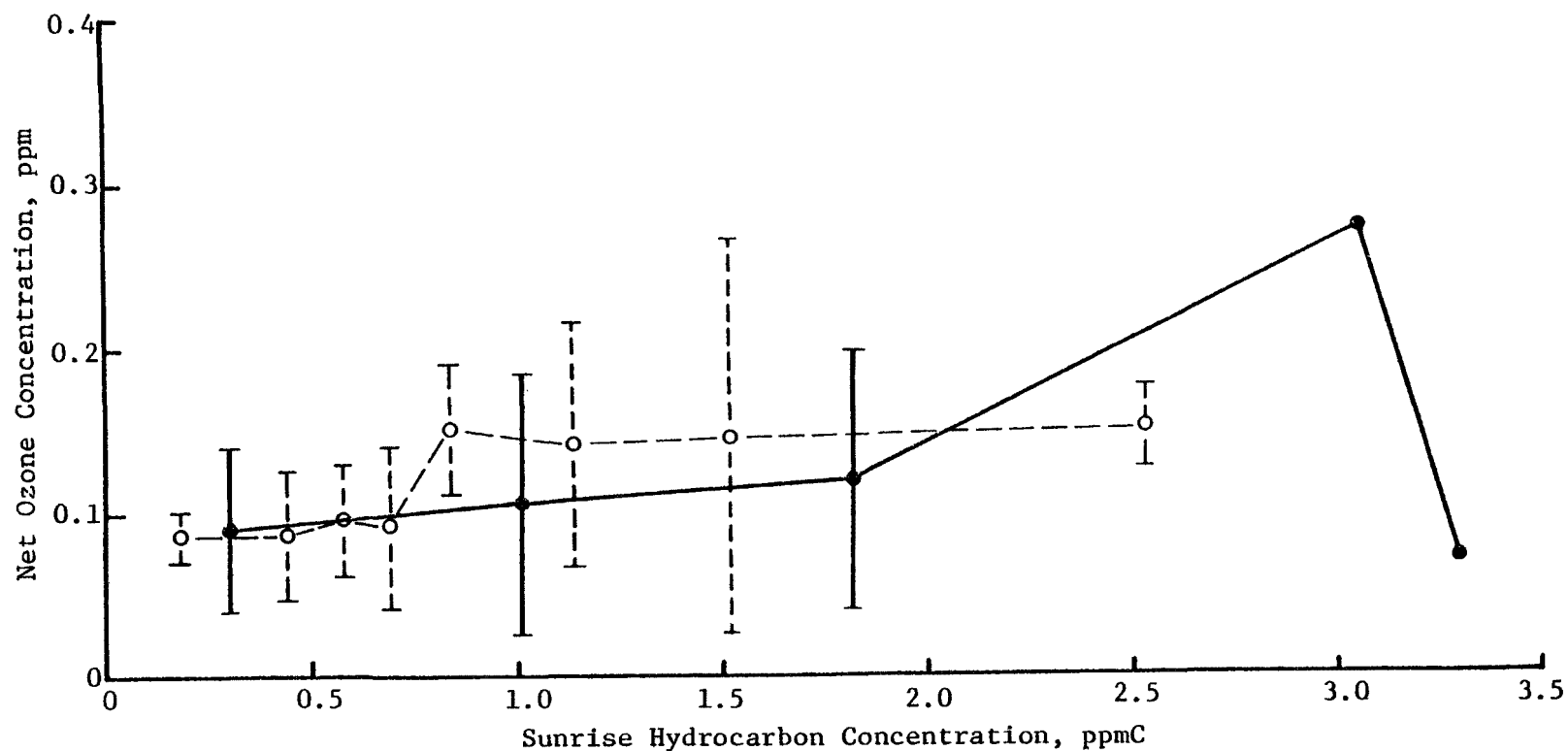


Figure 15. Third-Day Net Ozone Concentrations Versus Sunrise Hydrocarbon Concentrations for Dilution Experiments (---) and for Static Experiments (—). Points represent mean values; error bars represent  $\pm$  one standard deviation; and the absence of error bars indicates that only one data point was available.

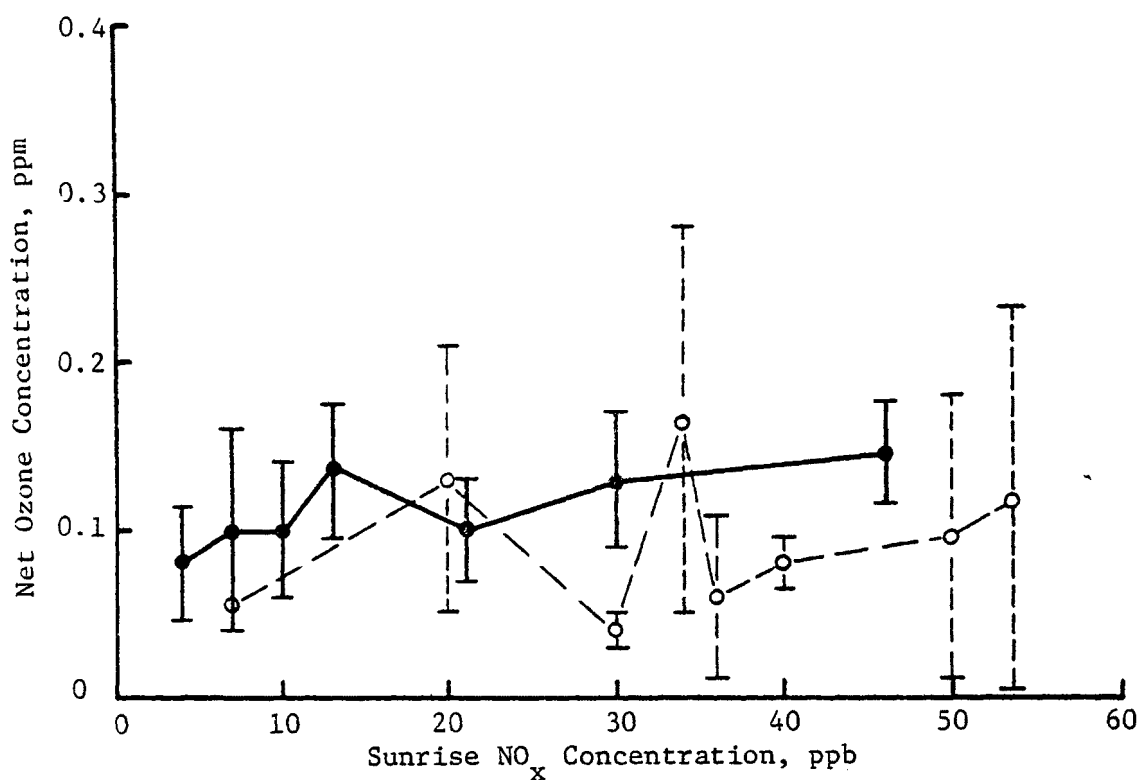


Figure 16. Third-Day Net Ozone Concentration Versus Sunrise NO<sub>x</sub> Concentrations for Static Experiments (---) and for Dilution Experiments (—). Points represent mean values; error bars represent  $\pm$  one standard deviation; and the absence of error bars indicates that only one data point was available.

### Analysis of Individual Experiments

The nine sets of four-chamber experiments that were considered in this analysis are also identified in Table 4. Data from these experiments were examined to determine the effects of such independent variables as initial [HC] and [NO<sub>x</sub>], dilution rate, and time of initiation of dilution on the maximum and net concentrations of ozone produced during each of the three days of an experiment.

The bar graphs of Figures 17, 18, and 19 may be used to compare maximum and net ozone production during static experiments with those from experiments conducted at various dilution rates. Experiments conducted at each of the four target initial [HC] and [NO<sub>x</sub>] conditions were considered as separate cases in each of these figures (case 1: 10 ppmC of HC/1 ppm of NO<sub>x</sub>; case 2: 5 ppmC/0.24 ppm; case 3: 5 ppmC/0.71 ppm; and case 4: 1 ppmC/0.1 ppm). Each of the figures is similar except for the time of initiation of dilution (Figure 17 at sunrise, Figure 18 at NO-NO<sub>2</sub> crossover, and Figure 19 at 1700). Also, the first bar for each day represents the results of the corresponding static experiment for that particular case.

Net O<sub>3</sub> concentrations are represented by the shaded areas and the minimum O<sub>3</sub> concentrations by the nonshaded areas. On the first day, the maximum and net O<sub>3</sub> concentrations are identical and are shaded. On the second and third days, the sum of the shaded and nonshaded areas represents the maximum O<sub>3</sub> concentration.

For the experiments in which dilution was initiated at sunrise (see Figure 17), the O<sub>3</sub> maxima decrease with increasing dilution rate on the first and second days, and in three of four cases on the third day. First-day O<sub>3</sub> maxima are greater than second-day values, which in turn exceed third-day values with only a single exception. Second- and third-day minimum O<sub>3</sub> levels decrease with increasing dilution rate. On the second day, the largest net O<sub>3</sub> occurs at 39 percent dilution--exceeding levels under both static and 95 percent dilution conditions. On the second day, at 95 percent dilution, the net [O<sub>3</sub>] exceeds the static levels in two of four cases. Third-day net [O<sub>3</sub>], compared to the second-day levels, increase for the static experiments but decrease for the dilution experiments with one exception.

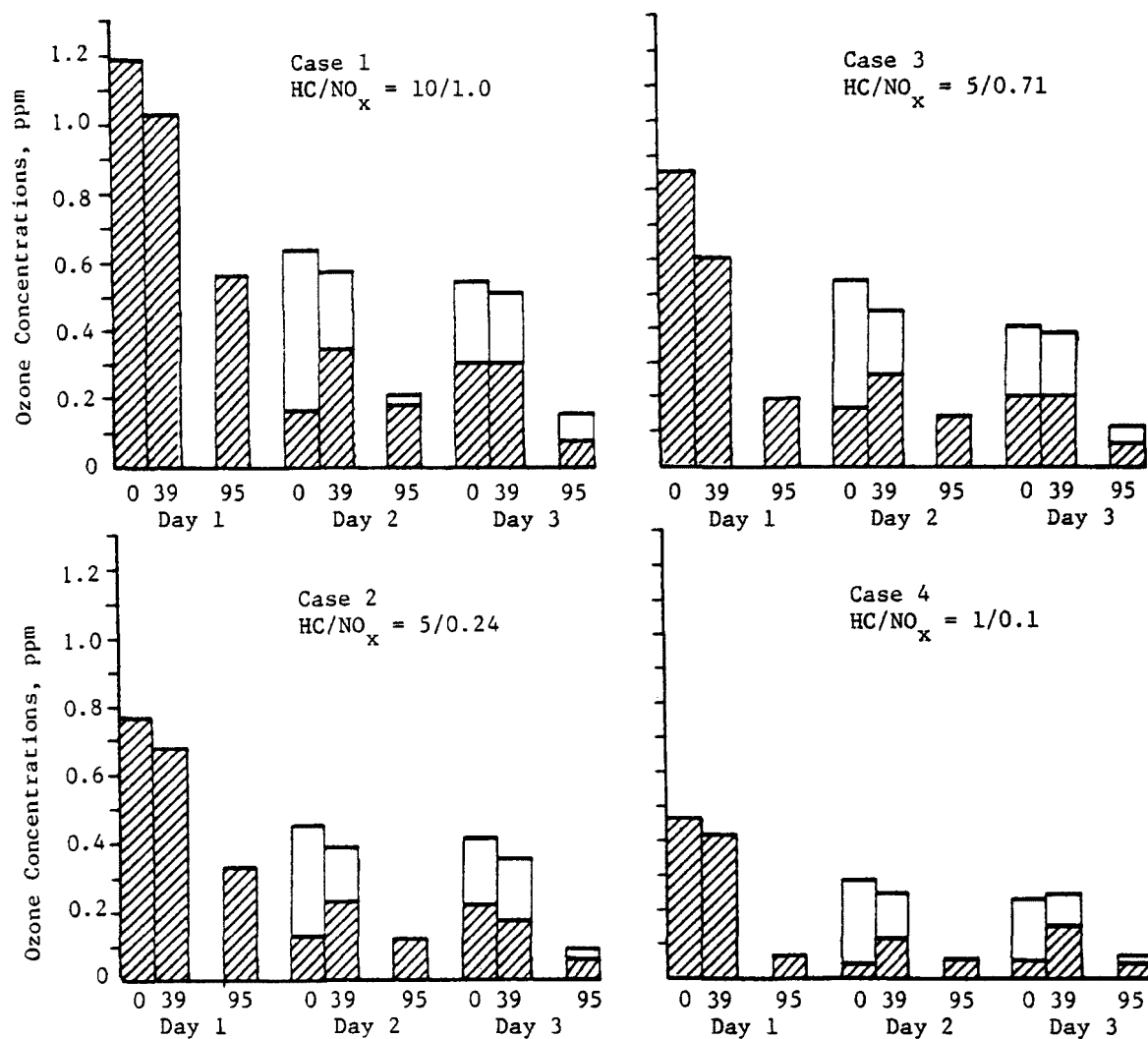


Figure 17. Maximum and Net Ozone Concentrations for Static Experiments and for Dilution Experiments Initiated at Sunrise (Shaded Areas are Net  $[O_3]$  and Open Areas are Minimum  $[O_3]$ ). Note that the first-day maximum net  $[O_3]$  are identical and that on subsequent days the maximum  $[O_3]$  equals the sum of the minimum and the net ozone concentrations.



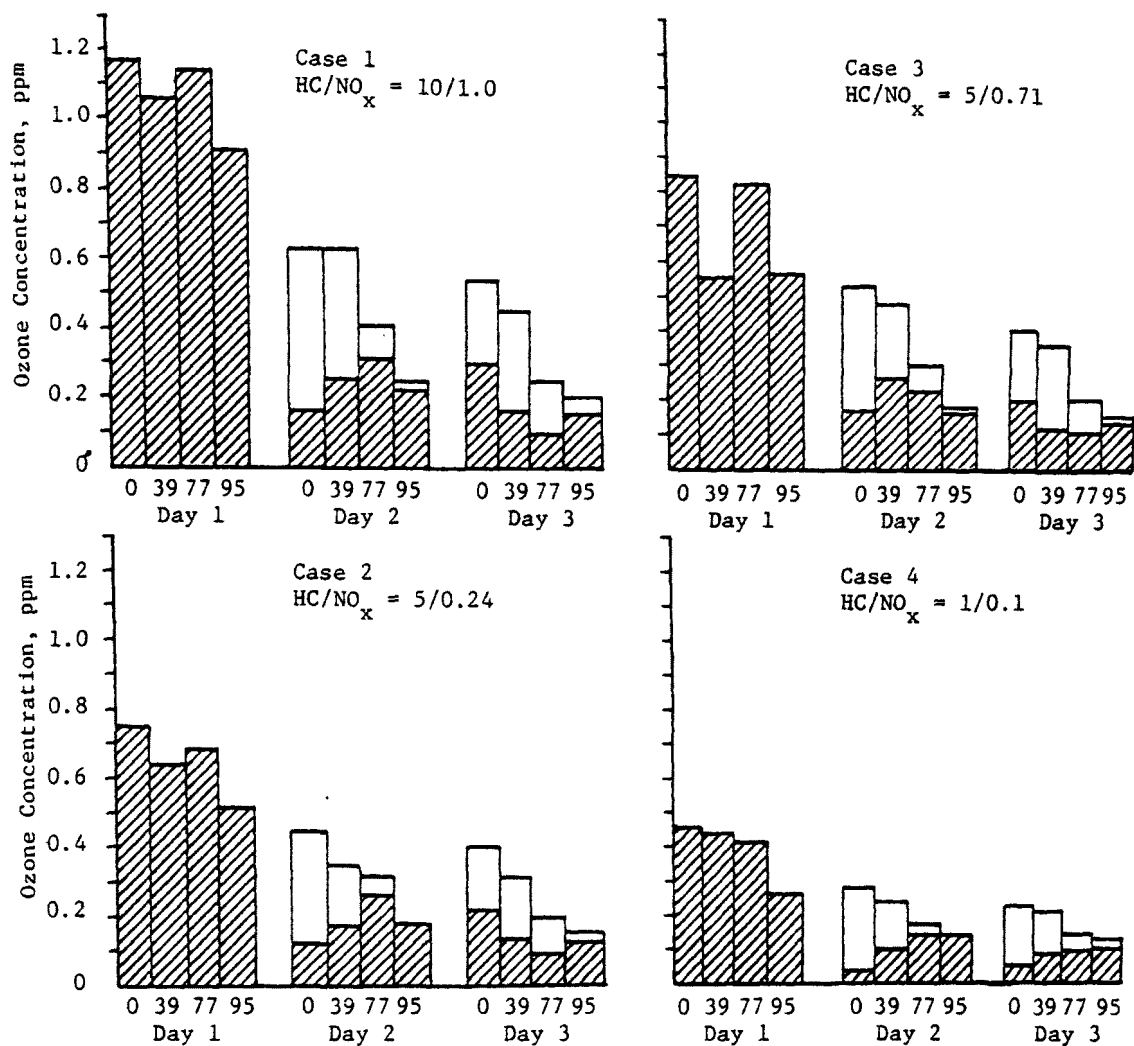


Figure 18. Maximum and Net Ozone Concentrations for Static Experiments and for Dilution Experiments Initiated at Crossover (Shaded areas are net [O<sub>3</sub>] and open areas are minimum [O<sub>3</sub>].) Note that the first-day maximum and net [O<sub>3</sub>] are identical and that on subsequent days the maximum [O<sub>3</sub>] equals the sum of the minimum and the net ozone concentrations.

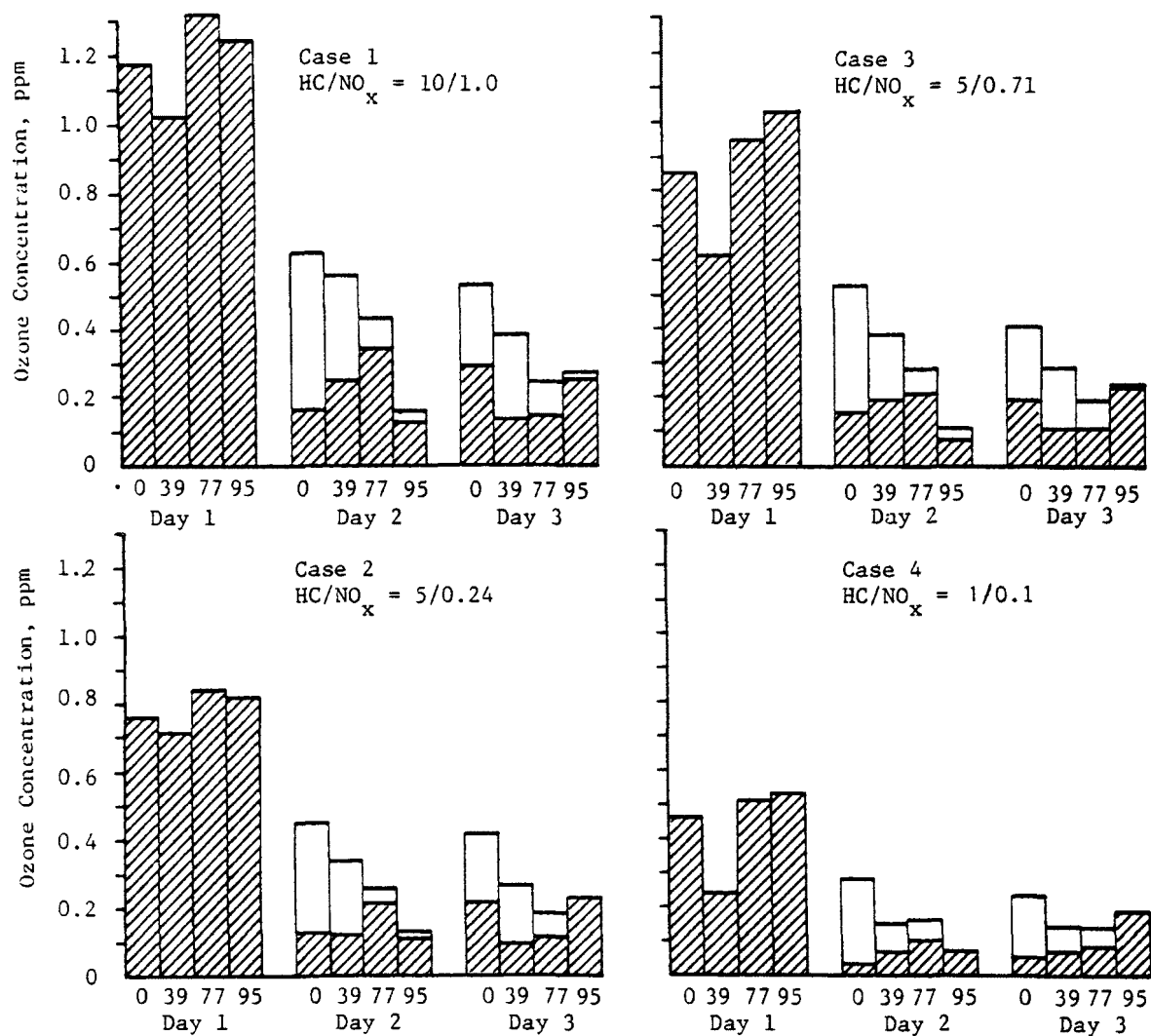


Figure 19. Maximum and Net Ozone Concentration for Static Experiments and for Dilution Experiments Initiated at 1700 (Shaded areas are net  $[O_3]$  and open areas are minimum  $[O_3]$ .) Note that the first-day maximum and net  $[O_3]$  are identical and that on subsequent days the maximum  $[O_3]$  equals the sum of the minimum and the net ozone concentrations.

Results from the experiments in which dilution was initiated at NO-NO<sub>2</sub> crossover are presented in Figure 18. If the first-day results from the 27 August 1975 experiment (39 percent dilution) are not considered, then the first-day O<sub>3</sub> maxima decrease with increasing dilution rate. Across all these experiments, the second- and third-day maxima also decrease with increasing dilution rate. First-day O<sub>3</sub> maxima are greater than second-day values, which in turn exceed third-day levels. Ozone minima decrease with increasing dilution rate on the second day and in two of four cases on the third day. Second-day net [O<sub>3</sub>] is greater for dilution than for static conditions, with the largest increase at 77 percent in three of four cases. Compared to second-day levels, third-day net [O<sub>3</sub>] increases for static experiments but decreases for dilution experiments.

Figure 19 depicts the results from experiments in which dilution was initiated at 1700. Since for these conditions dilution was initiated after the first-day O<sub>3</sub> maxima were achieved; comparison of the first-day maxima permits an assessment of precision under various environmental and operational conditions. Except for the 4 November 1975 experiment (39 percent dilution), which may have been heavily influenced by seasonal effects, the precision is excellent. With a single exception, the second-day O<sub>3</sub> maxima decrease with increasing dilution rate and, except at 95 percent dilution, this occurs on the third day as well. First-day O<sub>3</sub> maxima are greater than second-day values, which in turn exceed third-day levels except at 95 percent dilution. Ozone minima decrease with increasing dilution rates on the second day and, with a single exception, on the third day. On the second day the largest net [O<sub>3</sub>] occurs at 77 percent dilution. Net [O<sub>3</sub>] on the second day at 39 and 77 percent dilution exceeds the static values with a single exception. In three of four cases, however, the static levels exceed those at 95 percent dilution. The second-day net [O<sub>3</sub>] are greater than the third-day levels for 39 and 77 percent dilution; whereas the third-day levels are greater than the second-day values for the static and 95 percent dilution conditions. Third-day net [O<sub>3</sub>] at 95 percent dilution exceeds static levels in three of four cases and levels at 39 and 77 percent dilution. Static third-day net [O<sub>3</sub>] also exceeds levels at 39 and 77 percent dilution in three of four cases.

The maximum and net ozone results that are presented in Figures 17, 18, and 19 are displayed in an alternate format in Figures 20 and 21. Those experiments in which dilution was initiated at the same times are presented in each of three separate graphs within each of these figures. Within each graph the three run days are treated separately. The ozone concentrations achieved at each of the four target initial concentrations on a given day are plotted. It should be noted that Case 1 corresponds to target initial HC/NO<sub>x</sub> conditions of 10 ppmC/1 ppm, Case 2 to 5/0.24, Case 3 to 5/0.71, and Case 4 to 1/0.1. Thus, within each day the cases are ordered on the graphs such that they are in increasing order of both hydrocarbons and oxides of nitrogen concentrations (order: 4, 2, 3, 1). The connected symbols represent a common target dilution rate. Results from both static and dilution experiments are included to permit their comparison. It should also be noted that since first-day maximum and net ozone concentrations are identical, the first-day results in Figures 20 and 21 are also identical.

Ozone maxima shown in Figure 20 generally increase with increasing precursor concentration. First-day ozone maxima display an increasing trend with both hydrocarbon and NO<sub>x</sub> concentrations. The erratic first-day behavior of Case 3 is due to the low HC/NO<sub>x</sub> ratio for this case. Under these conditions, NO<sub>x</sub> is in excess and the formation of O<sub>3</sub> may be slowed by NO inhibition. Thus, the system may tend to be light-limited and therefore more sensitive to environmental variables than the other cases. The erratic behavior noted on the first day of Case 3 is not present on the second and third days.

Maximum ozone concentrations on both the second and third days generally increase with increasing first-day precursor concentration and also with increasing first-day maximum ozone. Thus, based on maximum daily concentrations, it is difficult to separate the influence of second- and third-day ozone generation by precursors remaining after the first day's reaction from the fraction of first-day ozone that remains on subsequent days. This consideration prompted the development of the net ozone analysis.

Under both static and dilution conditions (except 95 percent at 1700), first-day ozone maxima are greater than second-day values, which in turn are greater than third day levels.

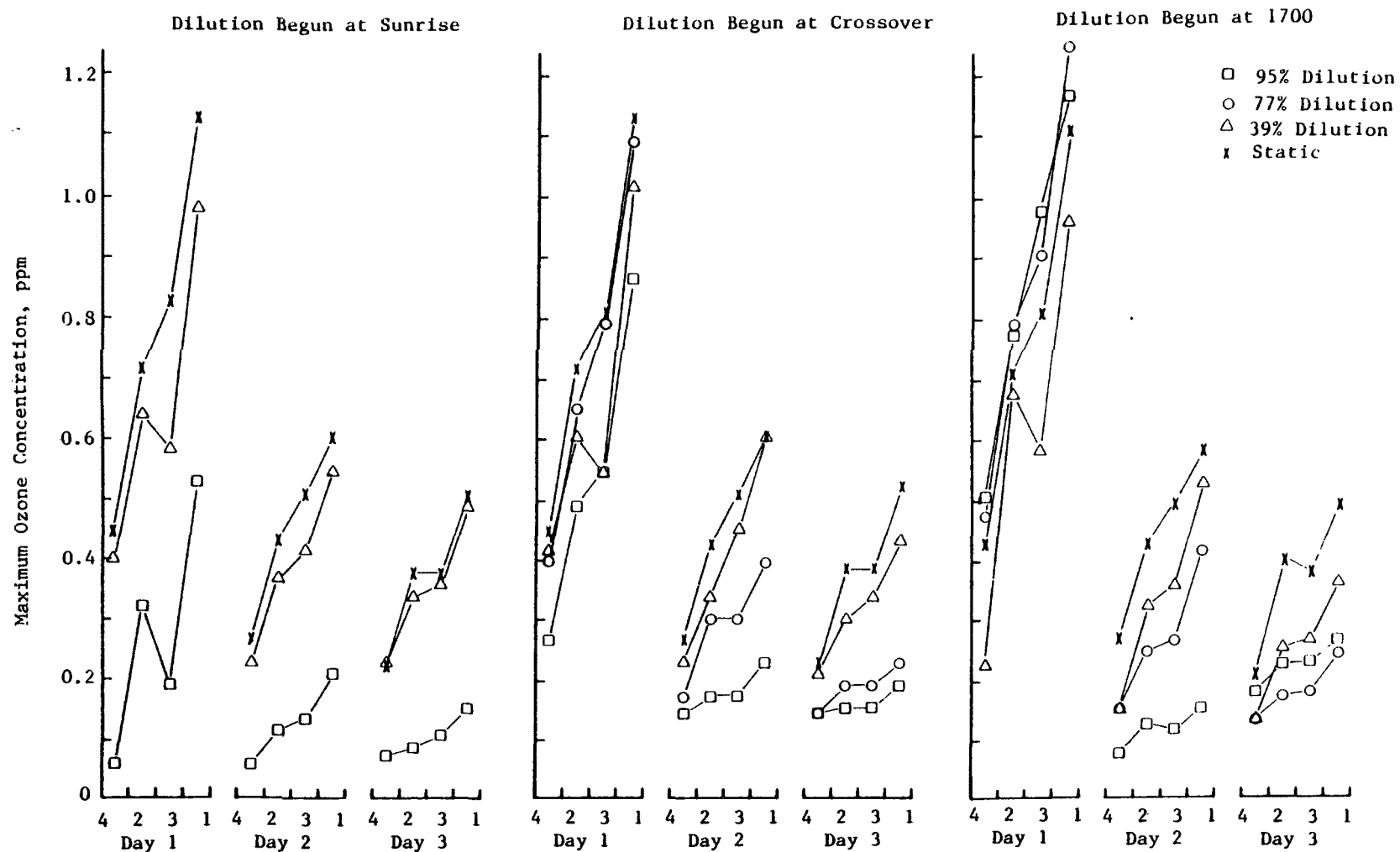


Figure 20. Maximum Ozone Concentrations Plotted by Case Number and Day for Dilution Beginning at Sunrise, 1700, and Crossover.

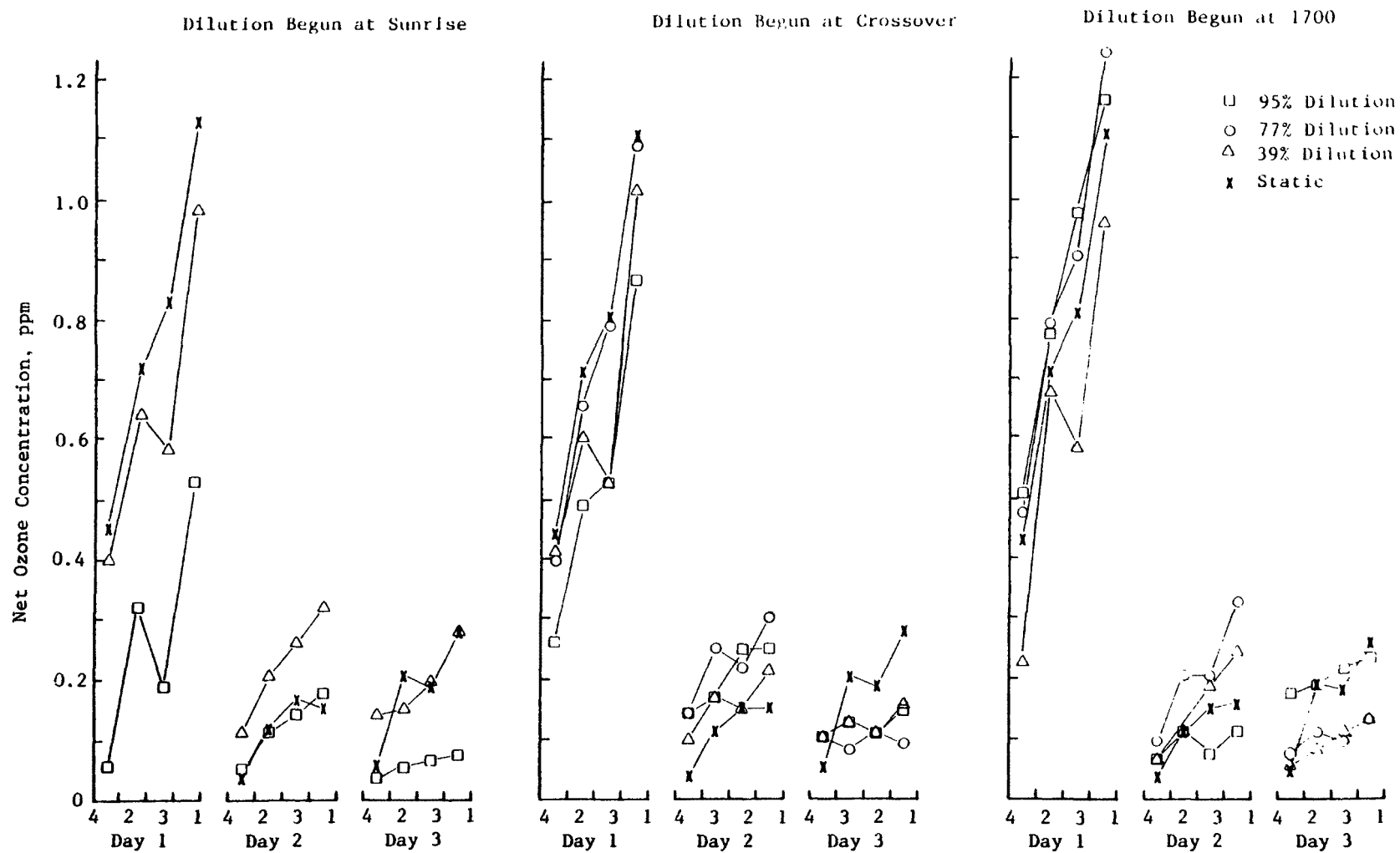


Figure 21. Net Ozone Concentrations Plotted by Case Number and Day for Dilution Beginning at Sunrise, 1700, and Crossover.

In no case examined in the current study did dilution cause first-day ozone levels to exceed those of corresponding static experiments.\* Although increased first-day ozone concentrations under dilution conditions have been reported<sup>42,43</sup>, no attempt was made in the current study to duplicate the reported conditions. During 18 November 1975 experiments, however, the maximum ozone concentrations generated under different dilution conditions were comparable. In this experiment each chamber had the same target initial HC and NO<sub>x</sub> conditions (5.0 ppmc and 0.24 ppm). Different dilution rates were initiated in each chamber at NO-NO<sub>2</sub> crossover. Under static conditions the [O<sub>3</sub>]<sub>max</sub> was 0.49 ppm; at 39 percent dilution 0.49 ppm; at 77 percent 0.39 ppm, and at 95 percent 0.32 ppm. Thus, it seems likely that under the appropriate conditions, maximum ozone concentrations generated under dilution conditions could exceed the corresponding static levels.

For those cases in which dilution was begun at sunrise or at crossover, first-day maximum ozone concentrations are generally reduced by dilution. This reduction is most apparent at 95 percent dilution. The impact of dilution on first-day [O<sub>3</sub>]<sub>max</sub> is more apparent when dilution was initiated at sunrise than at crossover.

Second- and third-day static O<sub>3</sub> maxima are greater than the concentrations achieved in experiments in which dilution occurred. At a fixed time of initiation of dilution, maximum second- and third-day O<sub>3</sub> concentrations decrease with increasing dilution rate (except 95 percent at 1700). Although dilution acted to reduce second- and third-day [O<sub>3</sub>]<sub>max</sub>, the reduction was always less than proportional to the extent of dilution at the time of occurrence of the maximum concentration.

The second- and third-day net ozone concentrations presented in Figure 21 display a slight trend toward increasing with increasing first-day precursor concentration and also with increasing first-day maximum ozone levels. If it is assumed that the amount of ozone remaining from the first day does not influence second- and third-day ozone generation, then these results suggest that the apparent trend is caused by increased absolute quantities of precursors remaining on subsequent days after the first day's reaction.

---

\*Note that experiments in which dilution was initiated at 1700 were not considered, since the late introduction of dilution could not have influenced the first-day maxima.

It should be noted, however, that the net ozone concentrations on second and third days are frequently of the same magnitude as concentrations observed in purified air irradiations. Thus, the extent to which the chambers themselves affect the second- and third-day results cannot be defined at this time.

In general, the second-day net ozone concentrations in dilution experiments are greater than the corresponding third-day levels (except for 95 percent dilution at 1700).<sup>\*</sup> For static conditions, however, third-day net ozone concentrations are greater than second-day levels.

With few exceptions (95 percent dilution at sunrise and at 1700) the second-day net ozone concentrations in dilution experiments are greater than or equal to those for static experiments. Second-day net ozone concentrations generated at 39 and 77 percent dilution generally exceed those for static and 95 percent dilution. In contrast, except for case 4, the third-day net ozone concentrations in static experiments are greater than those for dilution experiments. There are no apparent trends for third-day net results under dilution conditions.

The amount of net ozone produced on the second and third day falls between 0.08 and 0.30 ppm in 80 percent of the cases. Thus, in the RTI smog chambers, aged photochemical systems displayed relatively high ozone-generative potentials.

The following generalizations may be drawn from inspection of Figures 17 through 21.

- For those experiments in which dilution was initiated before the maxima occurred, maximum first-day ozone concentrations are reduced under dilution in comparison to static conditions. In no case examined in the current study did dilution cause first-day ozone levels to exceed those of the corresponding static experiments.
- Second- and third-day ozone maxima also decrease with increasing dilution rate. The decrease is less than proportional to the extent of dilution.

---

<sup>\*</sup>Under these conditions, dilution was occurring at the time of maximum  $[O_3]$  on the second day; whereas dilution was not occurring on the third day. Thus, the impact of dilution at a high rate (95 percent) on the second day was sufficient to reduce the observed second-day ozone concentrations below those achieved during static conditions on the third day.



- First-day  $O_3$  maxima are greater than those produced on the second day, and second-day maxima are greater than those produced on the third day under static and dilution conditions.
- On both the second and third days, the minimum  $O_3$  concentrations decrease with increasing dilution rate.
- The second-day net ozone concentrations at 39 or 77 percent dilution are greater than at the corresponding levels under static conditions.
- The second- and third-day net ozone concentrations generated under dilution conditions may be greater than the corresponding levels under static conditions, although the maxima are lower. Thus, the maximum second- and third-day ozone concentrations are reduced by dilution but the ozone-generative potential is not.
- For dilution conditions, the second-day net ozone concentrations exceed third-day levels, while for static conditions the third-day levels exceed those for the second day.
- Second- and third-day net  $[O_3]$  generally range between 0.08 and 0.30 ppm. Thus the ozone-generative potential of aged photochemical systems in the RTI smog chambers is high and usually exceeds 0.08 ppm.

For experiments in which dilution was initiated before the first-day maximum  $O_3$  concentration occurred, dilution is expected to influence the behavior of the chemical systems in comparison to those of the corresponding static cases. On the average for static experiments, NO-NO<sub>2</sub> crossover was achieved 2.2 hours after sunrise at approximately 0734 EST. Chamber 2 with the highest target initial HC/NO<sub>x</sub> ratio (5.0/0.24) was the first to achieve crossover at 1.6 hours after sunrise. The lowest initial target HC/NO<sub>x</sub> ratio was in Chamber 3 (5.0/0.71), which was the slowest to achieve crossover at 3.1 hours after sunrise. Chambers 1 and 4 required intermediate times, 1.7 and 2.4 hours. The time to crossover may be reduced under dilution conditions.<sup>42,43</sup> Examination of the current data set for such comparisons, however, revealed too few cases to yield conclusive results.

The time required to achieve the first-day maximum  $O_3$  concentration was reduced under dilution conditions. In comparison to the time required under static conditions, the time to  $[O_3]_{\max}$  was reduced when dilution was initi-

ated at NO-NO<sub>2</sub> crossover. The time to [O<sub>3</sub>]<sub>max</sub> was reduced to a greater extent when dilution was initiated at sunrise. On the average, [O<sub>3</sub>]<sub>max</sub> was achieved at 9.4 hours after sunrise for the static runs. When dilution was initiated at NO-NO<sub>2</sub> crossover, [O<sub>3</sub>]<sub>max</sub> was achieved at 8.7 hours after sunrise, while the corresponding time requirement when dilution was initiated at sunrise was 7.8 hours.

The effect of dilution on the absolute magnitude of the first-day [O<sub>3</sub>]<sub>max</sub> can be explored by examination of Figure 22. The O<sub>3</sub> concentrations in these bar graphs are represented as percentages of the first-day [O<sub>3</sub>]<sub>max</sub> achieved under static conditions. These percentages are given at each of the tested dilution rates for each of the four target initial HC/NO<sub>x</sub> ratios. Also shown in these illustrations by broken lines is the theoretical percentage of the static [O<sub>3</sub>]<sub>max</sub> that would have resulted if the ozone produced with dilution were equal to the fraction of the chamber's volume that was present when the [O<sub>3</sub>]<sub>max</sub> was achieved.

In 13 of 20 dilution experiments, the ozone production exceeded the quantity expected if first-day ozone production were proportional to the extent of dilution. Although seasonal effects may account for the discrepancy between theoretical and achieved [O<sub>3</sub>]<sub>max</sub> for the 95 percent sunrise dilution experiments of 29 September 1975, in only three of the eight sunrise dilution cases does the measured [O<sub>3</sub>]<sub>max</sub> exceed the theoretical value.

In 10 of 12 crossover dilution cases the measured [O<sub>3</sub>]<sub>max</sub> exceeds the theoretical value. For many of these experiments the theoretical value is exceeded by over 30 percent.

These results suggest that in photochemically reacting systems of surrogate urban hydrocarbons and NO<sub>x</sub>, ozone production is sensitive to the time at which dilution is initiated. When dilution is begun at sunrise, ozone production may be reduced more nearly in proportion to the extent of dilution than when dilution is initiated at NO-NO<sub>2</sub> crossover. This behavior is somewhat surprising when it is considered that the average delay between sunrise and NO-NO<sub>2</sub> crossover is only 2.2 hours--from 0524 to 0734 EST.

When dilution is initiated at sunrise, the photochemical reactions are also being initiated. Dilution removes precursors that are important to the establishment and maintenance of various sequences of reactions instrumental in the generation of ozone. When dilution is initiated after photochemical

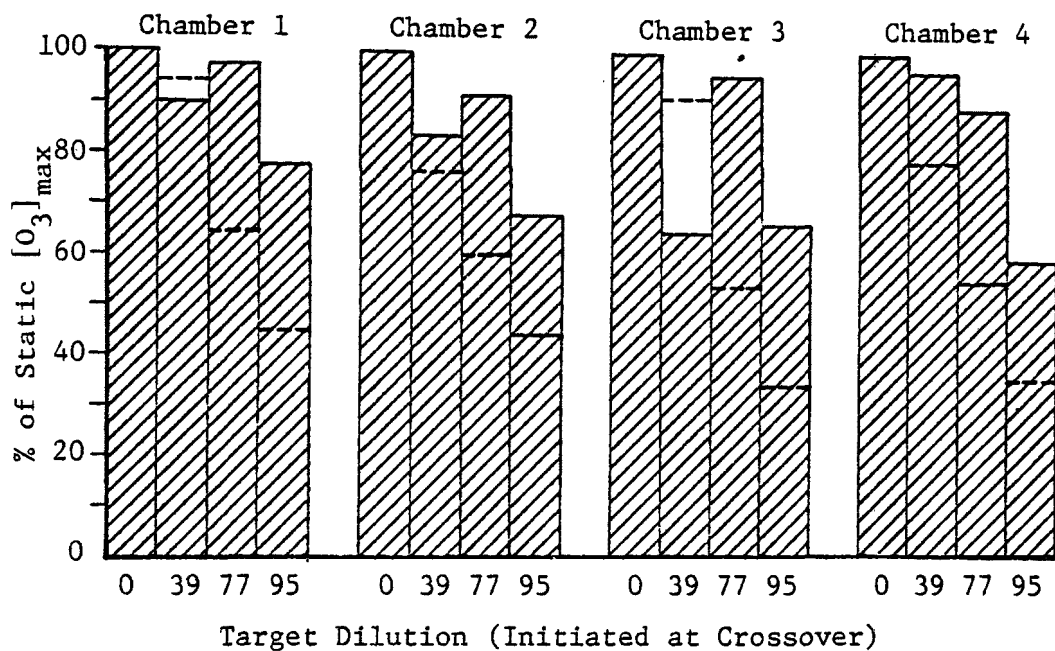
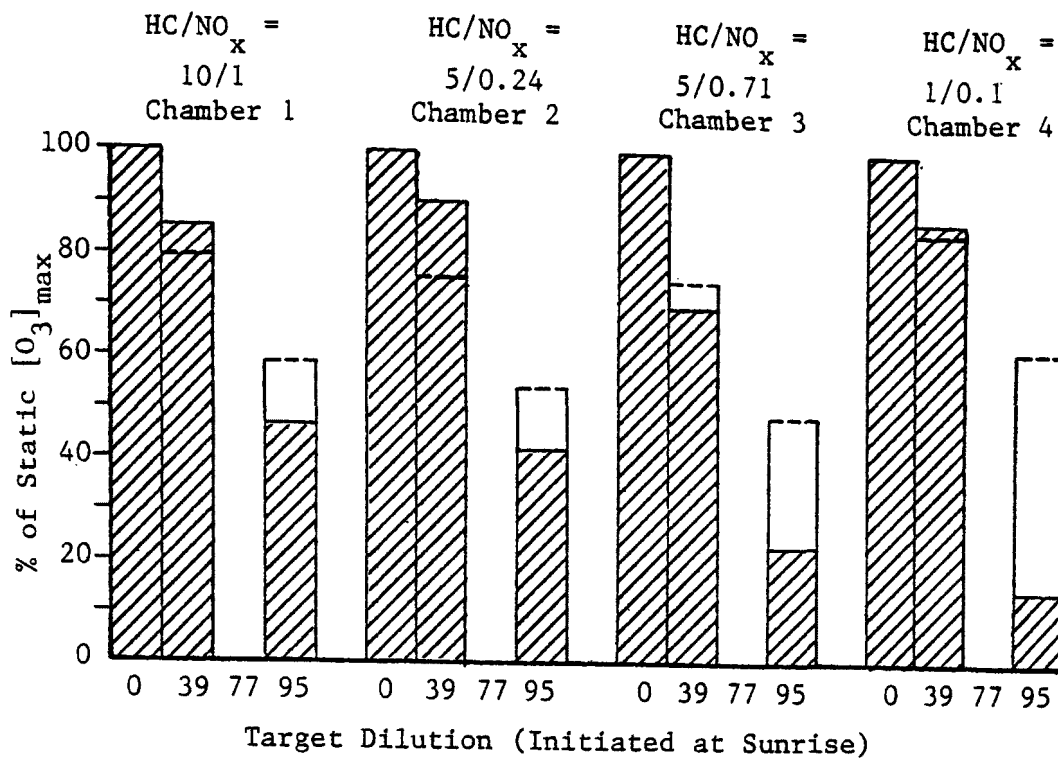


Figure 22. Maximum Ozone Concentrations Under Dilution Conditions Relative to the Maximum Ozone Concentration Obtained Under Static Conditions (Shaded area represents the percentage of the static maximum ozone concentrations achieved under dilution conditions; the broken line represents the percentage of the static maximum concentration estimated by applying the appropriate dilution factor to the static maximum ozone concentration.)

initiation reactions have occurred, the resulting oxidation of NO to NO<sub>2</sub> is well on its way toward establishing an appropriate ratio to permit ozone accumulation. Thus the finding that the [O<sub>3</sub>]<sub>max</sub> is sensitive to the time of initiation of dilution does not seem unreasonable in terms of the current understanding of the sequence of events leading to photochemical ozone generation. It is likely, however, that additional experimental investigations supplemented with modeling efforts will be required to identify the detailed mechanistic subtleties responsible for the observed behavior.

The findings that first-day ozone-generative potential is sensitive both to the dilution rate experienced by the reacting system and to the time at which dilution is initiated have implications to the real atmosphere. The descriptive discussion of urban meteorology and chemistry in Section 3 suggests that significant dilution begins at 0830 to 0930--3 to 4 hours after sunrise. The average time of crossover in the current study was 0734, 2.2 hours past sunrise. In addition, it is suggested that early morning (0600 to 0900 CST) hourly average NO<sub>x</sub> data indicate that up to 80 percent of the NO<sub>x</sub> may exist as NO<sub>2</sub>. Thus, if the St. Louis atmosphere is representative of most urban areas and if the current findings may be extrapolated to the larger dilution rates that prevail in an urban atmosphere, then the effects of atmospheric mixing on maximum urban ozone concentrations are less than proportional to the extent of dilution of the air parcel.

#### EXPERIMENTS CONDUCTED TO PROVIDE DATA FOR MODEL TESTING

Eight experiments were conducted in October of 1976 to provide EPA with data for model verification and testing. In these experiments, mixtures of propene and NO<sub>x</sub> were irradiated. Results from these experiments are summarized in Table 14, and individual data are presented in Volume 2 (Appendixes A and B).

The experiments conducted on 6 October in Chamber 3 and on 11 October in Chambers 3 and 4 can be compared directly. On 6 October the sunlight profile was "choppy" after 1015 EST. The solar radiation integrated both to the time of [O<sub>3</sub>]<sub>max</sub> and for the complete days was slightly higher on 11 October than on 6 October. In spite of the differences in irradiation, a higher ozone concentration was observed on 6 October. Inspection of the maximum ambient temperature levels on these two days suggests that the

TABLE 14. SUMMARY OF RESULTS FROM EXPERIMENTS CONDUCTED TO  
PROVIDE DATA FOR MODEL TESTING<sup>a</sup>

Run	T <sub>max</sub> °C	ΣSR Langleys	Chamber 1	Chamber 2	Chamber 3	Chamber 4
10-6-76	25.0	377				
HC			Propene	Propene	Propene	Propene
[HC]i <sup>b</sup>			1.35 (1.5) <sup>e</sup>	0.64 (0.7)	1.21 (1.5)	- (0)
[NO <sub>x</sub> ]i <sup>c</sup>			0.14 (0.1)	0.52 (0.5)	0.53 (0.5)	0.098 (0.1)
HC/NO <sub>x</sub> <sup>d</sup>			9.6 (15.0)	1.2 (1.4)	2.3 (3.0)	- (-)
t <sub>xo</sub>			8.39	10.34	9.45	14.63
[O <sub>3</sub> ] <sub>max</sub> <sup>c</sup>			0.39	0.08	0.47 <sup>f</sup>	0.009
10-11-76	18.9	420				
HC			Propene	Propene	Propene	Propene
[HC]i			0.68 (0.7)	2.36 (3.0)	1.26 (1.5)	1.17 (1.5)
[NO <sub>x</sub> ]i			1.57 (1.5)	1.68 (1.5)	0.55 (0.5)	0.50 (0.5)
HC/NO <sub>x</sub>			0.43 (0.47)	1.4 (2.0)	2.3 (3.0)	2.3 (3.0)
t <sub>xo</sub>			<sup>g</sup>	10.17	9.59	9.83
[O <sub>3</sub> ] <sub>max</sub>			0.00	0.02	0.37 <sup>f</sup>	0.25

<sup>a</sup>For individual data see Volume 2 (Appendixes A and B).

<sup>b</sup>Units ppmC of propene only; total hydrocarbon concentration slightly higher; see Appendix A.

<sup>c</sup>Units ppm.

<sup>d</sup>t<sub>xo</sub> is time of NO-NO<sub>2</sub> crossover in hours EST.

<sup>e</sup>Numbers in parentheses represent target values.

<sup>f</sup>Mixing fan turned off shortly after injection.

<sup>g</sup>Crossover did not occur.

6.1° C warmer conditions on 6 October may have been partially responsible for the higher ozone concentration on this day. This is consistent with the results of propane irradiations discussed in a subsequent section of this report.

The effects of stirring were examined in Chambers 3 and 4 on 11 October. Although a higher  $[O_3]_{\max}$  was observed in this single experiment with the mixing fan turned off shortly after reactant injection, the initial conditions were not identical, and this difference may be responsible for the apparent discrepancy. It is recommended that additional experiments be conducted to address this issue.

A comparison of results from experiments conducted in the RTI outdoor chambers with results from the evacuable indoor chamber at the Statewide Air Pollution Research Center (SAPRC)<sup>17</sup> at Riverside, California, is presented in Table 15. The agreement is generally good: the  $[O_3]_{\max}$  levels in the RTI experiments generally exceed those of the SAPRC experiments. The apparent agreement may be fortuitous in view of the differences in operating conditions for the two very different types of smog chambers. Ambient diurnal temperature and solar radiation profiles define the environmental conditions employed at the RTI facility. The duration of irradiation is normally 12 hours, from sunrise until sunset. In contrast, the SAPRC facility is operated at fixed temperature and irradiation intensity. The duration of SAPRC experiments is normally 6 hours.

#### OZONE-GENERATIVE POTENTIAL OF LOW REACTIVITY HYDROCARBONS

Hydroxyl radical attack on hydrocarbons is thought to be the major removal mechanism for these species in reacting photochemical HC/NO<sub>x</sub> systems. The rate constant for OH attack on olefinic hydrocarbons is much greater than that for alkane hydrocarbons. This accounts for the more rapid depletion of olefins in comparison to alkanes that has been observed both in ambient air and in smog chamber studies. Hydrocarbon data collected in the urban mix runs of the current study and presented in Volume 2 (Appendix A) confirm these observations.

The ozone-generative potential of many organics was established based on studies conducted in smog chambers. In an effort to reduce photochemical formation of ozone in polluted atmospheres, regulations on solvent emissions

TABLE 15. COMPARISON OF RTI OUTDOOR SMOG CHAMBER RESULTS  
WITH RESULTS FROM SAPRC INDOOR CHAMBER<sup>17</sup>

Run	T <sup>a</sup> °C	[HC]i ppmC	HC/NO <sub>x</sub> ppmC/ppm	[O <sub>3</sub> ] <sub>max</sub> ppm
RTI No. 1 10-6-76	25.0	1.35	9.6	0.39
EC - 11	29.7	1.34	9.9	0.23
RTI No. 3 10-6-76	25.0	1.21	2.3	0.47 <sup>b</sup>
RTI No. 3 10-11-76	18.9	1.26	2.3	0.37
RTI No. 4 10-11-76	18.9	1.17	2.3	0.25
EC - 7	30.9	1.41	2.4	0.38 <sup>c</sup>
EC - 13	29.2	1.50	2.6	0.37
EC - 57	30.1	1.59	2.7	0.24
EC - 52	30.1	1.65	2.8	0.31
EC - 51	30.0	1.66	2.9	0.29

<sup>a</sup>T is maximum daily temperature for RTI experiments; T is average run temperature for SAPRC experiments

<sup>b</sup>Mean RTI [O<sub>3</sub>]<sub>max</sub> = 0.36 ± 0.11 ppm.

<sup>c</sup>Mean SAPRC [O<sub>3</sub>]<sub>max</sub> = 0.32 ± 0.06 ppm.

were established to limit emissions of reactive organics and to be less restrictive on emissions of organics considered to be nonreactive. Through substitution of less reactive organics for the more reactive ones, not only could an increase in organic emissions result, but the substitute compounds such as alkane hydrocarbons, by virtue of their low reactivity, could persist in air parcels transported downwind from urban areas.

Results from the current study suggest that on the second and third days, early morning HC/NO<sub>x</sub> ratios were high, alkane hydrocarbons persisted, the ozone-generative potential was high, and the net ozone on both days generally exceeded 0.08 ppm. Other smog chamber studies have shown alkane hydrocarbons to produce considerable amounts of ozone when irradiated in the presence of NO<sub>x</sub> at high HC/NO<sub>x</sub> ratios.<sup>9,26,44-47</sup>

Dimitriades has recently suggested a procedure to identify low reactivity organics as those which would not under any circumstances yield ozone concentrations greater than 0.08 ppm.<sup>47</sup> The results of EPA smog chamber studies conducted at initial HC/NO<sub>x</sub> conditions of 4 ppm (v/v)/0.2 ppm were reported to suggest that propane is the boundary point between reactive and nonreactive organics. The experiments discussed in this section of the report were conducted to examine the ozone-generative potential of the nonreactive hydrocarbons, propane, ethane, and acetylene in light of the results of Dimitriades.

On 8 September 1976 four experiments were conducted with low reactivity hydrocarbons. Ethane, acetylene, and propane were investigated separately in each of three chambers. Target initial conditions were 4 ppm (v/v) of the hydrocarbon and 0.2 ppm NO<sub>x</sub> (20% NO<sub>2</sub>). The fourth chamber was employed as a control: 0.2 ppm NO<sub>x</sub> was added to purified air in this experiment. First-day maximum O<sub>3</sub> concentrations were high in the first three chambers: ethane produced 0.32 ppm; acetylene 0.45 ppm; and propane 0.65 ppm. A maximum ozone concentration of only 0.02 ppm was observed in the control experiment.

The significant differences between these results and those of Dimitriades,<sup>47</sup> prompted experiments to determine if the high concentrations were caused by chamber-related effects. Matched experiments involving the four RTI chambers and two UNC chambers were conducted on 20 September 1976.<sup>†</sup> The

---

<sup>†</sup>This experiment is discussed in detail in a subsequent section of this report.



same target initial conditions were employed that were used in the 8 September propane experiment. The average  $[O_3]_{\max}$  produced in the six chambers was  $0.21 \pm 0.03$  ppm. The close agreement between chambers having similar initial reactant conditions, experiencing similar environmental conditions, but having significant differences in volume and configuration suggests that chamber-related effects were not responsible for the high ozone concentrations produced on 8 September and again on 20 September. It is suggested that environmental differences were responsible for the absolute discrepancy in  $[O_3]_{\max}$  values observed on these two days (0.65 versus 0.22 ppm).

Four additional experiments were conducted to elucidate the ozone-generative potential of propane. On 27 October 1976, propane/ $NO_x$  mixtures were irradiated in three chambers, and the fourth was employed as a control. The same target initial HC/ $NO_x$  ratio of 60 ppmC/ppm was employed; however, target initial HC concentrations of 12, 6, and 3 ppmC were used to examine the effect of changing absolute concentration at a fixed HC/ $NO_x$  ratio on ozone production. At target initial HC/ $NO_x$  conditions of 12 ppmC and 0.2 ppm, an  $[O_3]_{\max}$  of 0.028 ppm was produced. No consistent trend was observed with decreasing absolute HC concentration. In the fourth chamber, purified air plus 0.06 ppm  $NO_x$  produced an  $[O_3]_{\max}$  of 0.002 ppm.

The final two propane experiments were conducted on 5 November 1976. Target initial HC/ $NO_x$  conditions were 3.0 ppmC/0.05 ppm. Twenty percent of the initial  $NO_x$  in chamber 3 was injected as  $NO_2$ ; whereas 100 percent of the injected  $NO_x$  was  $NO_2$  in chamber 4. The resulting maximum ozone concentrations were 0.041 and 0.062 ppm. These results suggest that at identical initial HC and  $NO_x$  concentrations, the maximum ozone concentrations can be enhanced by increased initial  $NO_2$  levels.

Selected results from the 14 experiments conducted with low reactivity compounds are presented in Table 16, and individual data are presented in Volume 2 (Appendixes A and B). Based on these results, there is an apparent reduction of the  $[O_3]_{\max}$  as ambient temperature decreases. Propane experiments conducted at the same initial conditions on 8 September, 20 September, and 27 October generated 0.65, 0.21, and 0.03 ppm with corresponding maximum daily temperatures of  $31.7^\circ$ ,  $29.4^\circ$ , and  $9.4^\circ$  C. Although these findings are somewhat confounded by different solar irradiation profiles, additional evidence suggesting a strong temperature influence on maximum observed ozone

TABLE 16. SUMMARY OF RESULTS FOR LOW REACTIVITY EXPERIMENTS<sup>a</sup>

Run	T <sub>max</sub> °C	ΣSR Langley's	Chamber 1	Chamber 2	Chamber 3	Chamber 4
9-8-76	31.7	567				
HC			Ethane	Propane	Acetylene	Control
[HC]i <sup>b</sup>			6.9(8.0) <sup>e</sup>	11.7(12.0)	5.6(8.0)	-(0)
[NO <sub>x</sub> ]i <sup>c</sup>			0.17(0.2)	0.18(0.2)	0.16(0.2)	0.17(0.2)
t <sub>xo</sub> <sup>d</sup>			10.36	8.85	10.33	14.10
[O <sub>3</sub> ]max <sup>c</sup>			0.32	0.65	0.45	0.029
9-20-76	29.4	383				
HC			Propane	Propane	Propane	Propane
[HC]i			10.2(12.0)	11.1(12.0)	11.3(12.0)	10.3(12.0)
[NO <sub>x</sub> ]i			0.21(0.2)	0.22(0.2)	0.21(0.2)	0.21(0.2)
t <sub>xo</sub>			9.07	8.68	8.93	9.12
[O <sub>3</sub> ]max			0.20	0.20	0.18	0.21
10-27-76	9.4	366				
HC			Propane	Propane	Propane	Control
[HC]i			5.5(6.0)	10.4(12.0)	3.1(3.0)	-(0)
[NO <sub>x</sub> ]i			0.10(0.1)	0.21(0.2)	0.06(0.05)	0.06(0.05)
t <sub>xo</sub>			10.65	11.04	10.22	f
[O <sub>3</sub> ]max			0.039	0.028	0.047	0.002
11-5-76	11.7	328				
HC					Propane	Propane
[HC]i					2.6(3.0)	2.8(3.0)
[NO <sub>x</sub> ]i					0.06(0.05)	0.05(0.05)
t <sub>xo</sub>					10.47	g
[O <sub>3</sub> ]max					0.041	0.062

<sup>a</sup>For individual data see Volume 2 Appendixes A and B).<sup>b</sup>Units ppmC of target compound only; total hydrocarbon concentration slightly higher; see Appendix A.<sup>c</sup>Units ppm.<sup>d</sup>t<sub>xo</sub> is the time of NO-NO<sub>2</sub> crossover in hours EST.<sup>e</sup>Numbers in parentheses represent target values.<sup>f</sup>Crossover did not occur.<sup>g</sup>Crossover did not occur; NO<sub>x</sub> was injected as NO<sub>2</sub>.

concentrations is presented in Table 17. This comparison of results from the current study with those reported by other investigators<sup>45,47</sup> suggests that the maximum ozone concentrations generated by low reactivity compounds are highly temperature sensitive. In addition, they show a favorable comparison between the  $[O_3]_{\max}$  values of the 8 September RTI outdoor smog chamber experiments and those of the NAPCA indoor smog chamber.<sup>45</sup> Mechanistic justification for the extreme temperature sensitivity of ozone production by the low reactivity organics cannot be offered based on these results. Isolation of the causal factors from among the tens and perhaps hundreds of chemical reactions involved in the photooxidation of propane is difficult without the aid of a computer simulation model. Recent findings however of the strong temperature dependence of PAN decomposition and possibly of pernitric acid decomposition as well suggest that these reactions could be instrumental in accounting for the temperature sensitivity of ozone production by low reactivity organics.

Results from experiments conducted in the RTI smog chambers suggest that the criteria for determining reactivity should be modified. If a low reactivity hydrocarbon must not yield ozone in excess of 0.08 ppm in smog chamber investigations, then propane, ethane, and acetylene must be considered to be reactive organics.

The use of smog chamber data to establish the reactivity of organics is a controversial topic. Detailed discussion of the reactivity issue is beyond the scope of this report. A critical review of hydrocarbon reactivity has been published recently and should be consulted for more information on this subject.<sup>48</sup>

#### COMPARISON BETWEEN TWO OUTDOOR SMOG CHAMBER FACILITIES: MATCHED EXPERIMENTS

To investigate the extent to which matched initial reactant conditions would yield consistent results in outdoor smog chambers, matched experiments were jointly conducted at the University of North Carolina's Ambient Air Research Facility (UNC) and at the Research Triangle Institute's Outdoor Smog Chamber Facility (RTI). Each matched experiment was conducted on the same day at both facilities. Since the two facilities are located within 32 kilometers of each other, similar diurnal profiles of light intensity and ambient temperature are seen at each facility on any given day. These

TABLE 17. MAXIMUM OZONE CONCENTRATIONS GENERATED IN VARIOUS SMOG CHAMBERS USING LOW REACTIVITY HYDROCARBONS

Chamber	T <sub>max</sub> °C	Maximum Ozone Concentration <sup>a</sup>			
		Ethane	Acetylene	Propane	Blank <sup>b</sup>
RTI (9-8-76)	31.7	0.32	0.45	0.65	0.02
RTI/UNC (9-20-76)	29.4			0.21 <sup>c</sup>	
RTI (10-27-76)	9.4			0.028	0.002 <sup>d</sup>
NAPCA <sup>45</sup>	33.9	0.2 <sup>e</sup>	0.5 <sup>e</sup>	0.6 <sup>e</sup>	0.06 <sup>e</sup>
EPA <sup>47</sup>	22.2	0.08	0.13	0.11	0.04

<sup>a</sup>Unless noted otherwise, initial conditions 4.0 ppm(v/v) HC and 0.2 ppm NO<sub>x</sub>.

<sup>b</sup>Unless noted otherwise, a blank is clean air plus 0.2 ppm NO<sub>x</sub>.

<sup>c</sup>Average maximum ozone concentration from six chambers; see text.

<sup>d</sup>Clean air plus 0.06 ppm NO<sub>x</sub>.

<sup>e</sup>Initial conditions 6.0 ppm(v/v) HC and 0.2 ppm NO<sub>x</sub>.

variables are expected to be the major determinants of chemical behavior for any given set of initial reactant conditions. Performing the matched experiments on the same day, therefore, eliminates the possibility that differences in these variables would influence the results.

Although the chambers at both facilities are located outdoors and are fabricated from transparent FEP Teflon film to enable natural sunlight and ambient temperatures to govern the photochemical reactions, they are quite different in appearance, design, and manner of operation. Figure 23 permits comparison of the design and size of the two chamber types. RTI operates four side-by-side, 27-cubic-meter cylindrical chambers. The UNC gas-phase dual chamber is a much larger A-frame structure. Table 18 compares the physical and performance characteristics of the chambers. Major differences are: location (32 kilometers apart); shape; volume; surface-to-volume ratio; method of pretreatment of background air; and sample handling.

In these experiments, two types of hydrocarbons were used: an alkane (propane) which has a low reactivity and an olefin (propene) which has a high reactivity and which has frequently been used in smog chamber testing. Any substantial "wall effect" differences would be expected to be more evident in the propane experiment than in the propene experiment.

#### Cross Calibration Comparisons

To insure that a valid comparison could be made of the results obtained at both facilities, a detailed cross-comparison study was undertaken. In addition to investigating the hydrocarbon and NO standards that were used to calibrate the instruments, cross-measurements of initial hydrocarbon injections were made at both facilities. Based on measurements of three UNC- and five RTI-certified NO calibration standards, a common calibration was achieved to which all NO measurements were referenced. As the NO<sub>2</sub> and O<sub>3</sub> measurements were calibrated via gas phase titration, the NO<sub>2</sub> and O<sub>3</sub> results could also be validly compared. All hydrocarbon calibrations were referenced to an NBS-certified propane cylinder.\* Immediately following the predawn injection

---

\*It should be noted that while all the hydrocarbon concentrations reported in this subsection are referenced to a common calibration standard, the concentration reported in Appendix A are referenced to an RTI calibration standard which yields 8 percent lower values for propane and 7 percent lower values for propylene.

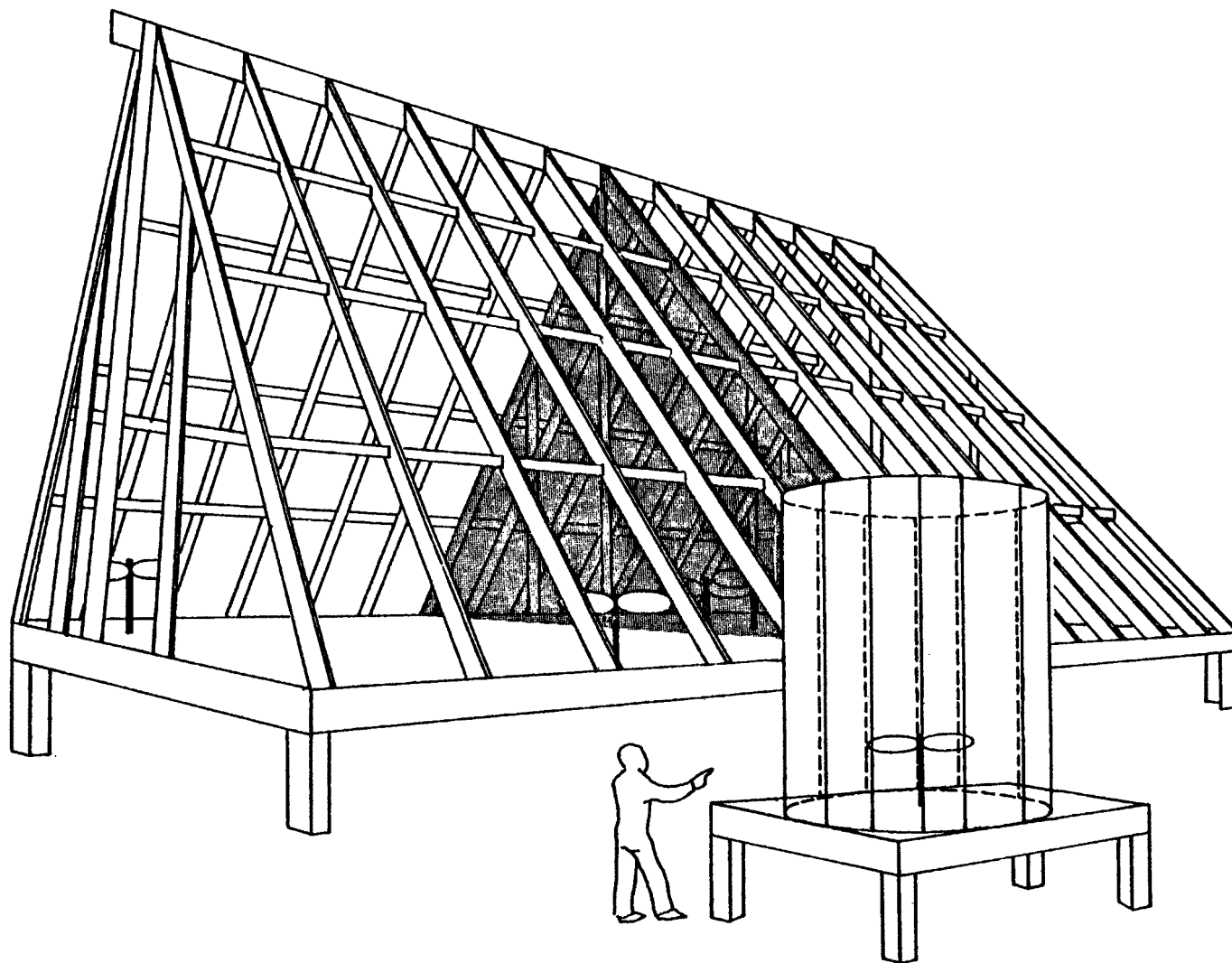


Figure 23. Comparison of the Designs and Sizes of the RTI (Foreground) and UNC (Background) Outdoor Smog Chambers. The Shaded Area is Hanging Teflon Film Separating the Two UNC Chambers.

TABLE 18. COMPARISON OF PHYSICAL AND CHEMICAL CHARACTERISTICS OF RESEARCH TRIANGLE INSTITUTE AND UNIVERSITY OF NORTH CAROLINA OUTDOOR SMOG CHAMBERS (a)

	Research Triangle Institute	University of North Carolina
Location	Research Park	Rural Area
Shape	4 Adjacent Cylinders	A-Frame Divided into Two Compartments
Dimensions, Meters (feet)	3.1 Dia x 3.7 H (10 Dia x 12 H)	9.1 W x 6.1 L x 6.1 H <sup>(e)</sup> (30 W x 20 L x 20 H)
Volume, m <sup>3</sup> (ft <sup>3</sup> )	27 (1000)	153 (5500) <sup>(e)</sup>
Surface Area, m <sup>2</sup> (ft <sup>2</sup> )	51 (580)	204 (2200) <sup>(e)</sup>
S/V, m <sup>-1</sup> (ft <sup>-1</sup> )	1.9 (0.58)	1.3 (0.40) <sup>(e)</sup>
Background Air Treatment	8-12 Hours Recirculation thru 0.5% Pd Catalyst (260°C) + Purafil	15-20 Turnovers with Rural Air, Start with 4-5 AM Rural Air
Sampling Handling	5 mm ID Teflon Lines <10 sec Residence Time	38 mm Glass Manifold 8 sec Residence Time Excess Air Returned
O <sub>3</sub> Half-Life, Hours <sup>(b)</sup>		
- Light <sup>(b)</sup>	10-25	18
- Dark <sup>(c)</sup>	17-40	48-70
Background Air O <sub>3</sub> Formation, ppm <sup>(d)</sup>	0.03-0.17	0.02 - 0.14
NO Oxidation Relative to Thermal Rate (Dark)	0.7-1.6	1.5 to 4.8

(a) Factors in common: material in both is 5 mil Teflon film and aluminum strips; both types use natural sunlight and ambient temperature (0 to 5°C rise above ambient in a day); both have reflective floors (aluminum under Teflon) to compensate for light transmission losses; both are stirred by fans.

(b) Function of temperature and season when measurement was made.

(c) Function of temperature when measurement was made.

(d) Function of temperature, season and background air when measurement was made.

(e) Data for each of the two chambers.

of reactants into the six chambers, two samples of each chamber's contents were collected in 25-liter Tedlar bags. One of these remained at the originating facility for hydrocarbon analysis while the second bag was transported to the other facility for analysis. The exception to this procedure was UNC's analysis of its chambers in real-time. This approach permitted two independent measurements of the initial hydrocarbon concentrations in each chamber.

### Background Conditions

To conduct a complete comparison it was important to determine the amount of preinjection chamber contaminants. This was particularly true in the case of the UNC facility where the injections are made into chambers containing rural ambient air. The preinjection measurements of 5 November 1976 were taken as representative of typical conditions (see Table 19). These indicated that NO levels were below the minimum detectable concentration (1 ppb) in all six chambers. Five ppb of NO<sub>2</sub> were seen in both UNC chambers while the four RTI chambers ranged between 0 and 5 ppb. The background air at the UNC facility contained 15 ppbV of hydrocarbons in the C<sub>2</sub> through C<sub>5</sub> range. Post-cleanup hydrocarbon concentrations in the RTI chambers were between 1 and 9 ppbV for the same group. In both cases, a significant fraction of the hydrocarbons were ethane and/or ethene (eluted at one peak) while the remainder was composed of traces of propane, propene, acetylene, normal butane, iso-butane, normal pentane, and isopentane.

### The Matched Experiment of 20-21 September 1976

The first matched experiment was conducted on 20-21 September 1976 and involved a propane/NO<sub>x</sub> chemical system. Target initial reactant concentrations for all six chambers were 4.00 ppmV propane and 0.20 ppm NO<sub>x</sub> (20% NO<sub>2</sub>). The propane was injected from common commercially supplied liquid propane tanks. Gas chromatographic analysis conducted at RTI revealed the contents to be 85% propane, 13% normal and iso-butane, 1% ethane and ethylene, and 1% methane on a volume basis. Nitric oxide and NO<sub>2</sub> were injected from high concentration gas cylinders.

Ideally, the initial reactant concentrations should be equal in all six chambers; measured initial concentrations shown in Table 20 indicate that all six chambers closely matched the target concentrations. After correc-



TABLE 19. MEASUREMENT OF PREINJECTION CHAMBER CONTENTS AND BACKGROUND AMBIENT AIR  
(DATA COLLECTED BEFORE DAWN ON 5 NOVEMBER 1976)

	UNC Background Air	Preinjection Chamber Contents					
		UNC Red	UNC Blue	RTI #1	RTI #2	RTI #3	RTI #4
Nitric Oxide (ppb)	—	0	0	0	0	0	0
Nitrogen Dioxide (ppb)	—	5	5	0	5	4	0
Ethane/Ethylene (ppbV)	6	—	—	1	5	5	4
Propane (ppbV)	2	—	—	0	1	1	1
Propylene (ppbV)	1	—	—	0	0	0	0
Acetylene (ppbV)	2	—	—	0	1	1	1
Isobutane (ppbV)	1	—	—	0	0	0	0
N-Butane (ppbV)	1	—	—	0	1	1	0
1-Butene (ppbV)	0	—	—	0	0	0	0
Trans-2-Butene (ppbV)	0	—	—	0	0	0	0
Isopentane (ppbV)	1	—	—	0	1	1	1
Cyclopentane (ppbV)	0	—	—	0	0	0	0
N-Pentane (ppbV)	1	—	—	0	0	0	0
Total Measured Hydrocarbons (C <sub>2</sub> thru C <sub>5</sub> ) (ppbV)	~15	—	—	~1	~9	~9	~7

TABLE 20. SUMMARY OF RESULTS FOR MATCHED EXPERIMENTS ON 20 AND 21 SEPTEMBER 1976

Target Injections	Propane	4.00 ppmV	NO	0.16 ppm		
	NO <sub>2</sub>	0.04 ppm	HC/NO <sub>x</sub> Ratio	20 ppmV/ppm		
Ambient Temperatures <sup>(a)</sup>	First Day Near Dawn (0800 EDT) 16°		First Day Maximum (1400 EDT) 23° C			
	Second Day Near Dawn (0800 EDT) 19° C		Second Day Maximum (1700 EDT) 27° C			
	<u>RTI #1</u>	<u>RTI #2</u>	<u>RTI #3</u>	<u>RTI #4</u>	<u>UNC Red</u>	<u>UNC Blue</u>
Initial Propane Concentration (ppmV) <sup>(b)</sup>						
- Analysis by UNC	3.73	4.06	3.86	4.12	4.61	4.27
- Analysis by RTI	3.81	4.13	4.21	3.83	4.92	4.57
Initial NO Concentration (ppm) <sup>(c)</sup>	0.170	0.175	0.166	0.168	0.166	0.165
Initial NO <sub>2</sub> Concentration (ppm) <sup>(c)</sup>	0.040	0.040	0.045	0.040	0.054	0.055
Initial HC/NO <sub>x</sub> Ratio (ppmV/ppm) <sup>(d)</sup>	18.1	19.2	20.0	18.4	21.0	19.4
Time of NO/NO <sub>2</sub> Crossover (EDT)	1004 <sup>(e)</sup>	0941 <sup>(e)</sup>	0956 <sup>(e)</sup>	1007 <sup>(e)</sup>	1020	1016
Time of Maximum NO <sub>2</sub> Concentration (EDT)	1308 <sup>(f)</sup>	1218 <sup>(f)</sup>	1228 <sup>(f)</sup>	1238 <sup>(f)</sup>	1308	1308
Maximum NO <sub>2</sub> Concentration (ppm) <sup>(c)</sup>	0.156	0.158	0.150	0.156	0.142	0.147
O <sub>3</sub> Concentrations (ppm) <sup>(c)</sup>						
- First Day Maximum	0.195	0.259	0.181	0.213	0.200	0.222
- Overnight Minimum	0.065	0.098	0.062	0.078	0.085	0.062
- Second Day Maximum	0.310	0.393	0.244	0.280	0.254	0.272
- Net Second Day Production	0.245	0.295	0.182	0.202	0.169	0.210

(a) Measured at the National Weather Service Forecast Office, Raleigh-Durham Airport.

(b) Corrected values based on hydrocarbon calibration standard cross-comparison.

(c) Corrected values based on nitric oxide calibration standard cross-comparison.

(d) Calculated from each facility's own measurements. Based on propane and NO<sub>x</sub> measurements only.

(e) Based on linear interpolation between hourly measurements.

(f) Sampling frequency: once per hour

tion for differences in the hydrocarbon calibration standards, the mean of the six RTI propane analyses was 4 percent higher than the mean of the UNC propane analyses. Based on the UNC analyses the UNC propane injections were an average of 13 percent higher than the RTI propane injections. This average increased to 17 percent for the RTI analyses. All NO injections were within 6 percent of each other. There was, however, a greater relative variation in the NO<sub>2</sub> injections. The initial NO<sub>2</sub> concentrations at the UNC facility were about 13 ppb higher than those at the RTI facility.

Two other variables that have major influences on the reactions that occur in the chambers are the diurnal profiles of light and ambient temperature. The total solar radiation profiles measured at each facility for 20 September 1976 are shown in Figure 24. Both profiles indicate that the day was partially cloudy with a fairly clear morning. The integrated light intensity from sunrise (approximately 0700 EDT) to near the times of the NO-NO<sub>2</sub> crossovers (1000 EDT) was 49.18 cal-cm<sup>-2</sup> at the RTI facility and 46.46 cal-cm<sup>-2</sup> at the UNC site. This indicates that the two facilities were exposed to very similar light conditions. The total solar radiation profiles for the second day of the experiment (not presented here) show a similar pattern of "choppy" sunshine although that sky was more overcast in the morning. It is assumed that the temperature profiles at the two facilities did not differ greatly from that measured at the nearby Raleigh-Durham Airport. The dawn and the daily maximum temperatures for both days were somewhat higher than those normally occurring in central North Carolina at this time of the year.

After the predawn reactant injections, a complex series of photochemical reactions began within the six chambers which ultimately led to smog formation. One indicator of the rate of the photochemical process is the time from dawn until the concentrations of NO and NO<sub>2</sub> are equal (crossover time). Modeling results suggest that this measure is relatively sensitive to any heterogeneous component of the reactions. If wall-related reactions differ in two smog chambers, these differences should be more strongly manifested for low reactivity chemical systems than for chemical systems of higher reactivity. The crossover times for the six chambers cluster rather closely around an average value of 184 minutes. RTI Chamber No. 2, however, achieved crossover in 88 percent of this time. This suggests that there may have

been surface-related processes occurring in this chamber. The two UNC chambers had crossover times about 8 percent longer than the average value, which indicates that surface-to-volume ratio still may be an influencing factor in large volume chambers for low reactivity chemical systems. Nevertheless, the close agreement of the six chambers for this variable points toward similar chemical behavior.

The ordering of the six chambers with respect to crossover times was roughly duplicated for the times to maximum  $\text{NO}_2$  concentration. The relative spread of the times about the average time of 348 minutes was approximately the same as the relative spread about the average crossover time. It should be noted, however, that the sampling frequency of the RTI measurements was once per hour; whereas, the UNC measurements were collected at 8-minute intervals for each of the two chambers. Consequently, the RTI-measured times to maximum  $\text{NO}_2$  concentration may be up to 30 minutes away from the actual times.

The two UNC chambers showed excellent agreement for their maximum  $\text{NO}_2$  concentrations as did the four RTI chambers. Nitrogen balances ( $\text{NO}$  plus  $\text{NO}_2$ ) at this stage of the reaction process are approximately 85 percent for RTI and 74 percent for UNC. Ratios of the maximum  $\text{NO}_2$  concentration to the initial  $\text{NO}_x$  concentration are about 74 percent in the RTI chambers and about 65 percent at the UNC facility. This latter value is somewhat larger than the average value of 58 percent found by the UNC group for lower initial concentrations of urban hydrocarbon mixture.<sup>49</sup>

The most interesting result of the propane experiment is to be found in the first-day maximum  $\text{O}_3$  concentrations. The agreement among all six chambers for this parameter and the time to maximum  $\text{O}_3$  concentration (see Figures 25 through 28) is impressive. While five of the six chambers closely cluster about an average value of 0.202 ppm (standard deviation: 0.016 ppm), however, RTI No. 2 is 28 percent higher. This is significant in the light of the excellent agreement in the other five chambers. This behavior is consistent with the earlier divergence of this chamber and also suggests the existence of unusual surface-related or chamber history-related processes in RTI No. 2. Since the maximum  $\text{O}_3$  concentrations in the other five chambers are in agreement, it is believed that wall-related effects play a much lesser role for these chambers in determining the magnitude of the maximum. The average

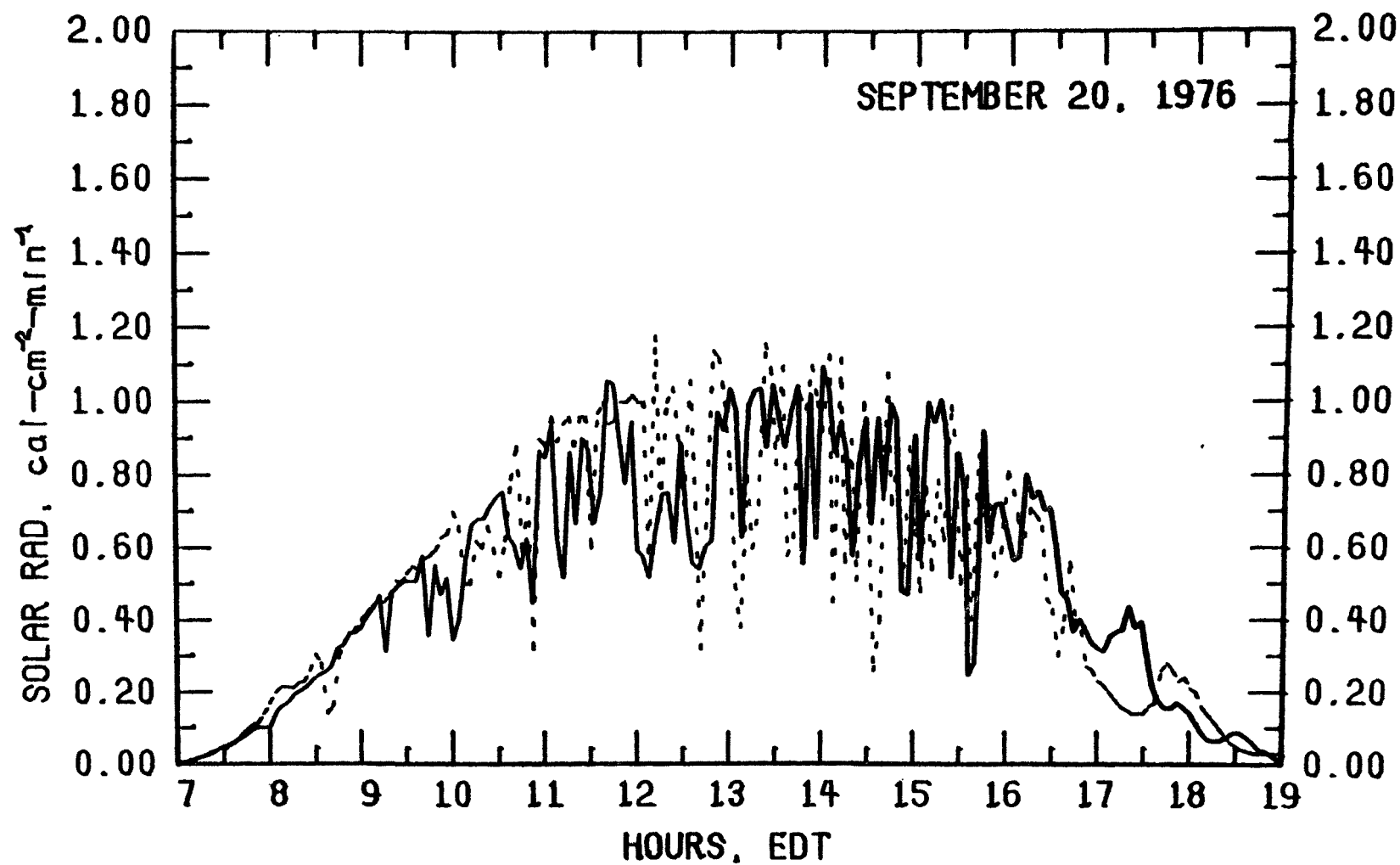


Figure 24. Total Solar Radiation Profiles for UNC (————) and RTI (- - - -) on September 20, 1976.

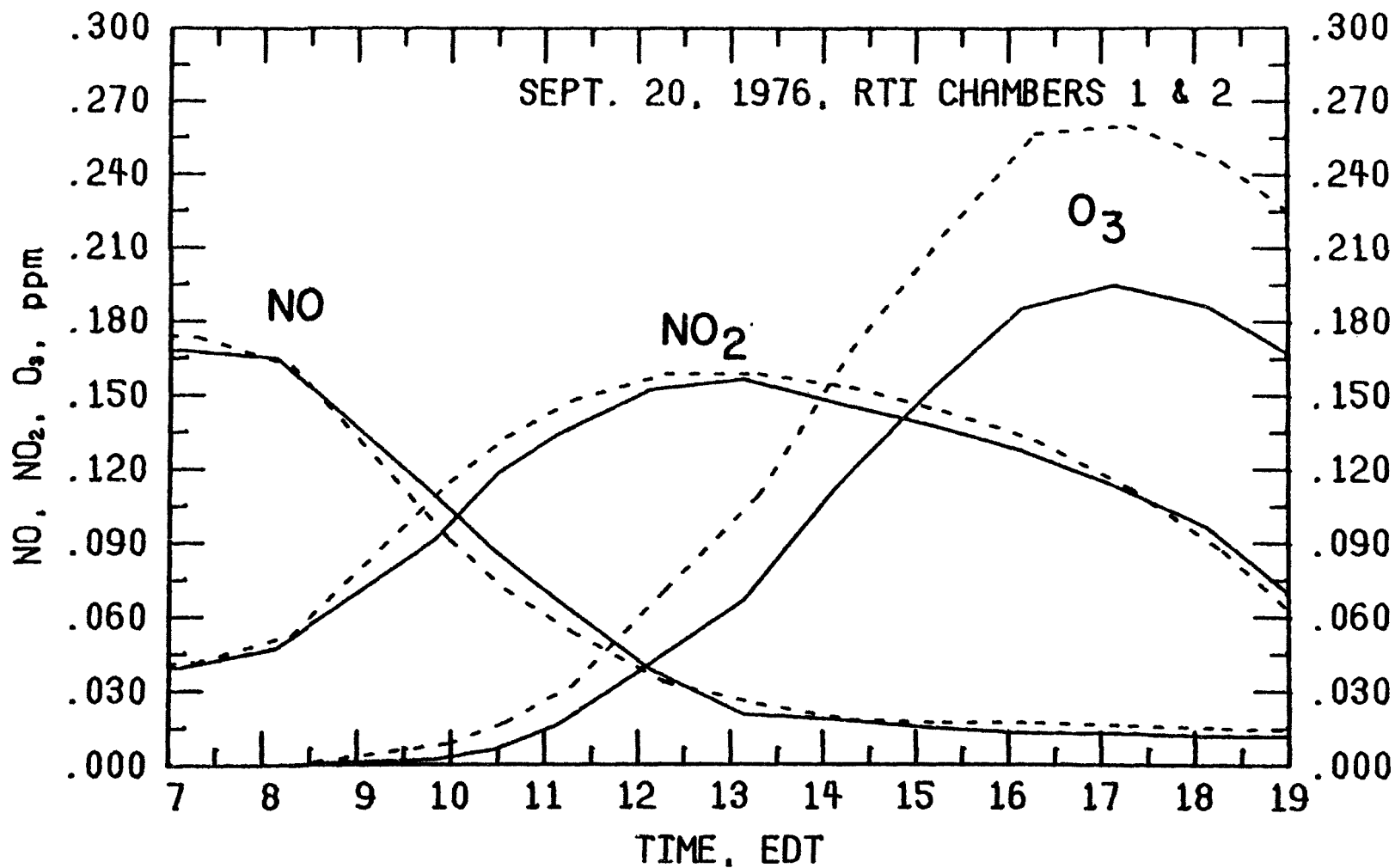


Figure 25, Nitric Oxide, Nitrogen Dioxide and Ozone Concentration Profiles for RTI Chamber 1 (—) and RTI Chamber 2 (---) on September 20, 1976,

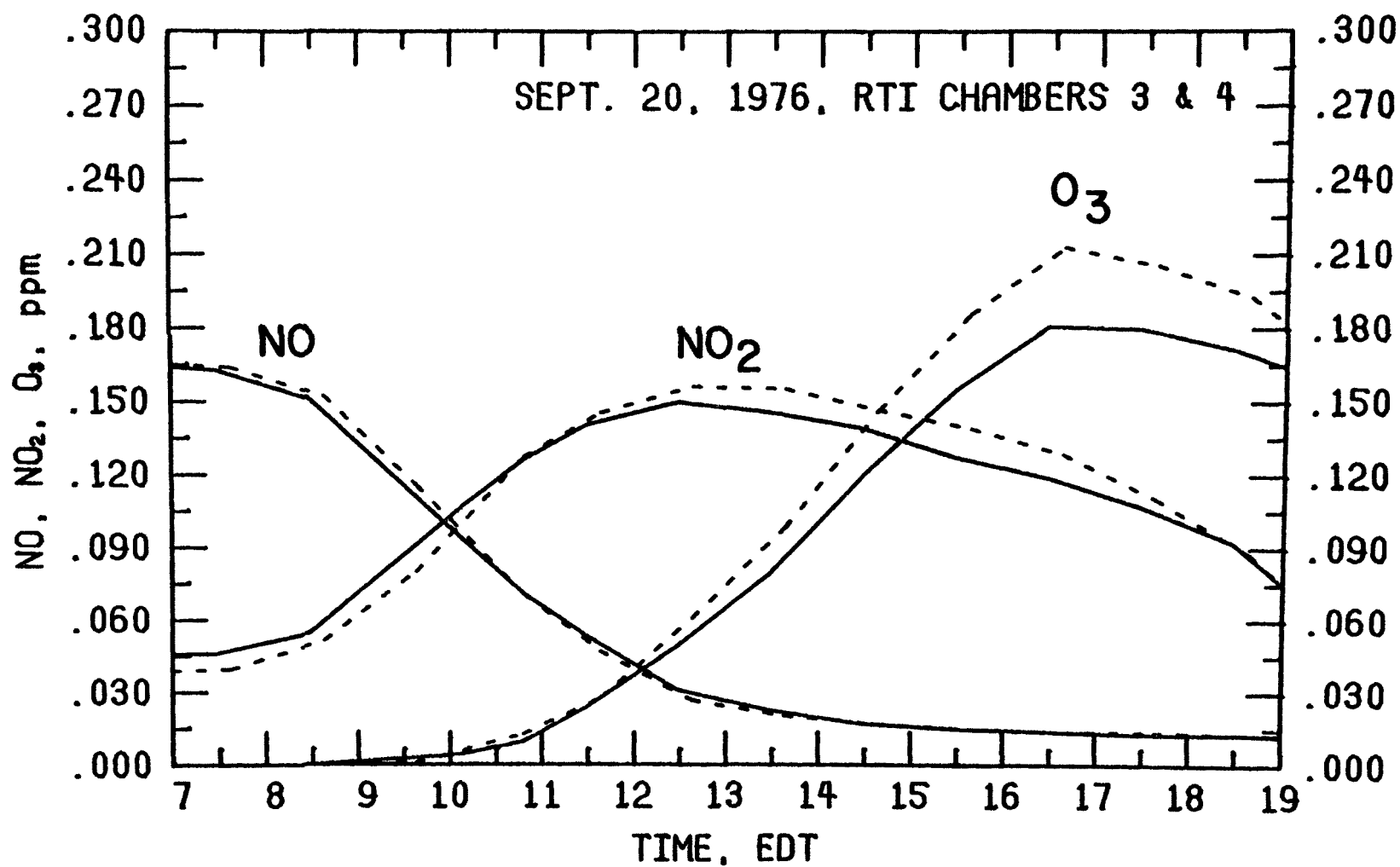


Figure 26. Nitric Oxide, Nitrogen Dioxide and Ozone Concentration Profiles for RTI Chamber 3 (—) and RTI Chamber 4 (---) on September 20, 1976.

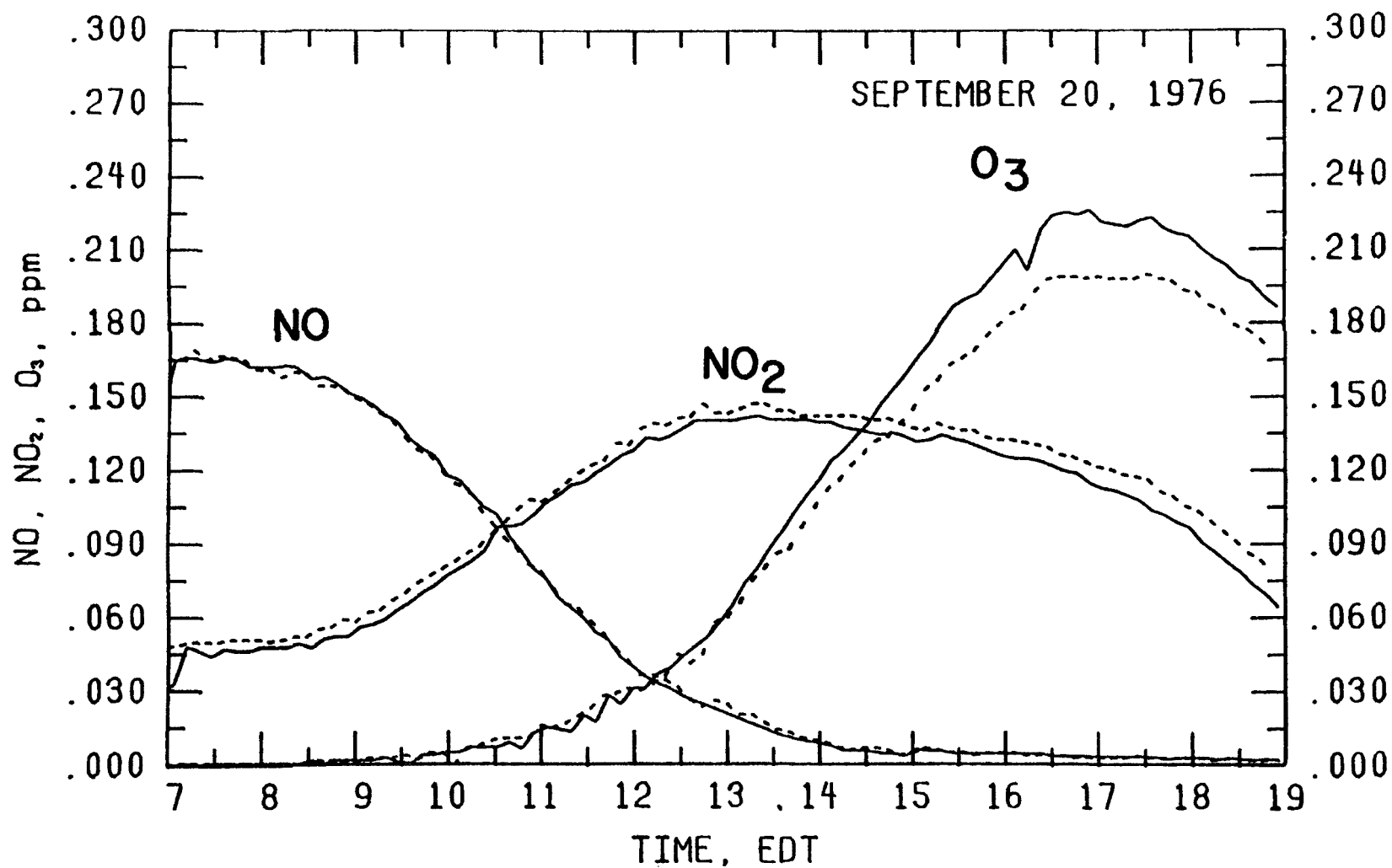


Figure 27. Nitric Oxide, Nitrogen Dioxide and Ozone Concentration Profiles for UNC Red Chamber (—) and UNC Blue Chamber (---) on September 20, 1976.



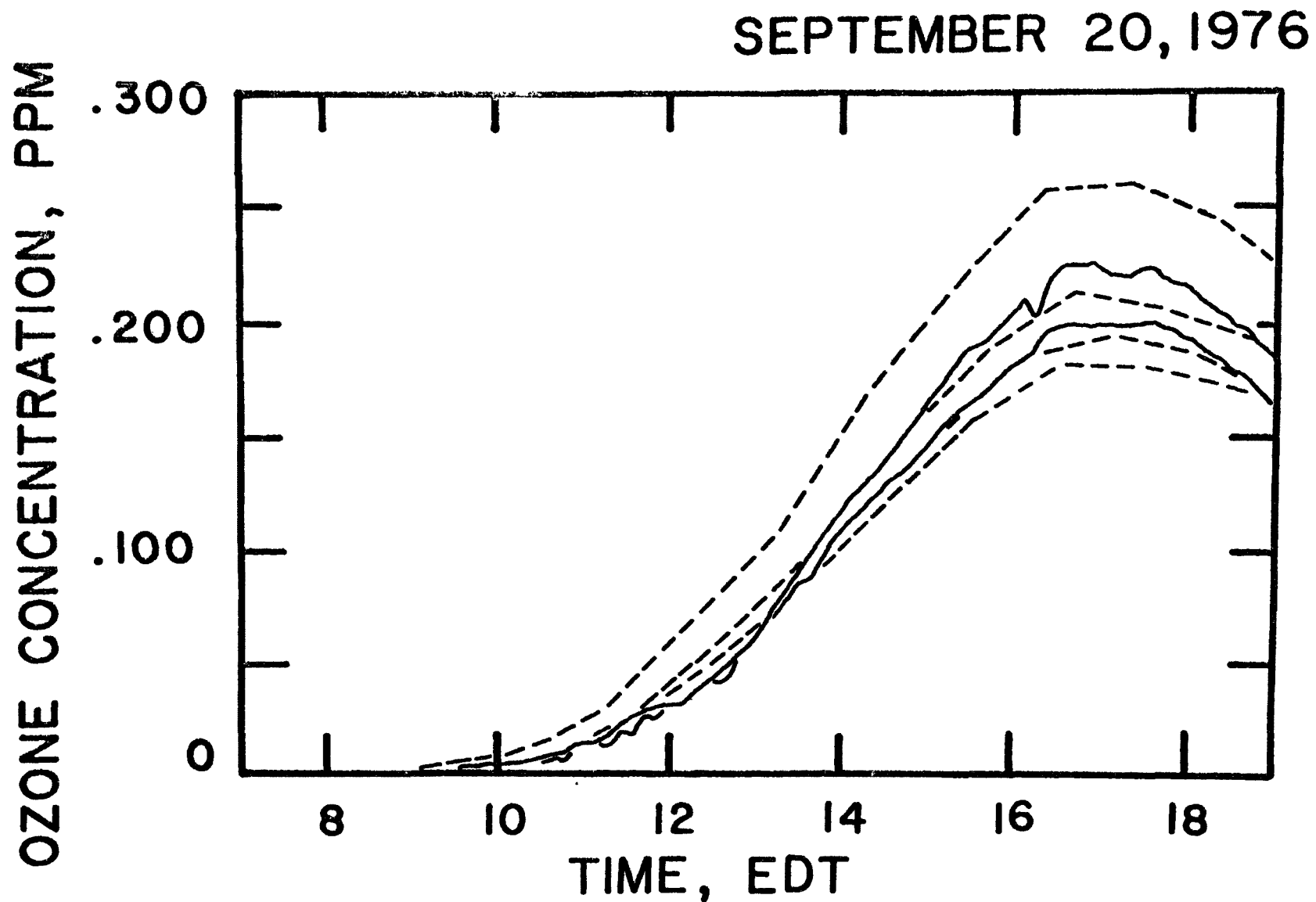


Figure 28. Ozone Concentration Profiles for the Two UNC Chambers (—) and the Four RTI Chambers (---) on September 20, 1976.

value of 0.202 ppm is substantially larger than the 0.11 ppm value which was measured in EPA's 400-liter Pyrex chamber for similar initial reactant concentrations.<sup>47</sup> This difference could be the result of different temperatures or light intensities, the presence of additional hydrocarbons in this experiment (see above) or different surface effects as judged by NO<sub>x</sub> behavior in the EPA and the outdoor chambers.

One of the several possible causes of high oxidant concentrations in rural areas is the long-range transport of "partially spent" photochemical systems from urban areas.<sup>50</sup> In such systems, low reactivity hydrocarbons are likely to play a significant role in second- and third-day oxidant formation. To investigate this possibility, the contents of the chambers were irradiated for a second day on 21 September 1976. As the differences between the overnight minimum and the second-day maximum O<sub>3</sub> concentrations indicate, substantial O<sub>3</sub> formation occurred on this second day. The RTI chambers formed between 95 and 126 percent of the previous day's maximum O<sub>3</sub> concentration while values of 85 and 95 percent were seen in the UNC chambers.

#### The Matched Experiment of 5 November 1976

The matched experiment of 5 November 1976 differed in several respects from the previous matched experiment: a higher reactivity hydrocarbon (propene) was used; two different sets of initial reactant concentrations were injected instead of one set for all the chambers and the experiment lasted only 1 day. Two chambers (RTI No. 1 and UNC Red) had target propene injections of 0.50 ppmV. Table 21 indicates that UNC Red came rather close to this target while RTI No. 1 overshot by about 18 percent. The other two chambers which were operated in this matched experiment (RTI No. 2 and UNC Blue) were intended to have initial propene concentrations of 1.33 ppmV. The UNC injection was close to this value. The RTI injection, however, was 13 percent low. Averaged across all four chambers, the RTI hydrocarbon analyses were 3 percent higher than those of UNC. Both facilities injected roughly 10 percent more NO and NO<sub>2</sub> than the target initial concentrations of 0.40 and 0.10 ppm.

Ambient temperatures for this experiment were rather low (5° C below normal for this date). Based on the results of previous UNC research on the effect of temperature on oxidant formation, the maximum ozone concentration should have been considerably less than that which would be expected on a

TABLE 21. SUMMARY OF RESULTS FOR MATCHED EXPERIMENT ON 5 NOVEMBER 1976

	RTI #2 and UNC Blue		RTI #1 and UNC Red	
Target Injections	Propylene	1.33 ppmV	Propylene	0.50 ppmV
	NO	0.40 ppm	NO	0.40 ppm
	NO <sub>2</sub>	0.10 ppm	NO <sub>2</sub>	0.10 ppm
	HC/NO <sub>x</sub> Ratio	2.66 ppmV/ppm	HC/NO <sub>x</sub> Ratio	1.00 ppmV/ppm
Ambient Temperatures <sup>(a)</sup>	Near Dawn (0800 EDT) 1°C		Maximum (1400 EDT) 11°C	
	<u>RTI #2</u>	<u>UNC Blue</u>	<u>RTI #1</u>	<u>UNC Red</u>
Initial Propylene Concentration (ppmV) <sup>(b)</sup>				
- Analysis by UNC	1.13	1.34	0.578	0.497
- Analysis by RTI	1.191	1.337	0.610	0.509
Initial NO Concentration (ppm) <sup>(c)</sup>	0.453	0.427	0.437	0.426
Initial NO <sub>2</sub> Concentration (ppm) <sup>(c)</sup>	0.103	0.130	0.112	0.106
Initial HC/NO <sub>x</sub> Ratio (ppmV/ppm) <sup>(d)</sup>	2.14	2.42	1.11	0.93
Time of NO/NO <sub>2</sub> Crossover (EDT)	1020 <sup>(e)</sup>	1000	1115 <sup>(e)</sup>	1132
Time of Maximum NO <sub>2</sub> Concentration (EDT)	1118 <sup>(f)</sup>	1104	1308 <sup>(f)</sup>	1436
Maximum NO <sub>2</sub> Concentration (ppm) <sup>(c)</sup>	0.476	0.487	0.420	0.417
Maximum O <sub>3</sub> Concentration (ppm) <sup>(c)</sup>	0.710	0.697	0.235	0.122

(a) Measured at the National Weather Service Forecase Office, Raleigh-Durham Airport.

(b) Corrected values based on hydrocarbon calibration standard cross-comparison.

(c) Corrected values based on NO calibration standard cross-comparison .

(d) Calculated from each facility's own measurements.

(e) Based on linear interpolation between hourly measurements.

(f) Sampling frequency: once per hour.

warm day.<sup>51</sup> On the other hand, the sky was cloudless throughout the major portion of the day. This would produce the largest amount of oxidants possible for this time of year given the observed temperatures. As illustrated in Figure 29, both facilities were exposed to nearly perfect light profiles from about 0745 until 1430 EDT.

In the high concentration chambers, it is seen that NO and NO<sub>2</sub> crossed over in UNC Blue in 135 minutes while RTI No. 2 took 20 minutes longer. This difference in crossover times can be most easily explained by observing that the initial hydrocarbon-NO<sub>x</sub> ratio for the RTI chamber was 12 percent lower than the value for the UNC chamber. As the difference appears to be associated with the initial reactant concentrations, it is not necessary to invoke wall-related effects. Assuming that this is the case, it would appear that such effects are not as influential in this experiment as in the previous one. This could be because the chamber wall history was different for this experiment, because the temperature was lower, or because the high reactivity propene/NO<sub>x</sub> chemical system may not be as sensitive to chamber contamination as the lower reactivity propane/NO<sub>x</sub> chemical system. There is insufficient evidence to draw any firm conclusions as to the true cause. The relationship between the two chambers' crossover times was maintained for the times of maximum NO<sub>2</sub> concentration (the earlier caution concerning this parameter is again stressed). Overall, the two chambers showed very good agreement as is shown in Figure 30.

The times to NO-NO<sub>2</sub> crossover were approximately equal in the low concentration propene chambers. RTI No. 1 was 17 minutes faster than UNC's crossover time of 227 minutes. This difference is somewhat less than what would be expected considering that the initial hydrocarbon-NO<sub>x</sub> ratio of the RTI chamber was 19 percent larger. Despite this close agreement in the early stages of the photochemical reactions, Figure 31 shows that the two chambers began to widely diverge shortly after the crossovers. RTI No. 1 had a NO<sub>2</sub> peak which occurred at least an hour before the NO<sub>2</sub> peak in UNC Blue. Afterwards, the decline of NO<sub>2</sub> was more rapid in the RTI chamber than in the UNC chamber. This behavior is consistent with the higher hydrocarbon-NO<sub>x</sub> ratio. It is not obvious, however, why this was not as strongly manifest in the times to NO-NO<sub>2</sub> crossover. It should be noted that there was nearly as large a relative difference in initial hydrocarbon-NO<sub>x</sub> ratios

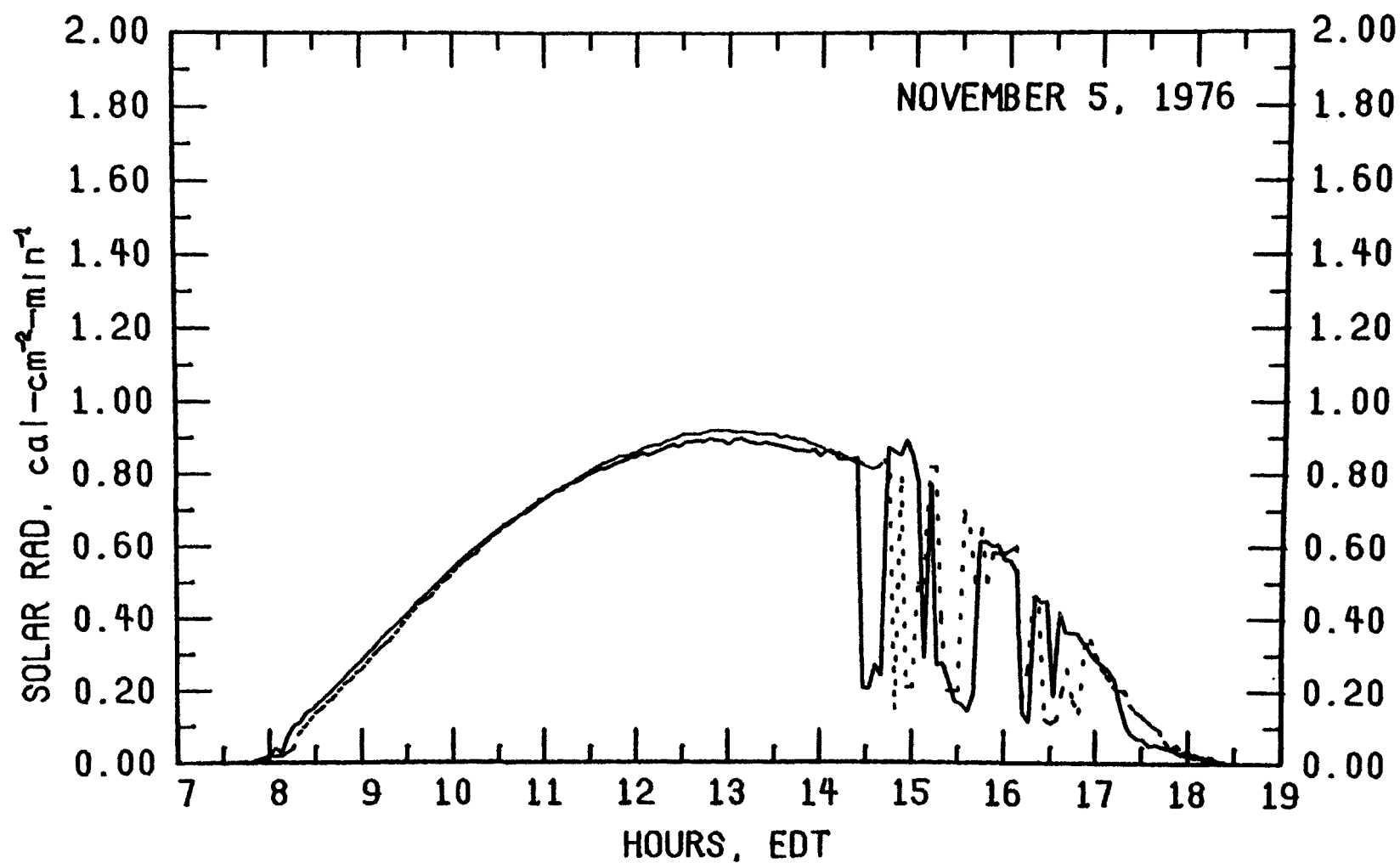


Figure 29. Total Solar Radiation Profiles for UNC (—) and RTI (- - -) on November 5, 1976,

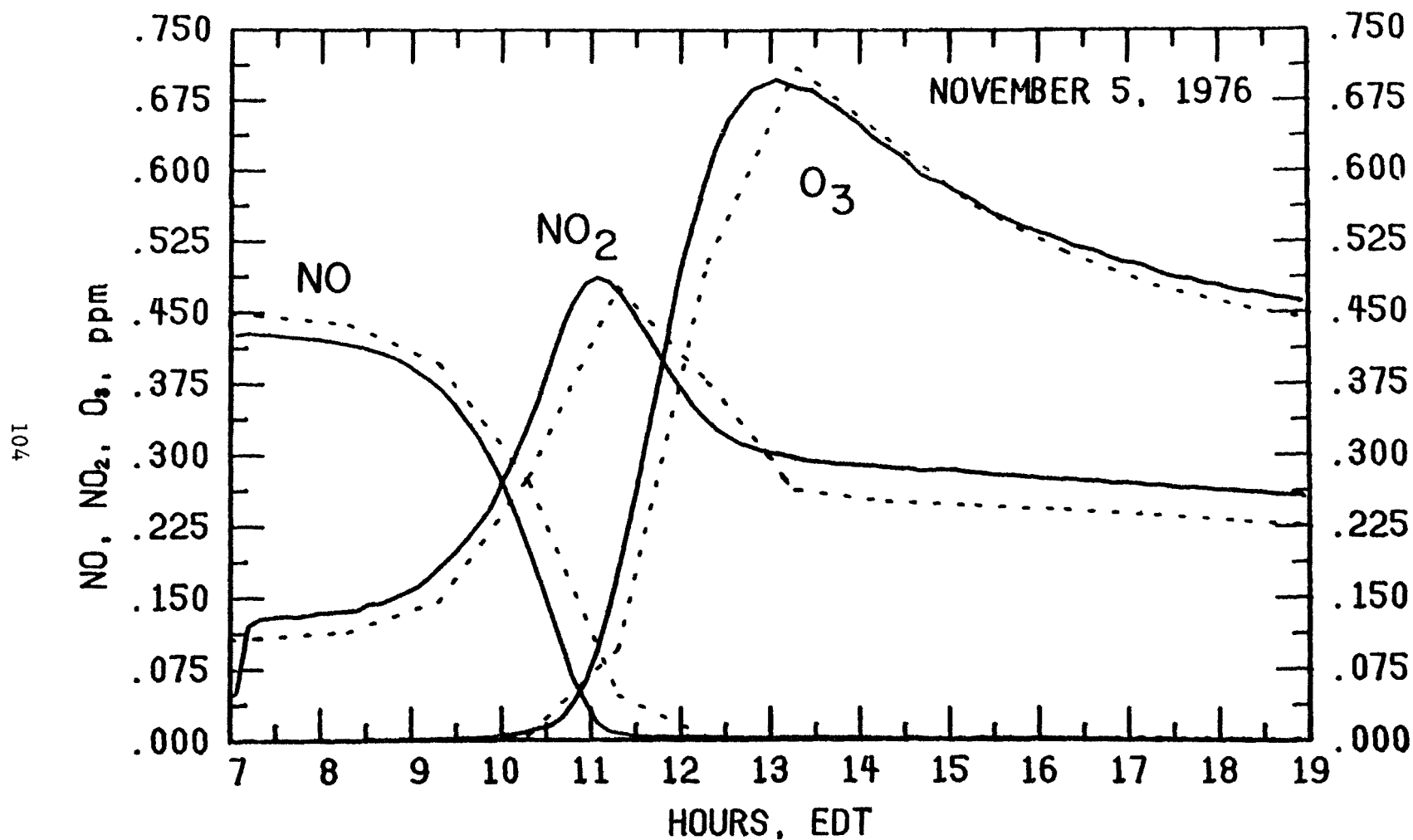


Figure 30. Nitric Oxide, Nitrogen Dioxide and Ozone Concentration Profiles for UNC Blue Chamber (—) and RTI Chamber 2 (---) on November 5, 1976.

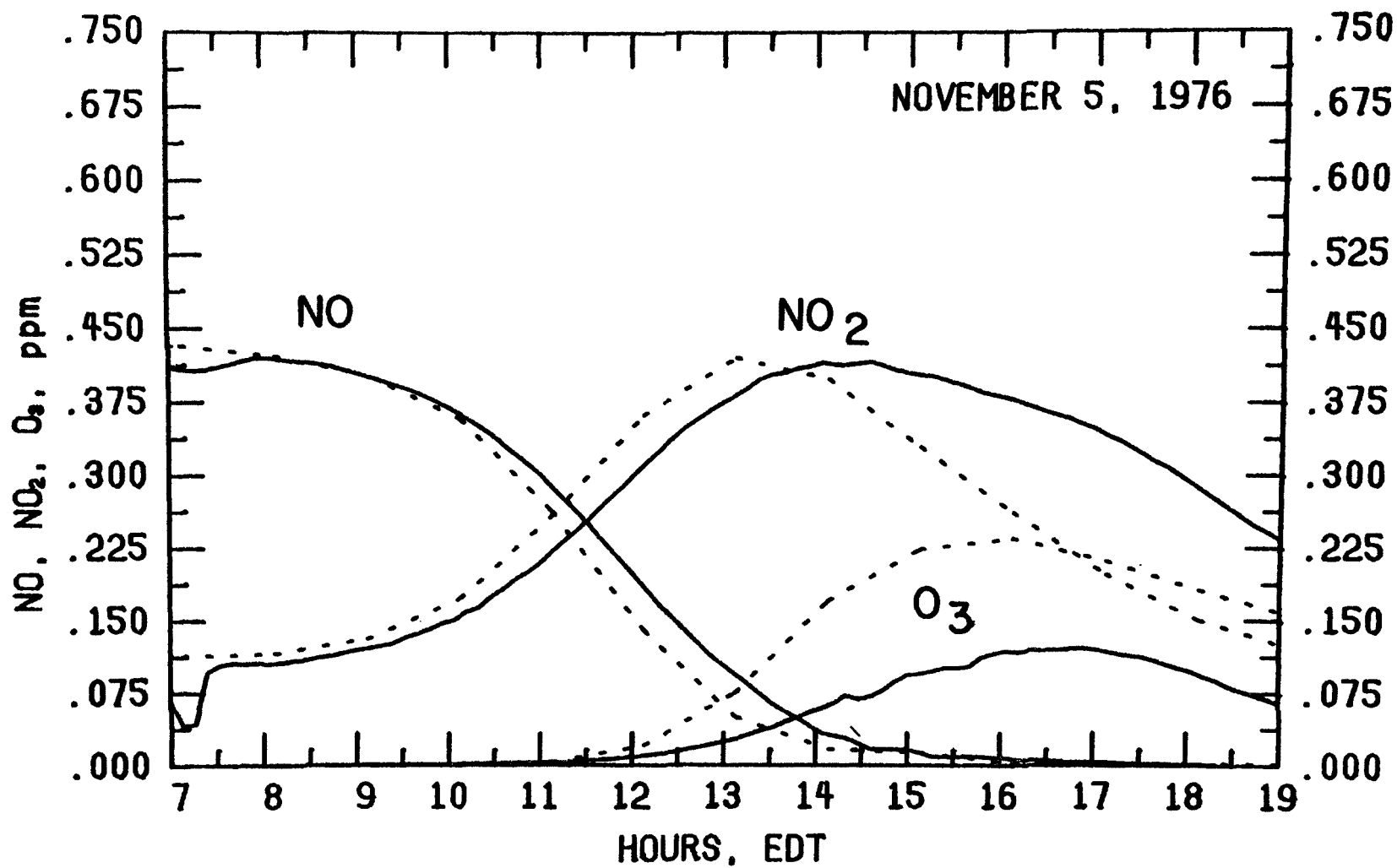


Figure 31, Nitric Oxide, Nitrogen Dioxide and Ozone Concentration Profiles for UNC Red Chamber (—) and RTI Chamber 2 (---) on November 5, 1976.

for the high concentration propene chambers and yet no large difference was observed for the  $\text{NO}_2$  concentration profiles. The implication is that the effect of variations in the ratio become more pronounced for lower initial hydrocarbon concentrations.

Nitrogen balances at the maximum  $\text{NO}_2$  concentration agreed well within the sets of matched chambers. In the high concentration propene chambers, RTI No. 2 showed a 94 percent nitrogen balance while 91 percent of the initial  $\text{NO}_x$  was still present in UNC Blue. For the two chambers having lower initial propene concentrations, the nitrogen balances were 85 percent for RTI No. 1 and 78 percent for UNC Red. It appears that the nitrogen balance improves with increasing initial hydrocarbon concentration when the initial  $\text{NO}_x$  concentration is held constant as was found by the UNC group.<sup>49</sup> The major  $\text{NO}_2$  loss up until the  $\text{NO}_2$  maximum is thought to be due to the formation of  $\text{HNO}_3$  by the reaction of  $\text{NO}_2$  with hydroxyl radicals. This is a thermal reaction and longer times to the  $\text{NO}_2$  maximum would tend to increase the  $\text{NO}_2$  loss by this pathway (assuming essentially the same average hydroxyl concentrations in the chambers).

In the high concentration propene chambers, there was very close agreement for the maximum  $\text{O}_3$  concentrations. The values measured in RTI No. 2 and UNC Blue were within 2 percent of each other. This result provides additional support to the belief that the chambers at the two facilities exhibit similar chemical behavior. Whatever had produced the deviant behavior of RTI No. 2 in the previous matched experiment was apparently not evident in this case (see above).

In contrast to the results for the high concentration propene chambers, the maximum  $\text{O}_3$  concentrations in the lower concentration chambers showed significant disagreement. RTI No. 1 produced nearly twice the ozone formed in UNC Red. An explanation for this behavior can be found in the initial reactant concentrations. The RTI chamber had an initial hydrocarbon- $\text{NO}_x$  ratio that was 20 percent larger than that of UNC Red. Since the maximum ozone surface is rather steep in low concentration regions, a small difference in the initial reactant concentrations can result in a large difference in the maximum ozone concentration. Since the surface flattens out as one moves along a constant  $[\text{NO}_x]$  line toward higher hydrocarbon concentrations, the observed differences in the initial concentrations of the high concentra-



tion propene chambers would not produce as large a disagreement in the maximum ozone concentrations as the same relative difference would produce at the lower initial concentrations. However, wall-related effects cannot be ruled out as a possible cause of the disagreement.

### Discussion

The results of an initial set of matched experiments comparing the chemical behavior of two outdoor smog chamber facilities have been presented. While it is not prudent to make definitive statements based on such a small number of experiments, the data that have been presented here support the belief that the four RTI and the two UNC outdoor smog chambers display very similar chemical behavior. It is likely that this is the result of the similarity of their wall materials and of the near-identical light intensity and temperature profiles that prevailed during the matched experiments. The excellent overall agreement of the results should increase confidence in the reliability of data obtained from outdoor smog chambers.



## REFERENCES

1. Holzworth, G. C., 1972. Mixing Heights, Wind Speeds and Potential for Urban Air Pollution Throughout the Contiguous United States. Environmental Protection Agency Publication No. AP-101.
2. Schere, K. L. and Demerjian, K. L., 1978. A Photochemical Box Model for Urban Air Quality Simulation. Proceedings, 4th Joint Conference on Sensing of Environmental Pollutants. American Chemical Society, Washington, D.C., pp. 427-433.
3. Jeffries, H. E., Kamens, R., Fox, D. L., and Dimitriadis, B., 1977. "Outdoor Smog Chamber Studies: Effect of Diurnal Light, Dilution and Continuous Emission on Oxidant Precursor Relationships" in International Conference of Photochemical Oxidant Pollution and its Control, Proceedings. Environmental Protection Agency Publication No. EPA-600/3-77-001, pp. 891-902.
4. Dodge, M. C., 1977. Effect of Selected Parameters on Predictions of a Photochemical Model. Environmental Protection Agency Publication No. EPA-600/3-77-048.
5. Office of Air Quality Planning and Standards, 1977. Uses, Limitations and Technical Basis of Procedures for Quantifying Relationships Between Photochemical Oxidants and Precursors. Environmental Protection Agency Publication No. EPA-450/2-77-021a.
6. Office of Air Quality Planning and Standards, 1978. Procedures for Quantifying Relationships Between Photochemical Oxidants and Precursors: Supporting Documentation. Environmental Protection Agency Publication No. EPA-450/2-77-021b.
7. Decker, C. E., Sickles, J. E., II, Bach, W. D., Vukovich, F. M., and Worth, J. J. B., 1978. Project Da Vinci II: Data Analysis and Interpretation. Environmental Protection Agency Publication No. EPA-450/3-78-028.
8. Personal Communication, Edwin L. Meyer, Jr., Office of Air Quality Planning and Standards, Environmental Protection Agency, June 12, 1978.
9. Sickles, J. E., II, 1976. Ozone-Precursor Relationships of Nitrogen Dioxide, Isopentane and Sunlight Under Selected Conditions. Doctoral Dissertation. Department of Environmental Sciences and Engineering, University of North Carolina, Chapel Hill, North Carolina.
10. Ripperton, L. A., Sickles, J. E., II, and Eaton, W. C., 1976. Oxidant-Precursor Relationships During Pollutant Transport Conditions. Environmental Protection Agency Publication No. EPA-600/3-76-107.

11. Khang, S. J., and Levenspiel, O., 1976. The Mixing Rate Number for Agitator-Stirred Tanks. Chemical Engineering, October 11, p. 141.
12. Jeffries, H., Fox, D., and Kamens, R., 1975. Outdoor Smog Chamber Studies: Effect of Hydrocarbon Reduction on Nitrogen Dioxide. Environmental Protection Agency Publication No. EPA-650/3-75-011.
13. Butcher, S. S., and Ruff, R. E., 1971. Effect of Inlet Residence Time on Analysis of Atmospheric Nitrogen Oxides and Ozone. Analytical Chemistry, 43: No. 13, p. 1890.
14. Bufalini, J. J., Kopczynski, S. L., and Dodge, M. C., 1972. Contaminated Smog Chambers in Air Pollution Research, Environmental Letters, 3: No. 2, p. 101.
15. Bufalini, J. J., Walter, T. A., and Bufalini, M., 1977. Contamination Effects on Ozone Formation in Smog Chambers. Environmental Science and Technology, 11: No. 13, p. 1181.
16. Jones, A. C., and Mindrup, R. F., Jr., 1976. Regional Air Pollution Study: Gas Chromatograph Laboratory Operations. Environmental Protection Agency Publication No. EPA-600/4-76-040.
17. Pitts, J. N., Jr., Darnall, K. R., Winer, A. M., and McAfee, J. M., 1977. Mechanisms of Photochemical Reactions in Urban Air: Volume II. Chamber Studies. Environmental Protection Agency Publication No. EPA-600/3-77-014b.
18. Dimitriadis, B., 1967. Methodology in Air Pollution Studies Using Irradiation Chambers. Journal of Air Pollution Control Association, 17: No. 7, p. 460.
19. Scofield, F., Levy, A., and Miller, S. E., 1969. I. Design and Validation of a Smog Chamber, National Paint, Varnish and Lacquer Association Publication No. 797.
20. Grasley, M. H., Appel, B. R., Burstain, I. G., Laity, J. L., and Richards, H. F., 1969. The Relationship of Smog Chamber Methodology to Hydrocarbon Reactivity in Polluted Air. American Chemical Society, Division of Organic Coating and Plastics Chemistry, 29, p. 422.
21. Powers, T. R., 1977. Effect of Hydrocarbon Composition on Oxidant-Hydrocarbon Relationships. Environmental Protection Agency Publication No. EPA-600/3-77-109a.
22. Doyle, G. J., 1970. Design of a Facility (Smog Chamber) for Studying Photochemical Reactions under Simulated Tropospheric Conditions. Environmental Science and Technology, 4: No. 11, p. 907.
23. O'Brien, R. J., 1974. Photostationary State in Photochemical Smog Studies. Environmental Science and Technology, 8: No. 6, p. 579.

24. Bufalini, J. J., and Altshuller, A. P., 1965. Kinetics of Vapor Phase Hydrocarbon-Ozone Reactions. Canadian Journal of Chemistry, 43, p. 2243.
25. Jaffe, R. J., Smith, F. C., Jr., and Last, K. W., 1974. Study of Factors Affecting Reactions in Environmental Chambers: Final Report on Phase II. Environmental Protection Agency Publication No. EPA-650/3-74-004a.
26. Heuss, J. M., February 10-12, 1975. Smog Chamber Simulation of the Los Angeles Atmosphere. A paper presented at the Environmental Protection Agency Scientific Seminar on Automotive Pollutants, Washington, D.C.
27. McNelis, D. N., 1974. Aerosol Formation from Gas-Phase Reactions of Ozone and Olefin in the Presence of Sulfur Dioxide. Environmental Protection Agency Publication No. EPA-650/4-74-034.
28. Kuhlman, M. R., 1974. The Ambient Aerosol Research Facility: Design Criteria and Validation. Master's Thesis. Department of Environmental Sciences and Engineering, University of North Carolina, Chapel Hill, North Carolina.
29. Hampson, R. F., Jr., and Garvin, D., Eds., 1975. Chemical Kinetics and Photochemical Data for Modeling Atmospheric Chemistry. NBS Technical Note 866.
30. Handbook of Chemistry and Physics, 1962. Forty-third Edition, Chemical Rubber Publishing Company, Cleveland, Ohio.
31. U.S. Department of Health, Education, and Welfare, 1970. Air Quality Criteria for Hydrocarbons. National Air Pollution Control Administration Publication No. AP-64.
32. Local Climatological Data: National Weather Service Forecast Office, Raleigh-Durham Airport. U.S. Department of Commerce, National Climatic Center, Ashville, North Carolina.
33. Federal Register, 1976. Measurement of Photochemical Oxidants in the Atmosphere. 41: No. 195, p. 44049.
34. Intersociety Committee, Method 406, 1972. Methods of Air Sampling and Analysis. American Public Health Association, Washington, D.C.
35. Winer, A. M., Peters, J. W., Smith, J. P., and Pitts, J. N., Jr., 1974. Response of Commercial Chemiluminescent NO-NO<sub>2</sub> Analyzers to Other Nitrogen-Containing Compounds. Environmental Science and Technology, 8: No. 13, p. 1118.
36. Intersociety Committee, Method 403, 1972. Methods of Air Sampling and Analysis. American Public Health Association, Washington, D.C.

37. Federal Register, 1971. Appendix E--Reference Method for Determination of Hydrocarbons Corrected for Methane. 36: No. 84, p. 8198.
38. Harrison, J. W., Timmons, M. L., Denyszyn, R. B., and Decker, C. E., 1977. Evaluation of the EPA Reference Method for Measurement of Non-methane Hydrocarbons. Environmental Protection Agency Publication No. EPA 600/4-77-033.
39. Intersociety Committee, Method 110, 1972. Methods of Air Sampling and Analysis. American Public Health Association, Washington, D.C.
40. Intersociety Committee, Method 111, 1972. Methods of Air Sampling and Analysis. American Public Health Association, Washington, D.C.
41. Young, H. D., 1962. Statistical Treatment of Experimental Data. McGraw-Hill Book Co., Inc., New York, N.Y., pp. 76-79.
42. Fox, D. L., Kamens, R., and Jeffries, H. E., 1975. Photochemical Smog Systems: Effect of Dilution on Ozone Formation. Science, 188: p. 1113.
43. Sickles, J. E., II, Ripperton, L. A., Eaton, W. C., and Wright, R. S., 1978. Atmospheric Chemistry of Potential Emissions from Fuel Conversion Facilities: A Smog Chamber Study. Environmental Protection Agency Publication No. EPA-600/7-78-029.
44. Bufalini, J. J., Gay, B. W., and Kopczynski, S. L., 1971. Oxidation of n-Butane by Photolysis of NO<sub>2</sub>. Environmental Science and Technology, 5: No. 4, p. 336.
45. Altshuller, A. P., Kopczynski, S. L., Wilson, D., Lonneman, W. A., and Sutterfield, F. D., 1969. Photochemical Reactivities of n-Butane and Other Paraffinic Hydrocarbons. Journal of the Air Pollution Control Association, 19: No. 10, p. 787.
46. Zafonte, L. and Bonamassa, F., 1977. Relative Photochemical Reactivity of Propane and n-Butane. Environmental Science and Technology, 11: No. 10, p. 1015.
47. Dimitriadis, B. and Joshi, S. B., 1977. "Application of Reactivity Criteria in Oxidant-Related Emission Control in the USA" in International Conference of Photochemical Oxidant Pollution and Its Control: Proceedings. Environmental Protection Agency Publication No. EPA-600/3-77-001, pp. 705-710.
48. Calvert, J. G. and Jeffries, H. E., 1977. International Conference on Oxidants, 1976. Analysis of Evidence and Viewpoints. Part II. The Issue of Reactivity. Environmental Protection Agency Publication No. EPA-600/3-77-114.
49. Jeffries, H. E., Fox, D. L., and Kamens, R., "Photochemical Conversion of NO to NO<sub>2</sub> by Hydrocarbons in an Outdoor Chamber", Journal of the Air Pollution Control Association, 26 (5): 480, 1976.

50. Jeffries, H. E., Sickles, J. E., II and Ripperton, L. A., "Ozone Transport Phenomena: Observed and Simulated." Presented at the 69th Annual Meeting of the Air Pollution Control Association, Portland, Oregon, June 27-July 1, 1976.
51. Kamens, R. M. and Jeffries, H. E., "Progress Report on Winter Oxidant Study in UNC Outdoor Chamber," EPA Grant 800916, Univeristy of North Carolina, Department of Environmental Science and Engineering, May 4, 1976.

**TECHNICAL REPORT DATA**  
(Please read Instructions on the reverse before completing)

1. REPORT NO. EPA-600/3-79-078a		2.		3. RECIPIENT'S ACCESSION NO.	
4. TITLE AND SUBTITLE OXIDANT-PRECURSOR RELATIONSHIPS UNDER POLLUTANT TRANSPORT CONDITIONS Outdoor Smog Chamber Study Volume 1				5. REPORT DATE August 1979	
				6. PERFORMING ORGANIZATION CODE	
7. AUTHOR(S) J.E. Sickles, II, L.A. Ripperton, W.C. Eaton, and R.S. Wright				8. PERFORMING ORGANIZATION REPORT NO.	
9. PERFORMING ORGANIZATION NAME AND ADDRESS Research Triangle Institute Research Triangle Park North Carolina 27709				10. PROGRAM ELEMENT NO.	
				11. CONTRACT/GRANT NO. 1AA603 AC-03 (FY-77) 68-02-2207	
12. SPONSORING AGENCY NAME AND ADDRESS Environmental Sciences Research Laboratory-RTP, NC Office of Research and Development U.S. Environmental Protection Agency Research Triangle Park, North Carolina 27711				13. TYPE OF REPORT AND PERIOD COVERED Final 6/75 - 6/78	
				14. SPONSORING AGENCY CODE EPA/600/09	
15. SUPPLEMENTARY NOTES Volume 2. Appendixes					
16. ABSTRACT <p>Multiple-day experiments were conducted in outdoor smog chambers to investigate the influence of simulated transport on ozone generation by various combinations of a surrogate urban hydrocarbon mixture and nitrogen oxides. The simulation of transport was accomplished by progressively diluting the contents of the chambers with purified air.</p> <p>First day ozone maximum concentrations were reduced under dilution conditions and were sensitive to both dilution rate and time at which dilution was initiated. Second and third-day ozone maxima were reduced at increasing dilution rates, but the reduction was less than proportional to the extent of dilution. The ozone-generative potential of an aged photochemical system generally exceeded 0.08 ppm.</p> <p>Additional experiments were conducted to examine the ozone-generative potential of low reactivity hydrocarbons, to provide data for testing and validation of a computer-based photochemical simulation model, and to compare the behavior of two types of outdoor smog chambers.</p> <p>Volume 1 contains all textual material. Volume 2 contains all the smog chamber analytical data for hydrocarbons, NO, O<sub>3</sub>, CO, CH<sub>2</sub>O, and condensation nuclei, as well as dilution and meteorological data.</p>					
17. KEY WORDS AND DOCUMENT ANALYSIS					
a. DESCRIPTORS		b. IDENTIFIERS/OPEN ENDED TERMS		c. COSATI Field/Group	
<ul style="list-style-type: none"> <li>* Air pollution</li> <li>* Ozone</li> <li>* Nitrogen oxides</li> <li>* Test chambers</li> <li>Solar radiation</li> <li>* Photochemical reactions</li> <li>Chemical analysis</li> </ul>				13B 07B 07C 03B 07E 07D	
18. DISTRIBUTION STATEMENT RELEASE TO PUBLIC		19. SECURITY CLASS (This Report) UNCLASSIFIED		21. NO. OF PAGES 126	
		20. SECURITY CLASS (This page) UNCLASSIFIED		22. PRICE	